9th JOINT STUDENT ONLINE SEMINAR on CIVIL INFRASTRUCTURES December 8-10, 2020

9th Joint Student Online Seminar on Civil Infrastructures

8-10 December 2020

Co-Organized by

International Center for Urban Safety Engineering (ICUS)
Institute of Industrial Science, The University of Tokyo, Japan

Regional Network Office for Urban Safety (RNUS),
School of Engineering and Technology,
Asian Institute of Technology (AIT), Thailand
&
Takeuchi laboratory,
Institute of Industrial Science, The University of Tokyo, Japan

Organizing Members

Prof. Kimiro Meguro (UT, Japan)
Prof. Wataru Takeuchi (UT, Japan)
Prof. Pennung Warnitchai (AIT, Thailand)
Prof. Hong Huang (Tsinghua Univ. China)

PREFACE

IIS has established a Regional Network Office for Urban Safety (RNUS) at SET, AIT since 2002 and dispatched young faculty members from Japan to Thailand to work for education and research including urban safety, remote sensing and GIS, infrastructure health assessment, flood risk monitoring. RNUS also serves to organize seminars and arrange IIS/U-Tokyo alumni parties every year. We recognize RNUS as one the core international liaison research offices in Paris and New York.

On the first day, Dr. Pennung Warnitchai, Dean of the Department of Civil Engineering, AIT, presented "Vibration control of buildings and structures-an Overview," and on the second day, Dr. Yudai Homma, Associate Professor of the Institute, presented "Mathematical Model for Social Distancing-Close relationship with architectural planning", and on the third day, Professor Wataru Takeuchi gave a lecture titled "Geospatical technologies towards one world, one health and earth".

This is the first event in the last 13 years which is fully organized via online conference style. I was concerned about the connection from countries with unstable internet environments, but the moderator from AIT was able to share the questions on chat and the discussion among the students progressed more than expected. There were 36 student presenters from 13 countries, including Thailand, Japan, Myanmar, India, Sri Lanka, Cambodia, Peru, Egypt, Indonesia, Nepal, China, Korea, and the Philippines, for a total of 132 participants over the three days, including the audience. The activities of the RNUS Thailand Office, which has been led by the International Center for Urban Safety Engineering (ICUS), will be expanded in cooperation with the Office of International Industry-Academia Collaboration.

May I ask each of you here today to lend your strength and support to AIT and IIS/UTokyo as it strives to enhance and expand ever-growing friendship and scientific exchange activities for excellent scientific researchers.

Thank you very much, Kopun-krap, Arigato-gozaimasu.

Wataru Takeuchi

▪ Program

9th Joint Student Online Seminar on Civil Infrastructures

Venue: Online Date: 8-10 December 2020

Field: D=Disaster I=Infrastructure E=Environment O=Others

Page	Date/ No.	Time	Name	Field	Affiliation	Title
8th Dec. 2020						
	Opening	19:00-	Prof. Pennung Warnitchai Prof. Takeuchi Wataru		AIT UTokyo	
	Special lecture	19:10-19-30	Prof. Pennung Warnitchai: Vibration Control of Buildings and Structures--an Overview			
2	1	19:30-19:40	Mr. Yokoe Yoshito (Japan)	D	Nagaoka Univ of Tech.	Seismic hazard assessment in Yangon City using the empirical earthquake evaluation method
3	2	19:40-19:50	Mr. Xinwei XI(china)	D	Tsinghua Univ	Research on the Safety Resilience Evaluation Model and Decision Optimization Method of Coastal Cities under Waterlogging
4	3	19:50-20:00	Ms. Ayaka Ikeda (Japan)	D	Nagaoka Univ of Tech,	Reproduce Past Earthquakes, 1987 Chibaken-Toho-Oki Earthquake (M6.7)
5	4	20:00-20:10	Mr. Martin Garcia-Fry (Peru)	D	Tohoku Univ.	Post-Disaster Operational Planning Process for Transit-Oriented Development with Secured Access to Livelihood Recovery
6	5	20:10-20:20	Mr. Atsuya Minagawa(Japan)	D	Nagaoka Univ of Tech	Study on amplification factor of maximum acceleration for seismic hazard assessment
7	6	20:20-20:30	Mr. Zhou Shiwei (China)	D	Tsinghua Univ.	Resilience assessment model on interdependent infrastructures
8	7	20:30-20:40	Ms. Achini Uppeka Ranasinghe (SriLanka)	O	AIT	Integration of Electrical Resistivity Imaging and Induced Polarization For Investigation of Subsoil Heavy Metal Contamination: A Case Study of Bang Yai Canal, Phuket Island, Thailand
9	8	20:40-20:50	Mr. Sanjiv Neupane (Nepal)	O	AIT	Evaluation of CORDEX regional climate model (RCMs) for future climate extreme projection in Bangkok and its vicinity, Thailand
10	9	20:50-21:00	Ms. Peetiya Nidhinandana (Thailand)	O	AIT	A Physical Modeling Study of Arrangements of Sheet Pile Wall in Sand Bed
11	10	21:00-21:10	Ms. Shakthi Kalpani Gunawardana(Sri Lanka)	O	AIT	Evaluation of SWAT model for hydrological simulation in the transboundary Srepok River Basin of the Lower Mekong Region
12	11	21:10-21:20	Mr. Saurav KC (Nepal)	O	AIT	Development of Framework to Assess the Groundwater Governance in Rapidly Urbanizing Cities

	9th Dec. 2020					
	Special lecture	19:00-19:20	Associate Prof. Yudai Honma: Mathematical Model for Social Distancing- Close Relationship with Architectural Planning -			
13	12	19:20-19-30	Ms. Nussarin Sudrohman (Thailand)	O	AIT	A study of the difference between tunnel precast system and fully precast system for townhouse construction
14	13	19:30-19:40	Mr. Jogo Boku (Korea)	O	UTokyo	Evaluation of Room Arrangements by Social and Spatial Network Analysis in Hospital Architecture
15	14	19:40-19:50	Mr. Nartmongkhol Songserm (Thailand)	O	AIT	Computer-aided Rock Classification using Python Programming
16	15	19:50-20:00	Ms. Kornkanok Sangprasat (Thailand)	O	AIT	Preliminary Analysis of Chiang Mai Earthquakes With Related To The Active Fault Zones of Thailand
17	16	20:00-20:10	Mr. Phattarasuda Witchayaphong (Thailand)	O	AIT	Influential Factors Affecting Travelers' Mode Choice Behavior on Mass Transit in Bangkok, Thailand
18	17	20:10-20:20	Mr. Mohamed ADEL (Egypt)	I	UTokyo	Evaluation of crack-bridging strength degradation in SFRC structural beams under flexural fatigue
		20:20-20:25	BREAK			

19	18	20:25-20:35	Mr. Nyi Linn Maung (Myanmar)	I	UTokyo	Formation and Transformation of Informal Settlements from Historical Viewpoint in Yangon, Myanmar
20	19	20:35-20:45	Mr. Kumar Avadh (India)	I	UTokyo	Investigation of local bond behaviour between corroded deformed reinforcement and uncracked concrete using DIC
21	20	20:45-20:55	Ms.Srikulnath Nilnoree (Thailand)	I	AIT	Development of Real-time Displacement Measurement Using Sampling Moiré Method in a Single Board Computer (a SBC)
22	21	20:55-21:05	Dr. Vikas Singh Kuntal (India)	I	UTokyo	Estimation of internal corrosion levels from surface racks of concrete using model predictive control in 3D RBSM
23	22	21:05-21:15	Saugat Shrestha (Nepal)	I	AIT	Suppression of Wind effects on structures using Plasma Actuators
24	23	21:15-21:25	Ms. Isrrah Malabanan (Philippines)	I	AIT	Simulation model development for traffic signal light control with emergency vehicle preferential treatment: A case study of Bangkok
25	24	21:25-21:35	Mr. Nogami Hiroki (Japan)	I	UTokyo	Model of Indirect Physical Contact within Social Activities

	10th Dec. 2020					
	Special lecture	19:00-19:20	Prof. Wataru Takeuchi: Geospatial Technologies Towards One World, One Health and One Earth			
26	25	19:20-19-30	Mr. Kumagai Taichi (Japan)	D	Nagaoka Univ. of Tech.	Numerical study on dynamic behavior of surface ground near the long-distance ground-flow area caused by the 2018 Sulawesi earthquake, Indonesia
27	26	19:30-19:40	Mr. Suzuki Haruki (Japan)	D	Nagaoka Univ. of Tech.	Estimating the ground characteristics of Koiwagawa area which caused house damages by the 2019 Off the Yamagata prefecture earthquake
28	27	19:40-19:50	Mr. Zamzam Multazam (Indonesia)	D	UTokyo	Experimental Study on simple retrofitting method for hollow blocks masonry walls
29	28	19:50-20:00	Mr. Takada Hikaru (Japan)	D	Nagaoka Univ. of Tech	Effects of surface ground characteristics on earthquake damage of wooden houses
30	29	20:00-20:10	Mr. Dheeraj Joshi (Indian)	D	UTokyo	Risk assessment of rail infrastructure in India to support business continuity plan
31	30	20:10-20:20	Mr. Nattapon Trumikaborworn (Thailand)	D	AIT	Tsunami Evacuation Simulation using Agent-based Modeling: a case study of Khao Lak, Thailand
		20:20-20:25	BREAK			
32	31	20:25-20:35	Mr. Sakanann Vann (Cambodia)	E	Prince of Songkla Univ.	Investigation of Seawater Intrusion Using Geoelectrical Survey in Coastal Aquifer of Phuket Island, Thailand
33	32	20:35-20:45	Mr. Daiki Shimizu (Japan)	E	UTokyo	Detection of drainage canal distribution and scenario evaluation of peat restoration measures in Indonesia
34	33	20:45-20:55	Ms. Syukratun Nufus (Indonesia)	E	Prince of Songkla Univ.	Empirical Model Of Thailand Shale Compaction Based On Geological Age Classification
35	34	20:55-21:05	Ms. Pragya Pradhan (Nepal)	E	AIT	Evaluation of CMIP5 General Circulation Model (GCMs) simulating precipitation and temperature in Koshi river basin,Nepal
36	35	21:05-21:15	Mr. Phanuphong Prajongkha (Thailand)	O	AIT	Evaluating Factors of Severe Injuries on Motorcycle Rear-end Collision in Thailand
37	36	21:15-21:25	Mr. Navindra Ganganath Liyanarachchi (SriLanka)	I	AIT	Rapid Identification of Seismic Damage in Tall Buildings by using Acceleration Response Time Histories
	Closing	21:25-21:45	Prof. Huang Hong Prof. Takeuchi Wataru		Tsinghua Univ. UTokyo	

Contents

・Special Lecture

- Prof. Pennung Warnitchai, AIT
- Vibration Control of Building and Structures--Overview

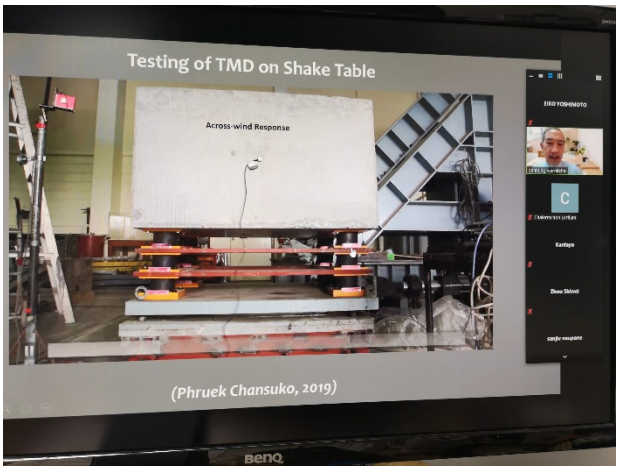

- Associate Prof. Yudai Honma, UTokyo
- Mathematical Model for Social Distancing –Close Relationship with Architectural

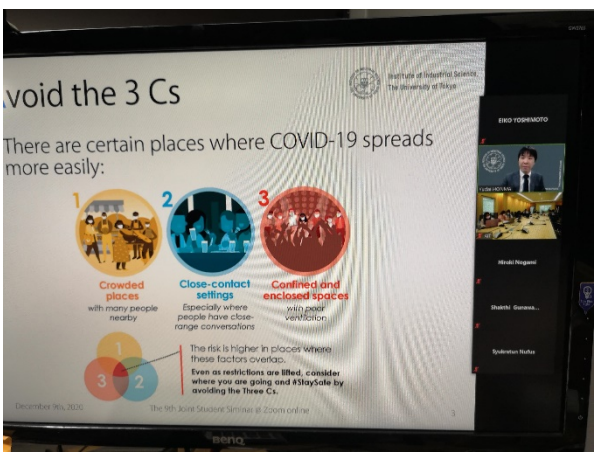

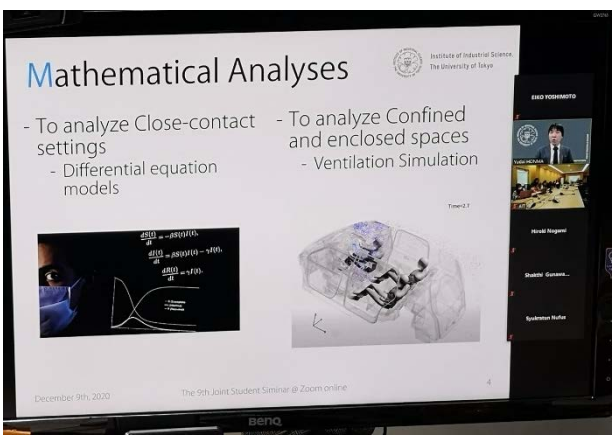

- Prof. Wataru Takeuchi, UTokyo
- Geospatial Technologies Towards One World, One Health and One Earth

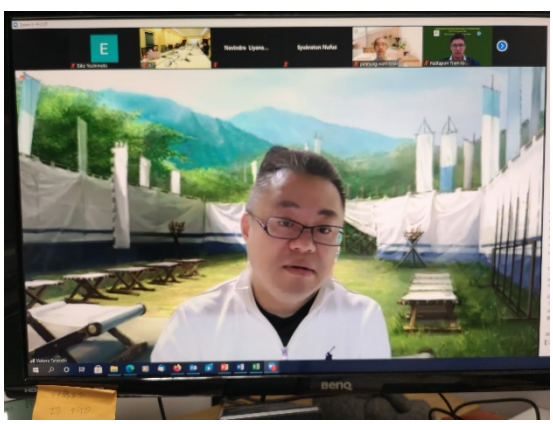

・Students posters

Seismic hazard assessment in Yangon City using the empirical earthquake evaluation method

Yoshito Yokoe, Nagaoka University Of Technology, Japan, M2

1. Background

・Seismic Risk in Myanmar

➢A number of large earthquakes have occurred in Myanmar in the past, such as the sagaing fault.

➢There is a high probability of more M7-class earthquakes in the future.

・SATREPS

➢SATREPS is conducting a building collapse risk assessment in Yangon. For example (Matsumoto (2019))

➢In these studies, the seismic motions on the engineering basis are uniformly calculated as 30 kine.

➢The purpose of this study is to obtain detailed engineering base waveforms for possible earthquake ground motions in Yangon city, and to create a seismic hazard map based on past earthquake motions.

yyyy/mm/dd/	epicenter	magunitude
1927/12/17	Yangon	M7.0
1930/05/05	Yangon	M7.3
1930/12/03	Bago	M7.3
1931/01/27	Kachin	M7.6
1946/09/12	Mandalay	M7.5

Past earthquakes that occurred on the sagaing fault

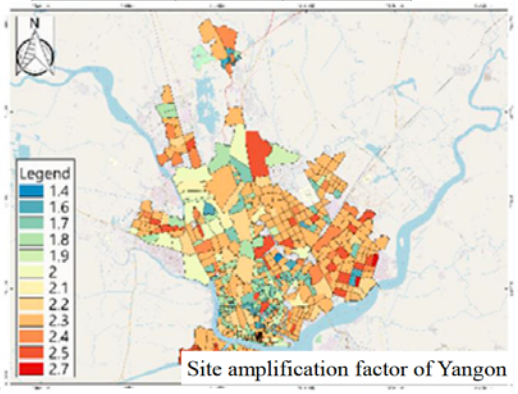

Site amplification factor of Yangon

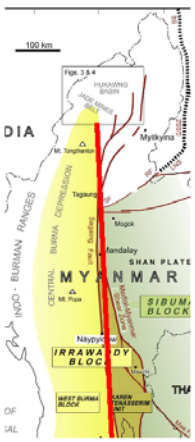

Sagaing fault location map

2. Scenario Earthquake

・Consider & Methods

➢The source fault model parameters were set based on previous studies.

➢ used EMPR, a strong motion prediction method developed by Sugito et al.

➢The effects of fault size, direction of rupture, and mode of rupture can be considered. The waveforms on an engineering basis can be obtained.

Mw= 0.88M+0.54 Central Disaster Prevention Conference (2004)

Log L= 0.6M -2.9 Matsuda (1975)

Log M0= 1.5Mw+9.1 Kanamori(1977)

L: length of the fault (km)

M : Magnitude

M0: Seismic moment (N-m)

Fault Parameters

Moment Magnitude (Mw)	7.0
Fault size(L×W)	30km × 15km
Epicenter depth	10km
Fault strike and slope	0°, 90°
Seismic moment(M_0)	3.52×10^{19} N・M

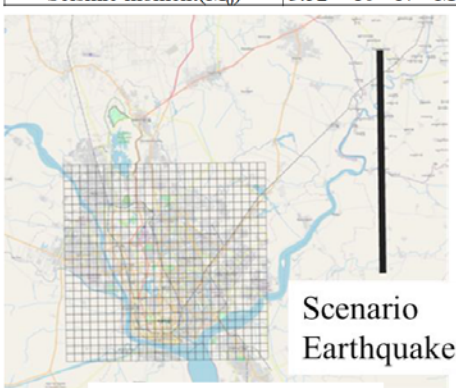

Site and Source Fault Location

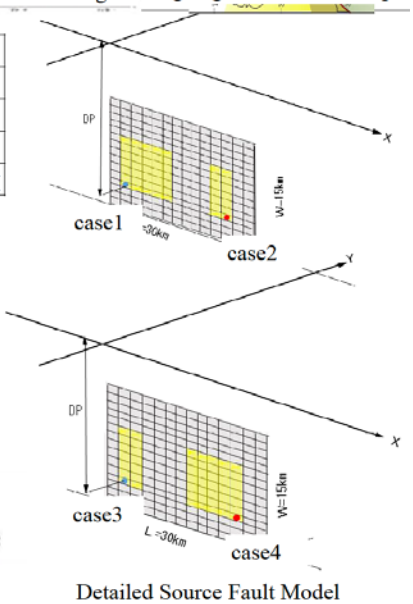

Detailed Source Fault Model

・Heterogeneity Considerations

➢The strong-motion generation area (SMGA) is set up with reference to the strong-motion prediction recipe in order to take heterogeneity of fault failure into account.

➢Two SMGAs were set up, with the large area accounting for 16% of the total area and the small area accounting for 6%.

➢A total of four cases were calculated in which the position of the fracture start point was placed at both ends of the SMGA and the position of the SMGA was changed.

$$Sa1=0.16 \times S, \quad Sa2 = 0.06 \times S$$

where $Sa1$= area of SMGA for large regions, and $Sa2$= area of SMGA for small regions S = area of the entire fault

3. Results

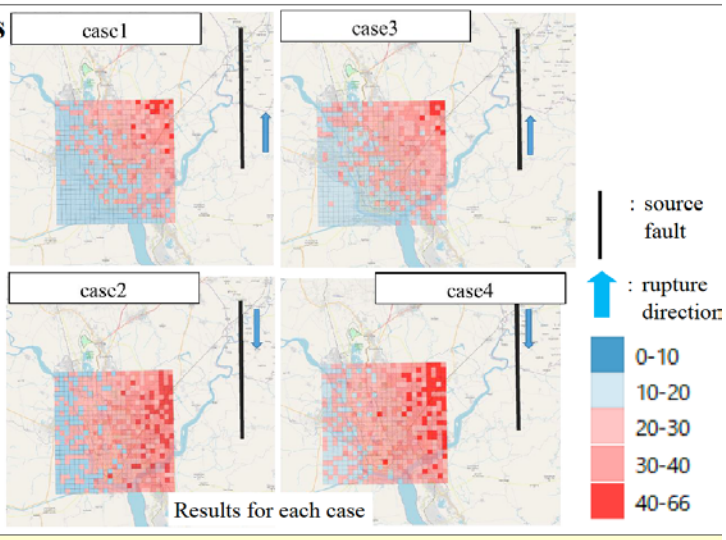

Results for each case

Name: Yokoe Yoshito TEL : +8190-8378-9186 E-mail: s173282@stn.nagaokaut.ac.jp. : Earthquake engineering HP: https://whs.nagaokaut.ac.jp/gee-l/index.html

Research on the Safety Resilience Evaluation Model and Decision Optimization Method of Coastal Cities under Waterlogging

Xinwei Xi, Tsinghua University, China, 3rd grades of postgraduate

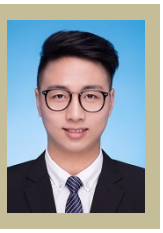

Urban waterlogging is a common urban disaster, and its destructive power is a major problem that restricts urban safety and social and economic development. This problem is more obvious in coastal cities due to frequent rainfall. How to quickly assess the safety and resilience of urban waterlogging in the case of insufficient numbers has become a problem that needs to be studied. This paper uses the combination of multi-criteria decision-making and Markov chain Monte Carlo method to give a solution.

As a typical coastal city in China and an internationally renowned city, Shenzhen has high rainfall and low altitude, as well as annual rainfall in the typhoon season, and waterlogging as a common disaster, posing challenges to security and resilience. So we took Shenzhen as a case, combined multi-criteria decision-making and Markov chain Monte Carlo method to quickly assess and optimize the waterlogging resilience.

The first part uses a multi-criteria decision-making scheme, based on GIS raster hydrological modeling, and can quickly assess the city's waterlogging safety resilience level under stable rainfall in the absence of urban drainage data. Multi-criteria decision-making methods are used to evaluate and score the waterlogging resilience level, carry out sensitivity analysis to streamline indicators, and consider regional conditions, risk preferences and moving window sizes to classify waterlogging safety resilience.

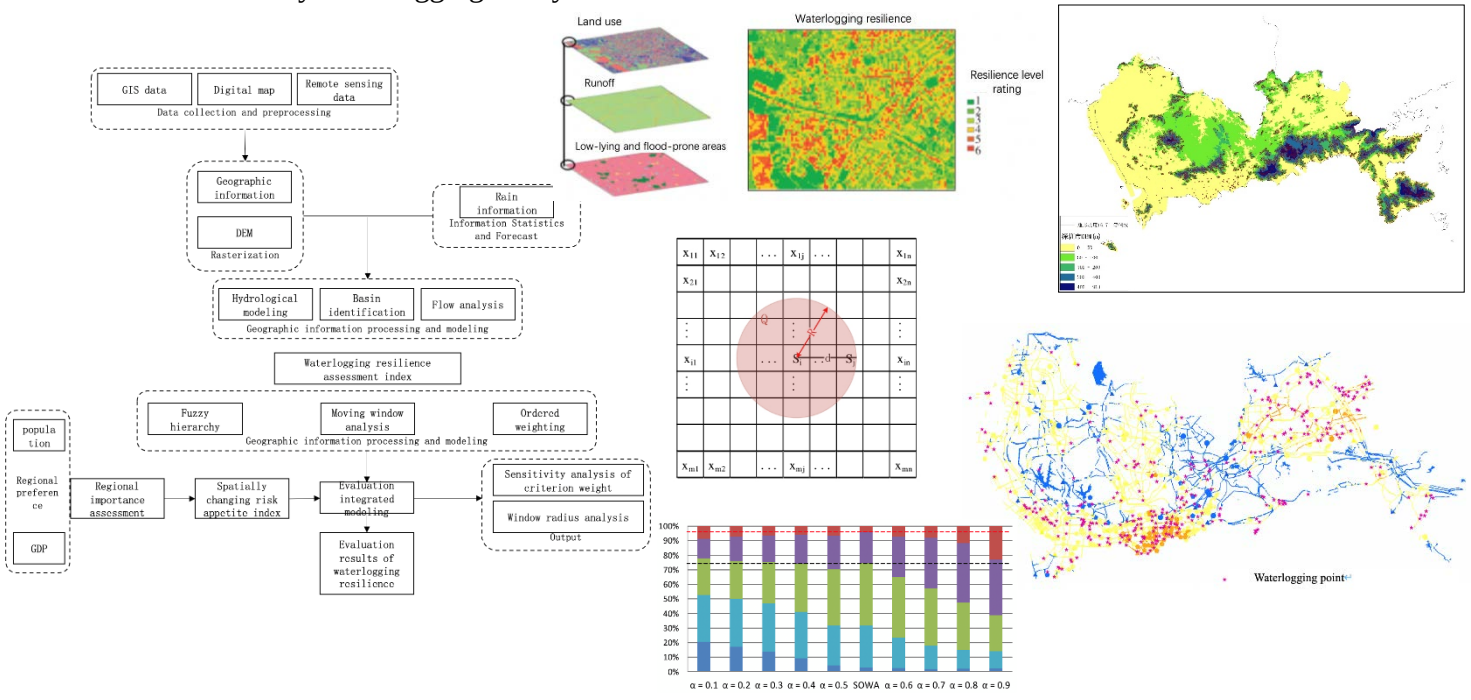

The second part is based on the results of the previous chapter, using Markov chain Monte Carlo method to simulate the dynamic changes in the resilience level of Shenzhen in the rainy season. The combination of MCMC method and difference improves the speed of simulation and convergence, and optimizes decision-making for resilience assessment. The recovery probabilities of different waterlogging resilience levels are converged, the recovery process is simulated, and sensitivity analysis is performed.

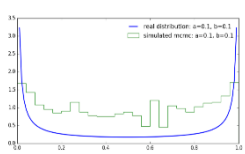

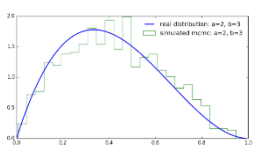

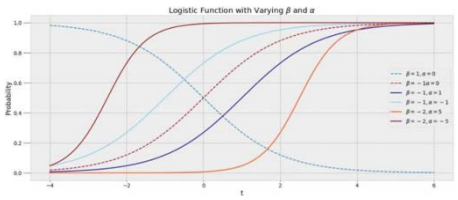

Based on the research conclusions, suggestions for improving the waterlogging resilience level of coastal cities are put forward and applied to actual production applications.

For further information, contact below.

Xinwei Xi, Hong Huang, Institute of Public Safety, Department of Engineering Physics, Tsinghua University

TEL: +86-188 0665 5592 E-mail: xxw18@mails.Tsinghua.edu.cn

Reproduce Past Earthquakes, 1987 Chibaken-Toho-Oki Earthquake(M6.7)

Ayaka Ikeda, Nagaoka University of Technology, Japan

Background

- In Japan, the earthquakes are very frequent.
- Tokyo metropolitan area is one of the most affected regions as it contains the largest part of the social infrastructure.

- IMPORTANT THINGS to do in order to reduce the earthquake damages:
  - Analyze and collect information related to the past earthquake damages.

⇩

1987 Chibaken-Toho-Oki Earthquake

Steps to Reproduce the Past Earthquakes

Step1 : Grasping the earthquake situation

Organizing and mapping the seismic motions using step 1's data making thus the implementation of the earthquake prevention measures easier.

Step2 : Making the Attenuation Relationship Formula appropriate for Tokyo metropolitan area

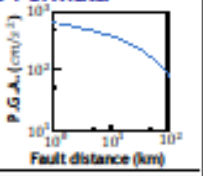

Step3 : Predicting the earthquake damages depending on the situation

Chibaken-Toho-Oki Earthquake

Latest earthquakes since modern Tokyo

- Date: December 17, 1987
- Epicenter Depth : 58 km
- Magnitude: M6.7
- Max Seismic intensity: 5

- NO TUNAMI.
- A lot of damage in the tile roofs of wooden houses

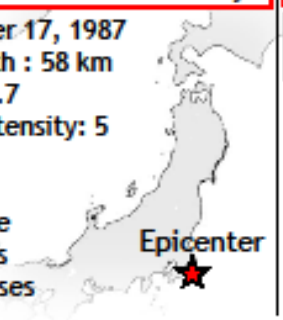

Earthquake Observation Records at the Time

Earthquake data are extremely scarce as far back as the past.

All 260 locations, 463 records!!

Network of Port Area Strong-motion Monitoring

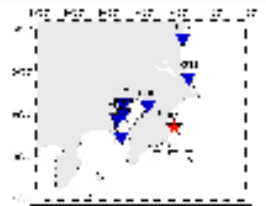

NOT comprehensive

Chibaken-Toho-oki earthquake Damage Assessment Report

LISTED DATA

the Peak Ground Acceleration (PGA)

With Building Name BUT

Address

Latitude and Longitude Coordinates

Seismometer installation coordinates must be identified !

Steps to Create The Earthquake Motions Distribution Map

There is a lack of data as we go back in the past.

Step1 : Identifying the Seismometers latitude-longitude coordinates

Is it still there? The name has changed?

Once you get the address...

Identify latitude-longitude coordinates on a GSI map!

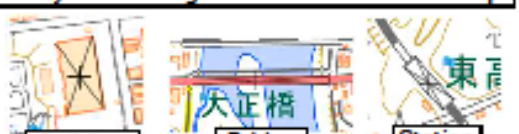

Step2 : Screening the Useful Data

In total, We identified 157 locations and179 records!

⇨ Creating the Map

Step3 : Calculating the PGV

In this report,

NS, EW, and UD components PGA

Horizontal Maximum

$$= \sqrt{\text{NS's PGA}^2 + \text{EW's PGA}^2}$$

Mapping based on the calculation's results and the location's information

The Earthquake Motions Distribution Map

Surface Record

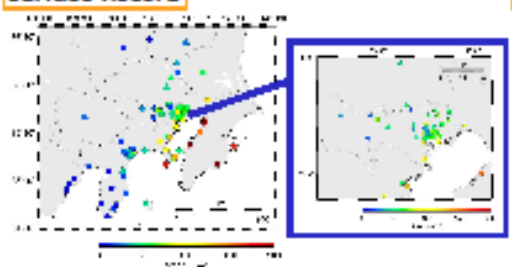

Underground Record

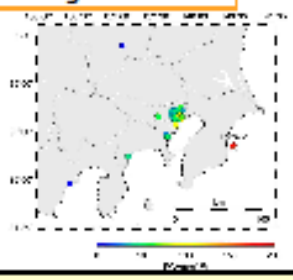

Future Prospects

In order to control and minimize the damages...

- What can be done ?

E.g.) Changing the magnitude,
Changing the epicenter's locations, etc...

⇩

The reproduction is required
the Attenuation Relationship Formula

⇩

Designing the earthquake prevention measures.

For further information, contact below.

Ayaka Ikeda, Earthquake Engineering Laboratory, TEL: +81-8084343459, E-mail: s183234@stn.nagaokaut.ac.jp
HP: https://whs.nagaokaut.ac.jp/gee-l/

A Post-Disaster Operational Planning Process for Transit-Oriented Development with Secured Access to Livelihood Recovery

Martin Garcia-Fry, Architect, Peru, Master Course

After the 2010 Merapi Volcano eruption, many villages were relocated in semi-urban settlements separated from their earlier livelihoods and with few options for diversification. Post-disaster resettlement is dependent on people's access to livelihoods as a means for short- and long-term recovery. The purpose of this study is to describe a systematic process of urbanization during the first ten years of recovery based on Transit-Oriented Development (TOD) that produces employment opportunities and less travel expenditures. In 2019, a field survey was conducted in the largest resettlement site of the Sleman Regency in Yogyakarta Province to evaluate the state of recovery; socio-demographic and land use data was subsequently processed to forecast urban development into the year 2030. Travel routines were simulated for 2019 and 2030 comparatively to quantify travel efficiency and ease of access to economic growth using urban form indices. The TOD provided 624 full-time jobs and consequently, 41,850m2 of residential demand due to concentrated building growth. The case study saw a 57% increase of neighborhood shopping and 21% new full-time job attainment for the displaced community. Efficiency reduced 33% of travel within the new settlement and a 57% reduction in total. Fuel consumption was decreased by 44%, equal to 109,752 grams of carbon dioxide (CO2). A balance in mobility modes was achieved with motorcycles (36%), public transportation (32%), and walking (32%) for the whole settlement. These results indicate inexpensive sustainable development with exposure to 3.2 times more transit volume allowing economies of scale to generate livelihood opportunities during post-disaster recovery.

3. Simulation A
Travel Schedules in 2019 with a New Settlement

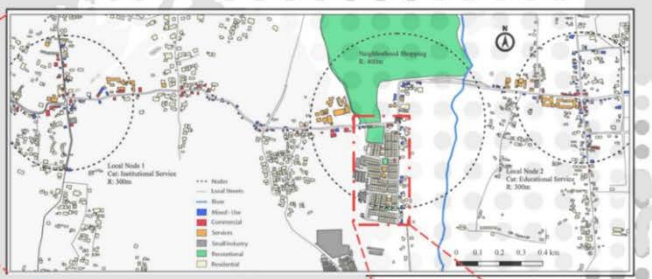

4. Simulation B
New Settlement & A Peri-Urban Development Process (2030)

2. Special Region of Yogyakarta, Cangkringan Sub-District

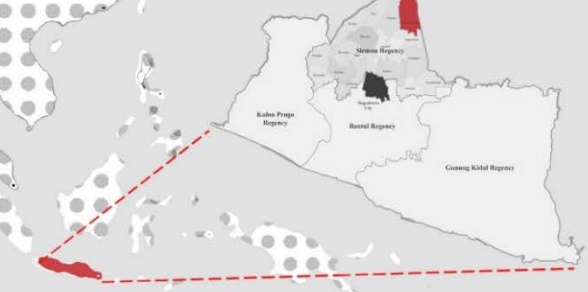

Findings

66% of all non-work tours occur within walking range, with all subjects walking to or from destinations increasing micro-business demand.

5. Simulation C
New Settlement
Peri-Urban Development (2030)
Public Transportation

1. Java Island, Indonesia

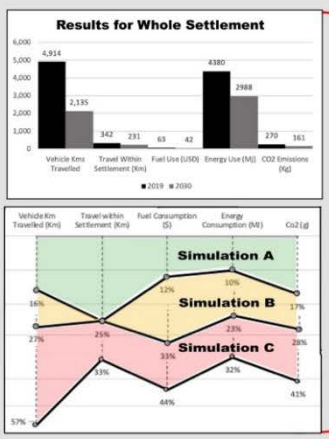

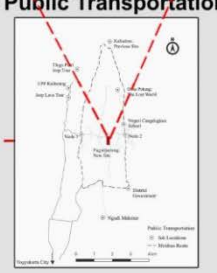

6. Transportation Route
(Key Destinations in the Cangkringan Sub-District)

8. Urban Form Results

- 37,442m2 of new construction
- Total transit volume 3.2 times larger by 2030
- 624 new full-time jobs in nodal development
- Neighborhood shopping increases by 57%

7. Travel Efficiency Tests

Next Steps: Consolidate a Urban Development Process for Instant Resettlement after Natural Disasters in Peri-Urban Areas

Contact:
Martin Garcia-Fry, 国際防災戦略研究分野, 東北大学災害科学国際研究所棟S402, Tel: +81-80-3193-4526, +022−752−2125,
E-mail: martingarciafry@gmail.com, Web: http://martingarciafry.com/

STUDY ON AMPLIFICATION FACTOR OF MAXIMUM ACCELERATION FOR SEISMIC HAZARD ASSESSMENT

Atsuya Minagawa, Nagaoka University of Technology, Japan, Master 2nd

INTRODUCTION

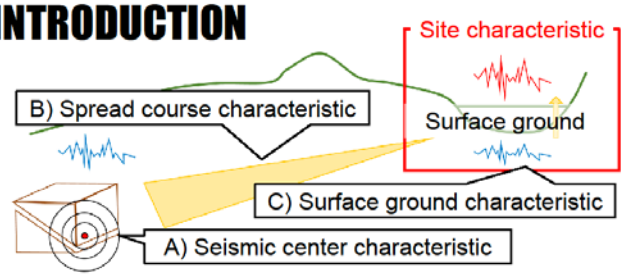

A,B,C→Seismic motion vibrating the structure

Yangon city

Sagaing fault

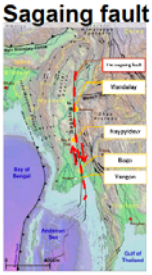

In Japan, the risk of earthquakes is high, and there are many efforts related to earthquake disaster prevention measures.
There are some countries that the risk is not properly evaluated.
In Yangon city, it is necessary to evaluate surface ground properties.

RESEARCH OBJECTIVE

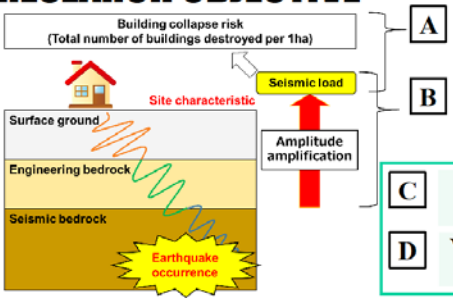

A	Building collapse risk assessment
B	Evaluation of ground amplification properties
C	The strong motion prediction
D	Vibration analysis of civil engineering structures

Previous studies and examination of earthquakes
Though A and B are evaluated focusing on velocity,
C and D are evaluated focusing on acceleration.

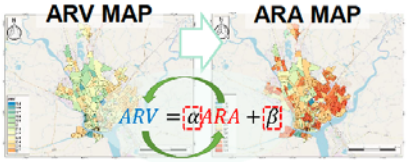

Research objective
Acceleration and velocity the expression of relations of the amplification factor is calculated.

ARV: Amplification Ratio of Velocity
ARA: Amplification Ratio of Acceleration

METHOD AND RESULT

1. Selection of examination points

vertical array observation

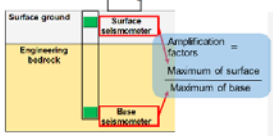

Amplification factor and vertical array observation
The amplification factor is calculated from the ratio of the maximum values of the base and the surface. There are no vertical array observations in Yangon to observe those records.
→The points similar to the geology of Yangon is selected from the strong motion data in Japan.

Topography of Yangon

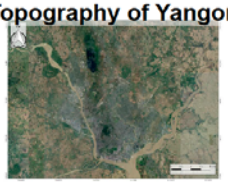

Columnar section of Yangon

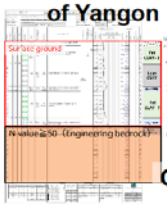

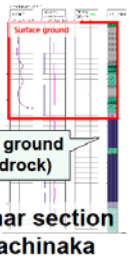

Columnar section of Hitachinaka

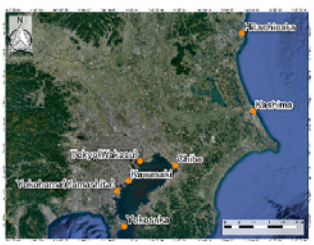

2. Integral and frequency range limitation

Conversion flow

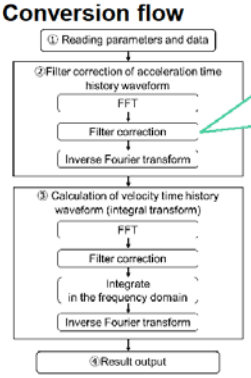

Filter correction

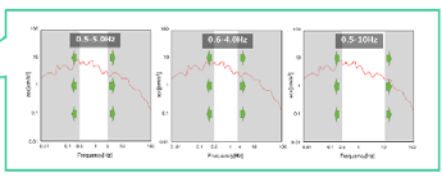

The acceleration waveform to the velocity waveform are converted. Filter correction is performed to limit the frequencies that are not related to building damage.

Points to consider when determining the filter range
(1) Natural period of buildings in Yangon: 0.5-1.0s (1.0-2.0Hz)
(2) Natural period of the ground in Yangon City: 0.3-0.9s (1.1-3.3Hz)
(3) Impact frequency during acceleration conversion: 0.2Hz or higher

3. Calculation of amplification factor and relational expression

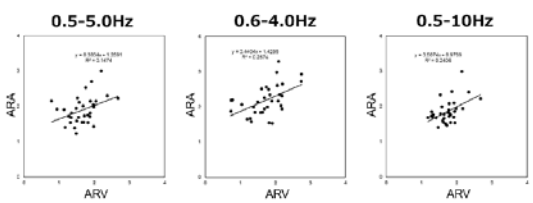

Filter section	0.5-5.0Hz	0.6-4.0Hz	0.5-10Hz
Relational expression	y=0.38x+1.3	y=0.44x+1.4	y=0.51x+0.98

SUMMARY

1. Selection of examination points
The presence or absence of bedrock affects the stable calculation of the amplification factor.

2. Integral and frequency range limitation
When performing integral conversion, it is necessary to limit the frequency with a filter.

3. Calculation of amplification factor and relational expression
From the result of "Hitachinaka", there was a relationship between ARA and ARV, but the result was that the same judgment could be made practically.

For further information, contact below.
Name: Atsuya Minagawa TEL: +8180-2252-2246 E-mail: 173277@stn.nagaokaut.ac.jp
Labo: Earthquake engineering HP: https://whs.nagaokaut.ac.jp/gee-l/index.html

Resilience assessment model on interdependent infrastructures ——take gas pipelines and power grids as an example

Student : Zhou Shiwei
Supervisor: Professor Huang Hong
Institute for Public Safety Research, Tsinghua University, Beijing, 10084, China

Abstract

In this research, a resilience assessment model of interdependent infrastructures was constructed in consideration of the absorptive, recovery and adaptive ability. The sensitivity analysis was carried out in gas pipelines and power grids aiming at identifying key nodes and pipe segments. Some improvement strategies to enhance resilience of the interdependent infrastructure was proposed in terms of absorptive, recovery and adaptive ability.

Introduction

An increasing number of countries are promoting the construction of Resilient Cities in recent years. Infrastructure resilience is a vitally important part of city resilience since infrastructure is the basis for maintaining normal operation of social and economic activities in a city. Additionally, the interdependency of infrastructures probably brings graver loss while facing disasters.

Research subjects

Literature retrieval

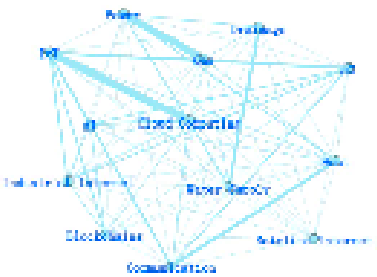

Fig.1 Infrastructure interdependency connection diagram based on Jaccard index

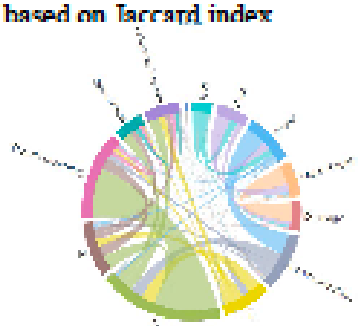

Fig.2 String figure of infrastructure interdependency based on Jaccard index

According to the results of literature retrieval, the interdependency of gas pipelines and power grids is fairly strong.

Methodology

Resilience assessment model on interdependent Infrastructures:

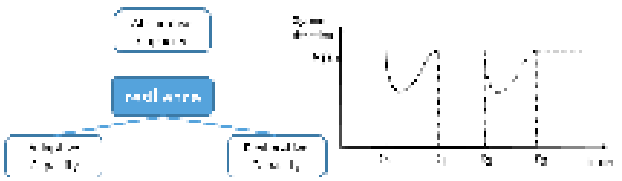

Fig.3 The function curve of infrastructure system

Interdependency: Geographic and Physical

Results

Gas pipelines

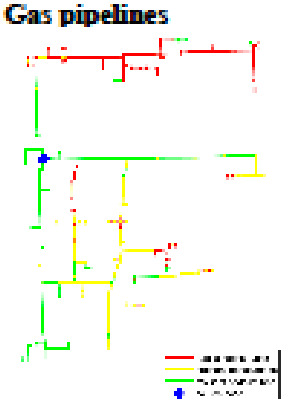

Power Grids（nodes）

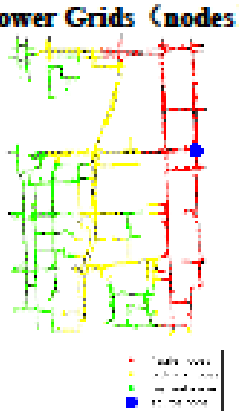

Power Grids（tubes）

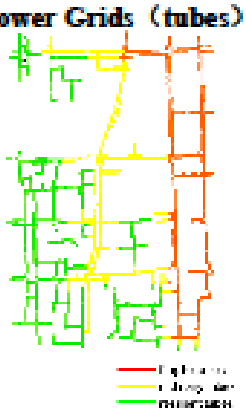

Resilience improvement strategies:

(1)Increase redundancy;
(2)Improve recovery plan;
(3)Reinforce key nodes and pipe segments.

Integration of Electrical Resistivity Imaging and Induced Polarization For Investigation of Subsoil Heavy Metal Contamination: A Case Study of Bang Yai Canal, Phuket Island, Thailand

Achini Uppeka Ranasinghe (Sri Lankan)

Master Degree Student of Geotechnical and Earth Resources Engineering
School of Engineering and Technology, Asian Institute of Technology

abstract

The long history of tin mining in Phuket island has polluted sediments in rivers, estuaries, and lakes. Although metal discharges were greater during the period of active tin mining in the eighteenth century, a significant amount of dissolved heavy metals still occur in the aquifer system. The quality of groundwater is affected by the characteristics of the media through which the water passes on its way to the groundwater zone of saturation. The contaminated discharge then enters the nearby waterways which eventually connects to the Bang Yai canal which is the largest river located in Phuket. Due to the river processes, the metal contaminants present are transported downstream and deposited in the canal bed. Often, the contaminants travel a considerable distance downstream from the mining sites. This study aims to demonstrate the benefits of integrating scientific investigating methods comprising electrical resistivity imaging (ERI) and induced polarization (IP) to attain the dispersion plums of contamination for a spatial investigation in an efficient way. ERI is a geo-electrical method based on different conductive properties of the subsurface materials while IP is based on the earth's capacity to hold an electrical chargeability over time. ERI alone may not identify the differences between the contamination of seawater and heavy metals, or even soft clay layers, thus ERI integrated with IP are used to obtain a more accurate spatial model for investigating subsurface contamination The survey lines of both ERI and IP were successfully conducted along Bang Yai canal as the study area for a quantitative assessment of the spatial contamination. Two-dimensional (2D) inversion models of the integration between ERI and IP from the resistivity and chargeability data show high-resolution subsurface overlying anomalies of the contamination. Finally, the research results are able to prove that the abandoned mining field is scientifically implied as being a contamination source dispersing along Bang Yai canal toward the Andaman Sea.

INTRODUCTION

Contamination is one of the main challenges related to groundwater. The entering of harmful pollutants such as heavy metals into the aquifer system degrades the quality of water and poses a risk to human health and the ecosystem. The long history of tin mining in Phuket island has polluted sediments in rivers, estuaries, and lakes. Although metal discharges were greater during the period of active tin mining in the eighteenth century, a significant amount of dissolved heavy metals still occur in the aquifer system. Heavy metals are non-biodegradable materials, so it remains in the environment for a long time which allows metal pollutants to spread through the groundwater system. Therefore, it is essential to assess the spatial dispersion of heavy metals to identify the contaminated area.

Many researchers have conducted studies to examine the heavy metal contamination in Phuket island. Suteerasak & Bhongsuwan (2008) investigated the heavy metal contamination in the sediments of the Bang Yai Canal in Phuket and observed elevated concentrations for Al, Fe, Sn, and Pb along the Bang-Yai canal. Geochemical studies were done by Akkajita et al. (2018) and Akkajit & Suteersak (2017) show the presence of heavy metal at the Bang-Yai catchment area.

Geo-electrical surveys are widely employed in characterizing contaminated sites. Electrical resistivity imaging (ERI) and induced polarization (IP) can be identified as the commonly used technique in environmental studies. However, in some geological conditions single method is insufficient in effectively recognizing the area of contamination. ERI doesn't provide reliable results if clay sediments are present in the investigated area (Pierwoła, 2013). In such cases, a combination of ERI and IP should be applied for unambiguous interpretation. Pierwoła (2013) investigated the influence of the deposited waste in a postmining landfill on the underground water using resistivity and induced polarization imaging methods in Buków, Poland. Puttiwongrak et al. (2019) used aqua regia and geo-electrical surveys (ERI & IP) to examine the heavy metal contamination in Saphan Hin, Phuket.

SITE DESCRIPTION

The study area covers the entire Bang Yai canal ("Khlong Bang Yai") in Phuket province, southern Thailand. Geo-electrical surveys were implemented at 5 stations along the Bang-Yai canal to examine subsoil contamination by the heavy metals as shown in Figure 1. Bang-Yai canal originates from Khuan Wa, Kathu waterfall area (Station 5) and flows down to the southeast direction through the Kathu Municipality with multiple short tributaries until it connects to the Andaman Sea at Saphan Hin (Station 1). The canal receives water flowing from the abandoned Tin (Sn) mining areas so there is a potential for heavy metal contamination of water and soil in the surrounding area of the Bang-Yai Canal.

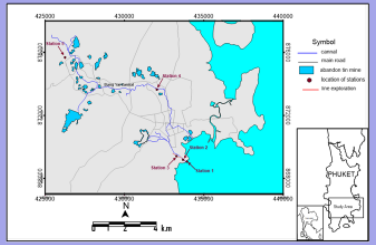

Figure 1 – Location 5 stations where geo-electrical surveys are performed

METHODOLOGY

Geo-electrical surveys (ERI & IP) were performed using AGI SuperSting R2 resistivity meter with a multielectrode switch system with 56 electrode channels which can measure both resistivity (ERI method) and chargeability (IP method). Five line surveys were conducted at five different station points along the Bang-Yai Canal as shown in Figure 1. Both resistivity (ρ) and chargeability were measured in all lines. Wenner electrode configuration was used for data acquisition in all stations as it is sensitive to the vertical variation of resistivity. A maximum profile length of 110m, 275m, 110m, 275m, and 82.5m and electrode spacing of 2m, 5m, 2m, 5m, and 1.5m was adopted for line 1, line 2, line 3, line 4 and line 5 respectively. The inversion of ρ and chargeability field data was carried out using AGI EarthImager 2D software. The inversion routine was based on the finite-difference model for ERI and linear inversion model for IP imaging. Table 1 shows the root mean square (RMS) error obtained and the number of iterations in 2D resistivity inversion of each survey line.

Table 1 : Root mean square and number of iterations of ERI inversion for all stations

	Line 1	Line 2	Line 3	Line 4	Line 5
RMS of ERI	15.63%	6.58%	11.48%	6.70%	4.79%
No of iterations	8	4	8	5	4

RESULTS

Resistivity is inversely proportional to the concentration of heavy metal therefore when soil is contaminated low resistivity is indicated in ERI results. However, low resistivity can also imply the presence of clay particles or seawater in the investigated area. To effectively identify the area of contamination IP imaging is also acquired for the same survey line. A strong IP effect can be observed when the high ion concentration is present hence high chargeability (≥ 30ms) can be detected in elevated heavy metal contamination. The combination of 2D ERI and IP inversions are used to clearly identify the contaminated zones in all stations. This is achieved by overlaying the inversion images of ERI and IP and isolating the common areas with low resistivity (≤ 1 Ohm-m) and high chargeability (≥ 30ms). Heavy metal contamination zones are present in all stations except station 5 which is located before mining sites. Therefore, tin mining sites can be identified as a probable source of heavy metal contamination. Generally, the river speed decreases as it approaches the sea so greater dispersion of heavy metal contaminates can be expected in this area. This might be the reason for the occurrence of a larger contaminated zone near the coastal region (Station 1 and Station 2).

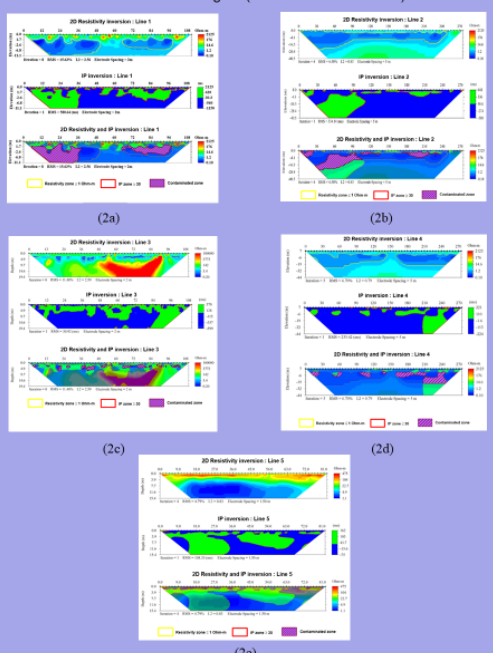

Figure 2 - 2D inversion results of contaminated interpretation (ERI, IP & overlaying result of ERI and IP) : (2a) Line 1, (2b) Line 2, (2c) Line 3, (2d) Line 4, (2e) Line 5.

CONCLUSION

The obtained results verify tin mining sites as a source of heavy metal contamination in the Bang-Yai area. A gradual increase in the contamination zone area is visible moving from Kathu waterfall (station 5) to the Saphan Hin area (station 1). The combination of resistivity and IP survey can be considered as an efficient approach to characterize a contaminated site. This is especially useful where impermeable, clayey sediments and seawater intrusion is present.

REFERENCE

Akkajit, P., & Suteersak, T. (2017). The study of historical contamination of Tin (Sn) and Zinc (Zn) in sediments at the Bang-Yai River estuary, Phuket Province. Journal of Applied Science, 16 (Special issue), 8-18. https://doi.org/10.14416/j.appsci.2017.10.s02

Akkajita, P., Jaileak, K., Suteersak, T., & Prueksakorn, K. (2018). Assessment of Heavy Metals in Sediment at Saphan Hin, Phuket. Chemical Engineering Transaction, 63, 301-306. https://doi.org/10.3303/CET1863051

Pierwoła, J., 2013. Investigation of Soil Contamination Using Resistivity and Induced Polarization Methods. *Polish Journal of Environmental Studies*, 22(6), pp.1781-1788.

Puttiwongrak, A., Suteerasak, T., Mai, P., Hashimoto, K., Gonzalez, J., Rattanakom, R. and Prueksakorn, K., 2019. Application of multi-monitoring methods to investigate the contamination levels and dispersion of Pb and Zn from tin mining in coastal sediments at Saphan Hin, Phuket, Thailand. *Journal of Cleaner Production*, 218, pp.108-117.

Suteerasak, T. & Bhongsuwan, T. (2008). Contamination of Heavy Metals Al, As, Cu, Cr, Mn, Ni, Pb, Sn, Zn and Fe in Sediment from Bang-Yai River in Phuket Province. วารสาร วิจัย และ พัฒนา มจธ., 31(4), 765-780

ACKNOWLEDGEMENT

I would like to thank Dr. Thongchai Suteerasak and Prince of Songkla University (PSU), Thailand for the support and assistance provided.

For further information, contact below.
Achini Ranasinghe, Geotechnical and Earth Resource Engineering (GTE) Laboratory, AIT TEL : +66-659706530, E-mail: ach.uppeka@gmail.com

Evaluation of CORDEX regional climate models (RCMs) for future climate extreme projection in Bangkok and its vicinity, Thailand

Sanjiv Neupane[1], Sangam Shrestha[1], Usha Ghimire[1], S. Mohanasundaram[1], Sarawut Ninsawat[2]

[1]Water Engineering and Management, School of Engineering and Technology, Asian Institute of Technology (AIT)

[2]Remote Sensing and Geographic Information System, School of Engineering and Technology, Asian Institute of Technology (AIT)

The 9th International Joint Student Seminar

8-10 December 2020

Asian Institute of Technology, Thailand

Abstract

This study focusses on evaluating a set of Regional Climate Models (RCMs) for future climate extreme projection in Bangkok and its vicinity, Thailand. Although a large number of RCMs are available nowadays in the CORDEX archive, the issue of their reliability for specific regions must still be confronted. This situation makes it imperative to sort out the most appropriate set of RCMs for the assessment of climate change impacts in the region. To this end, twenty-one RCMs with gridded resolution of 0.44° *044° from the CORDEX data portal were assessed for six climate indices; Consecutive Dry Days (CDD), Simple Daily Intensity Index (SDII), Number of extremely heavy precipitation days (R50mm), Maximum 1-day precipitation amount (RX1day), Mean of daily maximum temperature (TX mean) and Mean of daily minimum temperature (TN mean) using four performance indicators. The performance indicators used were correlation coefficient (CC), normalized root mean square deviation (NRMSD), absolute normalized root mean square deviation (ANRMSD) and average absolute relative deviation (AARD). The Entropy method was endorsed to acquire weights of these 4 indicators and weightage average techniques was used for ranking of 21 RCMs. The result demonstrated that the best model for one climate indices is not the same best model for other climate indices. In addition, the RCMs; WAS44_SMHI_RCA4_IPSL_CM5A_MR, WAS44_SMHI_RCA4_NCC_NorESM1_M, WAS44_SMHI_RCA4_CCCma_CanESM2, WAS44_SMHI_RCA4_ICHE_EC_EARTH and WAS44_SMHI_RCA4_MPI_ESM_LR are the top five best performing RCMs in Bangkok and its vicinity, Thailand, respectively. Therefore, they are recommended for the further investigation.

Overall Methodological Framework

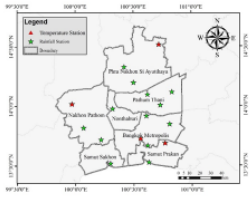

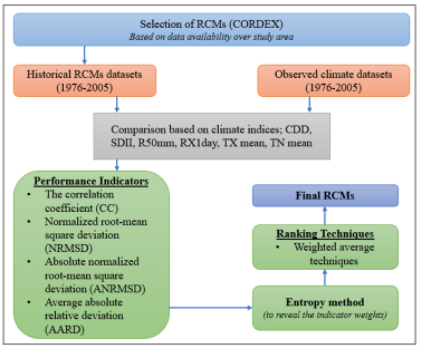

Entropy Method

Step 1: Formation of decision matrix which shows the performances of different alternatives (RCMs) with respect to various evaluation criteria (Performance indicators)

$$X = [X_{ij}]_{matrix} = \begin{bmatrix} X_{11} & \cdots & X_{1n} \\ \vdots & \ddots & \vdots \\ X_{m1} & \cdots & X_{mn} \end{bmatrix}$$ where, i = 1, 2...., m; j = 1, 2..., n

Step 2: Normalization of the decision matrix

$$rij = \frac{X_{ij} - min(X_{ij})}{\max(X_{ij}) - \min(X_{ij})}$$ where, i = 1, 2...., m; j = 1, 2..., n

$$rij = \frac{\max(X_{ij}) - X_{ij}}{\max(X_{ij}) - \min(X_{ij})}$$ where, i = 1, 2...., m; j = 1, 2..., n

Step 3: Determination of Entropy value (ej) for each evaluation criteria (performance indicators)

$$ej = \frac{-1}{\ln(m)} \sum_{i=1}^{m} f_{ij} * \ln(f_{ij})$$ where, i = 1, 2...., m; j = 1, 2..., n

$$fij = \frac{r_{ij}}{\sum_{i=1}^{m} r_{ij}}$$ where, i = 1, 2...., m; j = 1, 2..., n and 0<ej<1

Step 4: Calculation of Entropy weights (Wj) based on degree of diversification (Dj)

$$Dj = 1 - ej$$

$$Wj = \frac{D_j}{\sum_{j=1}^{n} D_j}$$ where, $\sum_{j=1}^{n} W_j = 1$

Weightage Average Technique

$$Vj = \sum_{j=1}^{n} r_{ij} W_j$$ where, j = 1, 2..., n; $\sum_{j=1}^{n} W_j = 1$; Wj>=0

Conclusions

- *Each indicator responds differently for various RCMs and climate indices and the best model for one climate indices is not the same best model for other climate indices.*
- *RCMs; WAS44_SMHI_RCA4_IPSL_CM5A_MR, WAS44_SMHI_RCA4_NCC_NorESM1_M, WAS44_SMHI_RCA4_CCCma_CanESM2, WAS44_SMHI_RCA4_ICHE_EC_EARTH and, WAS44_SMHI_RCA4_MPI_ESM_LR are the top five best performing RCMs in Bangkok and its vicinity, Thailand, respectively.*

Analysis of Performance Indicators for CDD

Model Serial	CC	NRMSD	ANRMSD	AARD
M1	0.029	0.593	0.166	0.547
M2	0.014	0.626	0.257	0.642
M3	0.174	0.968	0.795	1.193
M4	0.059	0.764	0.378	0.810
M5	0.001	0.618	0.198	0.601
M6	0.008	0.718	0.371	0.792
M7	0.090	0.632	0.407	0.447
M8	0.151	0.582	0.317	0.423
M9	0.029	0.553	0.147	0.571
M10	0.187	0.631	0.429	0.452
M11	0.206	0.526	0.139	0.429
M12	0.138	0.584	0.217	0.471
M13	-0.054	0.634	0.352	0.460
M14	0.138	0.537	0.156	0.425
M15	0.158	0.589	0.249	0.450
M16	0.044	0.625	0.378	0.432
M17	0.081	0.675	0.420	0.512
M18	0.018	0.650	0.372	0.499
M19	-0.203	0.719	0.427	0.584
M20	0.000	0.667	0.414	0.487
M21	0.039	0.624	0.356	0.459
Max	0.206	0.968	0.795	1.193
Min	-0.203	0.526	0.139	0.423
Max-Min	0.408	0.441	0.656	0.771

Application of Entropy Method and Weightage Average Technique for CDD

Model Serial	CC	NRMSD	ANRMSD	AARD	Weighted Average Value (Vj)	Rank
M1	0.566	0.848	0.958	0.838	0.790	8
M2	0.529	0.774	0.820	0.716	0.700	13
M3	0.923	0.000	0.000	0.000	0.272	21
M4	0.641	0.461	0.635	0.498	0.566	18
M5	0.498	0.794	0.909	0.769	0.730	12
M6	0.515	0.566	0.645	0.520	0.560	19
M7	0.716	0.761	0.591	0.968	0.752	9
M8	0.865	0.874	0.728	1.000	0.863	5
M9	0.568	0.940	0.988	0.808	0.813	7
M10	0.953	0.764	0.557	0.962	0.813	6
M11	1.000	1.000	1.000	0.992	0.998	1
M12	0.834	0.869	0.881	0.937	0.877	4
M13	0.364	0.755	0.675	0.951	0.665	16
M14	0.835	0.977	0.974	0.997	0.939	2
M15	0.883	0.858	0.831	0.965	0.883	3
M16	0.604	0.776	0.635	0.988	0.738	10
M17	0.694	0.664	0.571	0.884	0.699	14
M18	0.539	0.721	0.644	0.901	0.689	15
M19	0.000	0.564	0.561	0.791	0.449	20
M20	0.497	0.680	0.581	0.917	0.655	17
M21	0.593	0.779	0.669	0.953	0.736	11
ej	0.973	0.979	0.977	0.979	-	-
Dj	0.027	0.021	0.023	0.021	-	-
Wj	0.295	0.229	0.249	0.227	-	-

Weightage Average Value for all Climate Indices

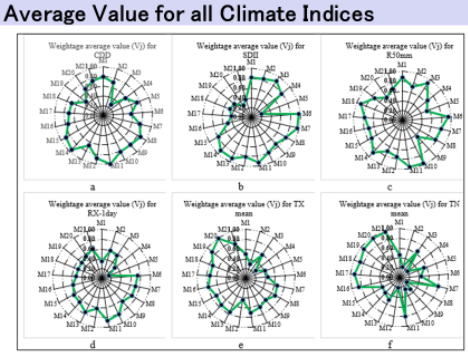

Final Selection of RCMs in Bangkok and its Vicinity, Thailand

Modal Serial	Rank in Bangkok and its vicinity						
	CDD	SDII	R50mm	Rx 1day	TX mean	TN mean	Rank Sum
M1	8	8	7	19	16	12	70
M2	13	7	13	12	20	18	83
M3	21	6	4	14	15	9	69
M4	18	13	18	20	21	20	110
M5	12	21	20	21	19	10	103
M6	19	1	3	4	17	13	57
M7	9	2	8	5	12	7	43
M8	5	10	9	6	11	21	62
M9	7	14	21	9	14	16	81
M10	6	11	1	2	13	17	50
M11	1	3	2	1	9	8	24
M12	4	9	11	11	18	19	72
M13	16	4	16	3	4	11	54
M14	2	5	6	7	6	14	40
M15	3	12	14	8	10	15	62
M16	10	15	15	13	3	6	62
M17	14	18	10	16	7	4	69
M18	15	16	5	17	8	5	66
M19	20	17	12	18	2	3	72
M20	17	20	19	15	1	2	74
M21	11	19	17	10	5	1	63

For further information, contact below.

Name: Sanjiv Neupane; Contact:+66-28532645; Email:mentosneupane26@gmail.com

A Physical Modeling Study of Arrangements of Sheet Pile Wall in Sand Bed

Asist. Prof. Dr. Thanadol Kongsomboon[1], Peetiya Nidhinandana[2], Siwakorn Soysak[3], Supavat Kongpanickul[4]
[1] Asist. Prof. [2,3,4]Student, Department of Civil Engineering, King Mongkut's Institute of Technology Ladkrabang (KMITL), Bangkok, Thailand
Presenter: Peetiya Nidhinandana, Asian Institute of Technology, Thai, Master of Engineering

In the big city, the development of underground construction has been increasing. That is the reason why people need to improve the retraining wall system to be more efficient. There are many usages of technics how to reduce wall movement for example, deeper length of sheet piles walls, anchored sheet pile wall, bracing system, various arrangement of sheet pile, etc. This research was the study of T-shape arrangement of sheet pile wall in the physical model using sand as the soil sample which has 29.9° of internal friction angle. We used the different length of web: 5, 10, 15 centimeters installed behind of the excavation side. The increases of soil resistance and area moment of inertia affected the movement behavior in each length of web. Refer to the relationship between the web length of T-shape models and the depth of the excavation, these could decrease the displacement of the retaining wall. We found that the T-shape with the web longer than the failure area of active resisting zone, it could develop more the moving resistance and reduce movement more effectively than the sheet pile with the web placed in the active resisting zone.

OBJECTIVES

- To study modeled sheet pile behaviors and soil failure in different excavation elevation via physical modeling in sand bed.
- To study and compare efficiency of wall displacement reduction in different web length of T-shape sheet pile arrangement.

SCOPE OF STUDY

1. Simulated Model dimension : 24x53x44 cm.
2. Sand represented as soils:

Ø (Direct Shear Test) = 29.9°
Ø (Slope Stability) = 31.5°
Specific Gravity = 2.603

%Finer (Sieve no.10-50)	
No.10	99.046%
No.20	72.378%
No.30	59.832%
No.40	26.088%
No.50	8.776%

3. Acrylic wall represented as a sheet pile:

Thickness = 1.50 mm.
Elastic Modulus = 58,199.88 ksc
Hex Bolts + Nuts 7 mm. Diameter

4. Water pressure and friction between wall and model are not considered.
5. Using image processing to capture the displacement with lens distortion correction.
6. Filling sand into the model by gravitational fall 30 cm. above the surface.

METHODOLOGY

▸The single wall behaviors (Fig 2) was used to determine 3 different web lengths of T-shape sheet piles:

1) 5 cm. - inside failure zone
2) 10 cm. - at failure zone
3) 15 cm. - outside failure zone

as shown in Fig 3.

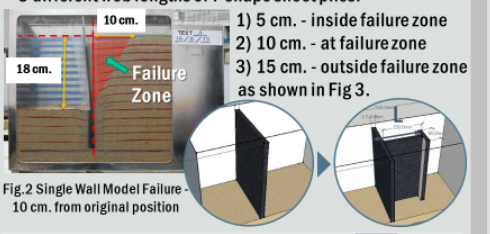

Fig.2 Single Wall Model Failure - 10 cm. from original position

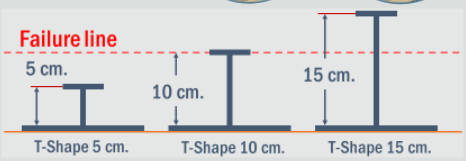

Fig.3 Top views of the model shown 3 different web lengths

▸ In an experiment, there were 3 steps as follows:

RESULTS

- As shown in Fig.4, displacements occurred in T-shape 5 cm., 10 cm., and 15 cm. smaller than in single wall respectively at the same excavation depth.
- For T-shape 5 cm., the wall suddenly failed at the 22-23 cm. excavation depth.
- For T-shape 10 cm. and 15 cm., the excavation can be continuously conducted until the base of wall (28 cm.) without failure plane found.

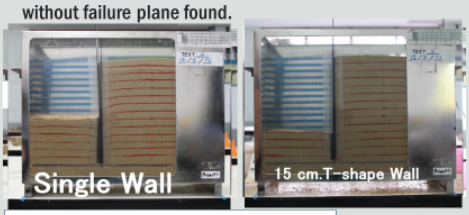

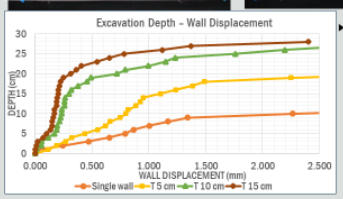

▸Rate of displacement was slow at beginning and started increasing after passing one excavation depth (Failure point).

Fig.4 The relationship curve between excavation depth – wall displacement

DATA ANALYSIS

Passive Force

- Passive force founded behind the flank of T-shape 5 cm. acts as the resistance at the beginning before the increment of active force drive the wall to fail.
- If the location of flank is out of the active zone (failure line in Fig.3), the passive force can resist active force effectively.

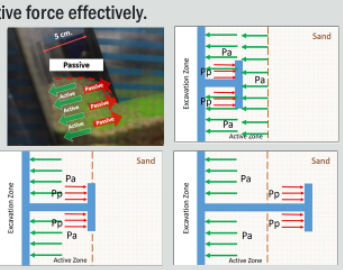

Fig.5 Active Force (Pa) and Passive Force (Pp) Behaviors

Location of web of T-shape

- Failure points for T-shape 5 cm. and 10 cm. are nearly same (excavation depths) because both T-shape model are still located in active zone.

Table 1: The failure point of different models

Model	Depth at failure (cm.)	Displacement at failure (mm.)	$\Theta = 45° + \frac{\Phi'}{2}$ at 23 cm. depth
Single Wall	14.9	8.40	65.25°
T-shape 5 cm.	21.1	5.40	61.25°
T-shape 10 cm.	21.3	0.84	N/A
T-shape 15 cm.	23.5	0.62	N/A

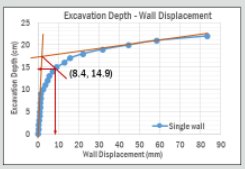

Fig.6 Example of Failure point given from graphical method

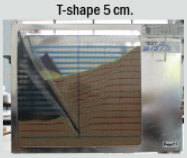

Fig.7 Sudden Failure of T-shape 5 cm. Wall

Displacement/Depth Ratio

- The ratio can be used to determine the efficiency of retaining walls.
- The trends of T-shape graph can be clearly described into 3 zones:
  - ✓ Zone A: Passive Force Develop,
  - ✓ Zone B: Passive Force Working,
  - ✓ Zone C: Failing.

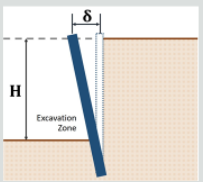

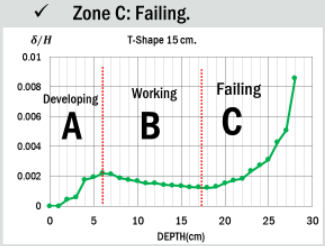

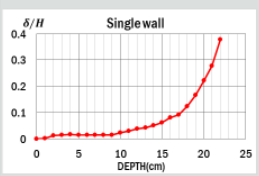

Fig.8 Depth and Displacement Relationship

- For the graph of single wall, there is not the development of passive force.

Area Moment of Inertia (I)

- Increment of area moment of inertia by T-shape arrangement cause smaller displacements due to the walls which can free stand for a while.
- When the active increased, the wall fell immediately as the T-shape walls change the way of movement from flexible bending to overturning and sliding like a gravity wall.

CONCLUSIONS

- T-shape can reduce wall movement, and the web longer than the failure zone could develop passive force at flank of "T" more effectively
- Higher area moment of inertia could change movement from flexible wall to gravity wall
- Development of passive force needs some initial displacement

REFERENCES

[1] Muni Budhu (2011): Soil Mechanics and Foundations 3rd Edition, John Wiley and Sons.
[2] Thanadol Kongsomboon (1996). Foundation Engineering, Course Book, Civil Engineering, KMITL, Bangkok

Other References

AWARDS & PUBLICATION

- March 2018: Publication in Engineering Journal of Research and Development, Volume 29 Issue 1, page 5-14 (January – March 2018)
- June 2017: Gold medal award of geotechnical engineering research Competition, The Engineering Institute of Thailand Under H.M. The King's Patronage, Thailand

For further information, please contact: PEETIYA NIDHINANDANA (Mai), Tel : +66-83-997-7990, E-mail: st121403@ait.ac.th , peetiya.pn@gmail.com

Evaluation of SWAT model for hydrological simulation in the transboundary Srepok River Basin of the Lower Mekong Region

Shakthi K. Gunawardana* , Sangam Shrestha**
*Graduate student in Water Engineering and Management, Asian Institute of Technology (AIT)
** Professor in Water Engineering and Management, Asian Institute of Technology (AIT)

The 9th International Joint Student Seminar on Civil Infrastructures
9-10 December 2020

Abstract

Srepok River Basin is a tributary of the transboundary 3S (Sesan, Srepok and Sekong) River Basin which constitute a significant part of Lower Mekong River Basin and shared among three countries: Cambodia, Vietnam, and Laos. Many dams are currently in operation and are planned to be constructed in future for energy generation. Hence, this has created pressure in water allocation in different sectors including maintenance of the environmental flow conditions for fish habitat. Therefore, this study utilized the Soil and Water Assessment Tool (SWAT) to model the hydrology of the Srepok River Basin. The SWAT model is part of the Mekong River Commission (MRC) Decision Support Framework, which was accepted by MRC member countries for water resources planning in the Lower Mekong Basin. Therefore, a SWAT model was developed utilizing six observed rainfall stations, one temperature station, and MRC land use and soil data. The developed model consists of 43 subbasins and 2270 hydrological response units. Sensitivity analysis was performed using the SWAT–CUP (SWAT Calibration and Uncertainty Programs) program and results showed that SCS runoff curve number as the most sensitive parameter. Model was calibrated for the period 1997–2001 and the performance in terms of Nash-Sutcliffe efficiency and coefficient of determination was 0.63 are 0.68, respectively. The simulated results will be used in future analysis to address pressing issues related to climate change and hydrological alterations due to hydropower developments in the Srepok River Basin.

Study Area

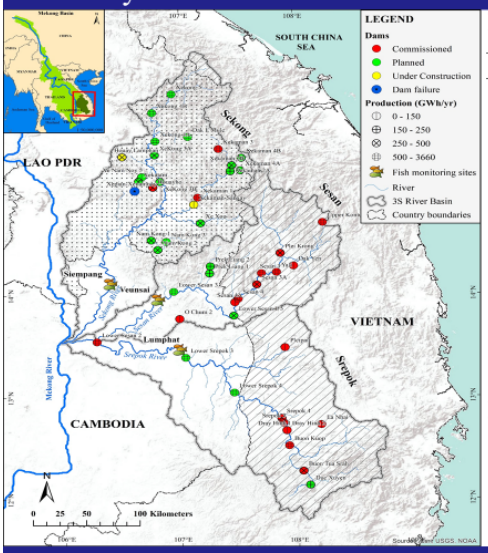

➢ **3S Basin**

– Only transboundary tributaries of the Mekong
– Sekong, Sesan and Srepok River Basin

- **Catchment area** - 78, 650 km² (10% of Mekong)
  Vietnam - 38%, Cambodia - 33%, Lao PRD – 29%
- **Elevation** - 80 m masl - 2040 m masl
- **Rainfall** - 1,500 mm - 3,000 mm
- **Temperature** – 19 ^{0}C - 36 ^{0}C
- **Mean annual flow** - 2,890 m^3/s
- **Rainy season** - May to November
- Fish species richness in the 3S River

	Sekong	Sesan	Srepok
Families	33	26	**33**
Species	213	133	**240**

➢ **Srepok River Basin**

- **Catchment area** - 30,940 km²
  Vietnam - 18,162 km², Cambodia - 12,780 km²
- **Elevation** - 140 m masl - 2,409 m masl
- **Rainfall** - 1,972 mm

Rainfall distribution in Srepok Basin

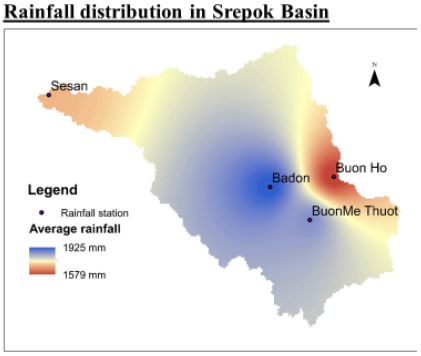

Minimum and maximum Temperature

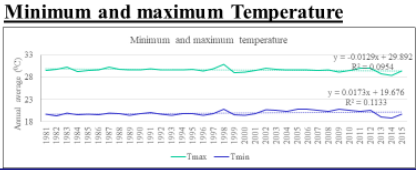

Methodology and data collection

SWAT: Soil & Water Assessment Tool
SWAT-CUP: SWAT Calibration and Uncertainty Program

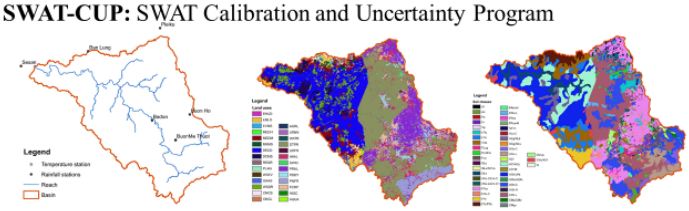

Rainfall stations: 6
Temperature station: 1

Land use classes: 28
Soil classes: 23
Mekong River Commission (MRC)

SWAT model development

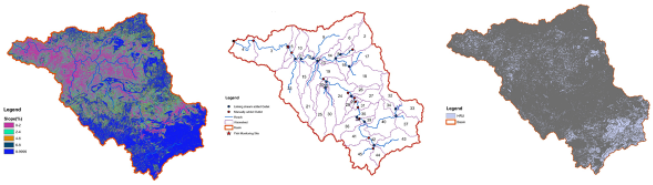

Slope: 5 classes
Sub basins: 45
HRU's: 2270

DEM: http://srtm.csi.cgiar.org

SWAT model calibration at Bandon station

Sensitivity analysis

Parameter	Definition	Min	Max	Fitted value
r__CN2.mgt	**SCS runoff curve number f**	35	98	-0.290
v__GW_DELAY.gw	**Groundwater delay (days)**	0	500	3.326
v__ALPHA_BF.gw	**Baseflow alpha factor (days)**	0	1	0.588
v__ESCO.hru	**Soil evaporation compensation factor**	0	1	0.970
v__CH_K2.rte	**Effective hydraulic conductivity in main channel alluvium**	-0.01	500	209.897

Water balance calculation

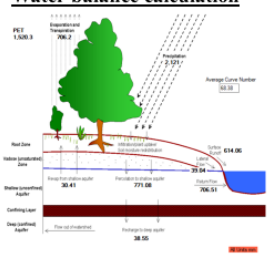

Inflow		Outflow	
Precipitation	2 121 mm	Evapotranspiration	706.20 mm
		Surface runoff	614.06 mm
		Lateral flow	39.04 mm
		Recharge	771.08 mm
Total	**2 121 mm**	**Total**	**2 130.28 mm**

Model performance indicator	Calibration (1997-2001)
Nash-Sutcliffe Efficiency (NSE)	0.63
Coefficient of Determination (R^2)	0.68
Percent Bias in volume (PBIAS)	-21.2
	Satisfactory performance

SWAT model validation

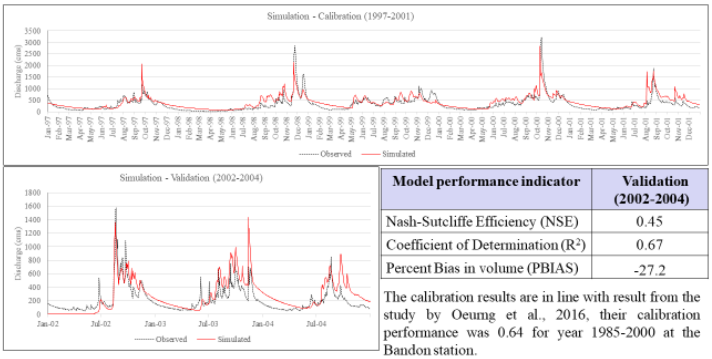

Model performance indicator	Validation (2002-2004)
Nash-Sutcliffe Efficiency (NSE)	0.45
Coefficient of Determination (R^2)	0.67
Percent Bias in volume (PBIAS)	-27.2

The calibration results are in line with result from the study by Oeurng et al., 2016, their calibration performance was 0.64 for year 1985-2000 at the Bandon station.

Conclusions

- The developed SWAT model captures the hydrological processes of the Srepok River Basin with a **satisfactory performance**

For further information, contact: shakthi.gunwardana01@gmail.com

Development of Framework to Assess the Groundwater Governance in Rapidly Urbanizing Cities

Saurav KC [a], Sangam Shrestha [a], Thi Phuoc Lai Nguyen [b], S. Mohanasundaram [a]
[a] Water Engineering and Management (WEM), [b] Regional and Rural Development Planning (RRDP)
Asian Institute of Technology (AIT),Thailand

The 9th International Joint Student Seminar
8-10 December 2020
Asian Institute of Technology (AIT), Thailand

Abstract

Groundwater, being a common-pool resource, and the source of one-third of all freshwater withdrawals for domestic, agricultural, and industrial sectors have been threatened due to its increased demand and exploitation. In addition to its vulnerability to availability and quality, the unfair access to the resource and its poor management has created challenges in urbanizing cities with increased possibilities for sectoral and right based conflicts. Thus, this study develops a framework for the diagnostic of the existing state of groundwater governance in rapidly urbanizing cities using an indicators-based approach. The framework comprises 4 dimensions (viz. technical; legal and institutional; cross-sectoral policy coordination; and operational) and 30 indicators addressing all the essential components of groundwater governance. Each indicator of the framework is rated using 2 variables (i) adequacy of provision and (ii) institutional capacity for implementation. The aggregation of all the elements of the framework provides a single quantitative value known as the Groundwater Governance Index (GGI). The GGI value signifies the existing state of groundwater governance which ranges from 0-3 where 0 represents the non-existence state of governance and 3 represents the optimal state of governance. The framework shall be useful for policy and decision-makers, managers, and related actors in visualizing the prevailing state of groundwater governance, understand the strengths, gaps, areas for improvement and develop strategies for strengthening groundwater governance and implementing effective operational management.

Overall Methodology

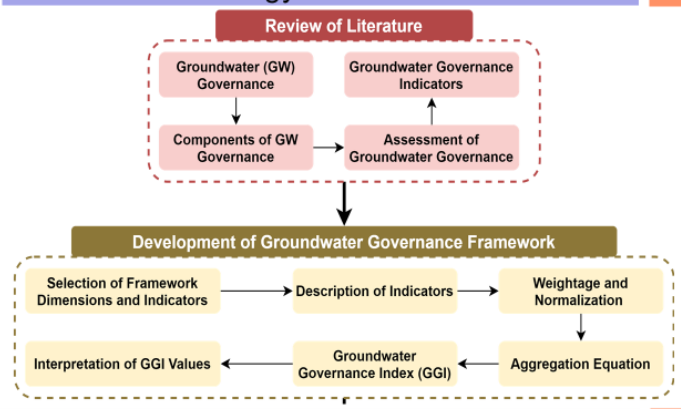

Aggregation of Elements

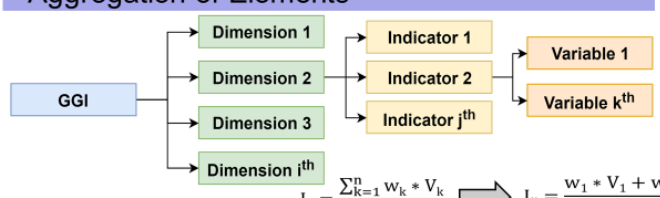

$$I_{ij} = \frac{\sum_{k=1}^{n} w_k * V_k}{\sum_{k=1}^{n} w_k} \Rightarrow I_{ij} = \frac{w_1 * V_1 + w_2 * V_2}{w_1 + w_2}$$

$$D_i = \frac{\sum_{j=1}^{n} w_j * I_{ij}}{\sum_{j=1}^{n} w_j} \Rightarrow D_i = \frac{w_1 * I_{i1} + w_2 * I_{i2} \dots\dots\dots + w_n * I_{in}}{w_1 + w_2 \dots\dots\dots w_n}$$

$$GGI = \frac{\sum_{i=1}^{n} w_i * D_i}{\sum_{i=1}^{n} w_i} \Rightarrow GGI = \frac{w_1 * D_1 + w_2 * D_2 + w_3 * D_3 + w_4 * D_4}{w_1 + w_2 + w_3 + w_4}$$

Where; GGI = Groundwater Governance Index; D = Dimension; I = Indicators; V = Variables; w = Weightage and i, j & k represents number of dimensions, number of indicators within in each dimensions and number of variables within each indicators respectively

Elements and Description of Framework

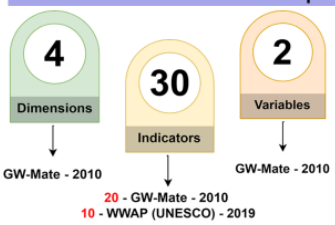

Measured in Relations to (Variables)

- Adequacy of existing governance provision
- Institutional capacity for their implementation

Rank/Rating	Level
0	Non-Existent
1	Incipient
2	Acceptable
3	Optimum

Dimension	S.N	Indicators
Technical	1	Existence of basic hydrogeological maps
	2	Groundwater body/aquifer delineation
	3	Groundwater-piezometric monitoring network
	4	Groundwater-pollution hazard assessment
	5	Availability of aquifer numerical management models
	6	Groundwater-quality monitoring network
	7	Availability of gender specific publications (guide) in Public Domain
Legal and Institutional	8	Waterwell drilling permits and groundwater use rights
	9	Instrument to reduce groundwater abstraction
	10	Instrument to prevent waterwell construction
	11	Sanction for illegal waterwell construction
	12	Groundwater abstraction and use charging
	13	Land-use control on potentially-polluting activities
	14	Levies on generation/discharge of potential pollutants
	15	Government agency as ground-water-resource guardian
	16	Community aquifer management organizations
	17	Gender responsive groundwater policies or legal frameworks
	18	Budget allocation for integrating gender concerns
	19	Gender inclusive groundwater management agencies (government)
	20	Customary land and water rights for indigenous groups or communities
	21	Agreements and commitments related to international human rights charters
Cross-Sector Policy Coordination	22	Coordination with agriculture development
	23	Groundwater-based urban/industrial planning
	24	Compensation for groundwater protection
	25	Sectoral coordination for sex disaggregated data
Operational	26	Transparency in groundwater services for all consumers
	27	Public participation in groundwater management
	28	Existence of groundwater-management action plan
	29	Inclusive participation in aquifer management organisations
	30	Gender sensitization training at government level

Interpretation of Results

Threshold	State of Governance	Description
0 - < 0.5	Non-Existent State of Groundwater Governance	The groundwater governance is at the non-existent state from a dimensional perspective. The area has no to highly insufficient provisions of technical resources, regulatory and legal outlines, policies for cross-sectoral coordination and operational plans. It faces several issues and conflicts due to the lack of institutional capacity for inclusive multi-stakeholder governance.
0.5 - < 1.5	Incipient State of Groundwater Governance	The groundwater governance is at the initial state from a dimensional perspective. The area has elementary provisions of technical resources, regulatory and legal outlines, policies for cross-sectoral coordination and operational plans. It faces some issues and conflicts due to the basic institutional capacity for inclusive multi-stakeholder governance.
1.5 - < 2.5	Acceptable State of Groundwater Governance	The groundwater governance is at a satisfactory state from a dimensional perspective. The area has fair provisions of technical resources, regulatory and legal outlines, policies for cross-sectoral coordination and operational plans. It faces very fewer issues and conflicts due to the decent institutional capacity for inclusive multi-stakeholder governance.
2.5 - ≤ 3	Optimum State of Groundwater Governance	The groundwater governance is at the most favorable state from a dimensional perspective. The area has adequate provisions of technical resources, regulatory and legal outlines, policies for cross-sectoral coordination and operational plans. It faces none to very little issues and conflicts due to the ample institutional capacity for inclusive multi-stakeholder governance.

Conclusion

- Groundwater governance framework for assessing the current state of groundwater governance in rapidly urbanizing cities was developed.
- The framework included 4 dimensions, 30 indicators and each indicators being rated in relation 2 variables.
- Groundwater Governance Index (GGI) was developed which ranges from 0 to 3, where 0 represents the non-existent state and 3 represents the optimal state of governance.

Note:
GW-MATE: Groundwater Management Advisory Team
WWAP: World Water Assessment Programme

For further information, contact: Saurav KC (er.saurav.kc@gmail.com)

A study of the difference between tunnel precast system and fully precast system for townhouse construction

Nussarin Sudrohman
Master degree student of Geotechnical and Earth Resources Engineering
School of Engineering and Technology, Asian Institute of Technology

abstract

The decision to buy a house for residence is affected by affordable price with high quality. That is become an important problem for the real estate business, especially townhouse business group. The townhouse is popular in the moderate-income group. Therefore, real estate developers must adapt for responding to the requirements. Nowadays, the fully precast system is applied instead the tunnel precast system. However, both systems have advantages and disadvantages. For this paper presents the difference between tunnel precast system and fully precast system for townhouse construction, studied on 3 factors, which are budget, construction time and quality control by comparing between the same living space with the similar type. As a result, it was found that the fully precast system used higher construction budgets but reduced the construction time, monitor process with quality control including. Moreover, reducing of the construction process has affected to the construction quality.

Introduction

Since townhouse construction techniques in Thailand have been developed, there are many alternative to constructions. So, constructors should recognize that the different techniques also have different advantages and disadvantages. Over the past year, tunnel technology and precast technology have been utilized to reach the construction requirements. Normally, for townhouse construction, three factors, which are budget, construction time and quality control, are considered. For this study, two construction techniques, which are tunnel precast and fully precast system, were compared by the same living space with the similar type.

Methodology

To learn about the differences between tunnel precast and fully precast system in terms of budget, construction time and quality control for townhouse construction, a townhouse block, which has 7 two-story house units with 81.51 m^2 area, was considered.

- For **budget**, bill of quantities (BOQ) and other expenses such as equipment and machine cost, and wage of labors and foreman were considered.
- **Construction time** for both construction systems were compared to find out the time difference and the works that may cause the delay time.
- For **quality control**, the number of inspection lists were compared.

Results

- **Budget**

The construction budgets were estimated from bill of quantities (BOQ) and other expenses as shown in table 1.

Table 1 Comparisons of budgets

Lists	Budget (Baht/ unit)		
	Tunnel precast	Fully precast	Difference*
1. Budget from BOQ	510,278	534,235	23,957
2. Other expenses			
• Mobile crane	4,000	-	4,000
• Formwork	7,143	-	7,143
• Labors	4,886	2,443	2,443
• Foreman	4,286	-	4,286
Total	**530,592**	**536,678**	**-6,086**

*Difference Budget = Tunnel precast budget – Fully precast budget

It presents that the tunnel precast townhouse requires a cheaper budget than fully precast townhouse for 6100 baht/ unit. Because it was cast in place and do not need to transport the prefabricated parts.

- **Construction time**

The construction time differences for a townhouse block of the two construction systems are shown in Gantt chart. It presents that the tunnel precast townhouse requires a longer time than fully precast townhouse for 5 days.

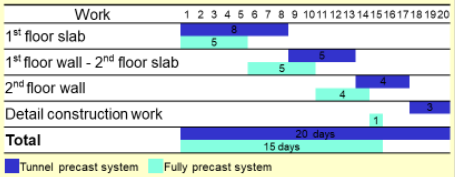

- **Quality control**

Compared to the inspection and quality control lists, the tunnel precast system has more items to check than the fully precast system. Because the 1st floor slabs and walls of a tunnel precast townhouse are cast in place, they must be inspected reinforcing steel, embedded materials and concrete pouring rate control. On the other hand, the slabs and walls of fully precast townhouse are prefabricated parts, which have been manufactured from the factory, and have precise sizes and shapes.

Fig. 1 Plan views of a 81.51 m^2 area townhouse unit

Conclusion

For this paper presents the difference between tunnel precast system and fully precast system for townhouse construction, studied on 3 factors, which are budget, construction time and quality control by comparing between the same living space with the similar type. As a result, it was found that the fully precast system used higher construction budgets but reduced the construction time, monitor process with quality control including. Moreover, reducing of the construction process has affected to the construction quality.

T-P Cheaper than Fully ⟫ 6100 ฿/ unit

T-P Slower than Fully ⟫ 5 days/ Block

T-P has more inspection items than Fully

Acknowledgement

This project was supported by Pruksa Real Estate Public Company Limited.

The 24th National Convention on Civil Engineering (NCCE 24)
Civil Engineer's Contribution to Thailand 4.0+
10-12 July 2019, Udonthani, Thailand

For further information, contact below.
Nussarin Sudrohman, TEL: +66877580913, E-mail: st120910@ait.asia
Download: https://thaince.org/wp-content/uploads/2019/ncce24.zip

Evaluation of Room Arrangements by Social and Spatial Network Analysis in Hospital Architecture

Jogo BOKU, Affliction, Republic of Korea, Master 2nd

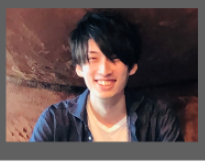

abstract

The purpose of this study is to clarify what factors are involved in designing the floor plans of modern hospital architecture. Modern hospitals consist of five major departments: Outpatient Dept., Diagnostic and Treatment Dept., Ward Dept., Management Dept. and Supply Dept. The hospital is a functional architecture consisting of a tree structure derived from these five departments.
This is also reflected in the plan of the building. In the initial stage, you design the architecture by considering these five departments as blocks and adjusting the examination of their area and layout.
This is called the block plan. Even though the hospital is a functional architecture, the quantitative rationale for them is unclear. This is because the block plan is planned on an empirical basis. Therefore, to quantitatively evaluate what components are essential for the block plan, we analyze and evaluate them from the following points of view using graph theory-based network analysis.(1) Based on the guideline of design, using the adjacency relationship between departments and rooms, which should be taken into account in any hospital, we express them as adjacency graphs and analyze the social network in the relationship between departments and rooms.(2) Based on the drawing of an actual hospital, the spatial network between departments and rooms is analyzed by using adjacent graphs.(3) Evaluate the arrangement of the rooms using the component values of eigenvectors belonging to the maximum eigenvalues of the adjacency matrix, called "convenient position-value".(4) A comparative analysis of the network graphs in (1) and (2), based on the convenient position-value in (3).By the above policy, we attempt to quantitatively evaluate the functional structure of hospital architecture. We quantitatively evaluate the functional structure of hospital architecture and present results that contribute to the optimization of future hospital planning.

Introduction

A hospital is a functional architecture, consisting of a tree structure subdivided around five departments. (Fig.1) In the initial stage, you design the architecture by considering these five departments as blocks and adjusting the examination of their area and layout. (Fig.2) This is called the block plan, and is a very time-consuming and complex task, like solving a puzzle. This study quantitatively evaluates and visualizes the relationship between this departmental arrangement and the rationale for the block plan that has been implemented empirically.

Fig.1 Hospital Structure

Fig.2 Block Plan

Methods

(1) Social Network

Based on “the Notes On Hospital Buildings”, the guideline, we create adjacency graphs from the description of rooms as "adjacent".

Fig.3 Notes On Hospital Buildings

(2) Spatial Network

Represents spatial connectivity in an actual hospital plan using adjacency graphs and adjacency matrix.

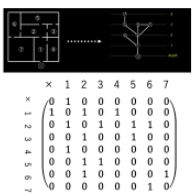

Fig.4 Adjacency Graph and Matrix

(3) Convenient Position-Value

We use a location evaluation index, “the convenient position-value”. It is found by calculating the component values of the eigenvector belonging to the largest eigenvalue of the adjacent matrix.

$$Ax = \lambda_{max}x \quad (1)$$

$$x_v = \frac{1}{\lambda_{max}} \sum_{u \in \delta(v)} x_u \quad (2)$$

A : the adjacent matrix
x : the eigenvector
λ_{max} : the largest eigenvalue
$\delta(v)$: the set of nodes to connect with node v
x_v : ingredient display of the (1) formula

Results

(1) Social Network

We visualize the closeness centrality of the social graph. It is mainly closeness-centered in the outpatient department, the medical department, and the rooms of the wards.

Fig.5 Social Graph Analysis

(2) Spatial Network

The actual hospital was based on the plan of Ohara General Hospital. Similarly, the closeness centrality showed higher values in areas such as elevator halls and corridors.

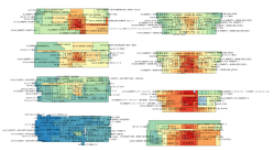

Fig.6 Ohara General Hospital Analysis

(3) Convenient Position-Value

We computed the distribution from the adjacency matrices obtained from (1) and (2) above by finding the convenient position-value.

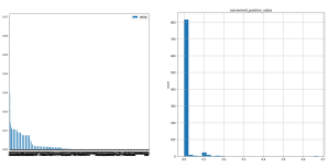

Fig.7 Distribution of the convenient position-value

Discussion

Comparing the closeness centrality of the social network in (1) and the spatial network in (2), we found that areas other than rooms such as corridors and cores, which were not mentioned in the guidelines, played an important bridging role.

In addition, the value of the convenient position-value in (3) is higher in the outpatient department and the diagnostic imaging department in both cases. This is a common feature with centrality analysis, and these sectors have a high potential for location.

So far we have combined all sectors for comparison, but in the future, it will be necessary to evaluate and analyze the locations according to the users.

Conclusion

The social network really reflected the tree structure, confirming the functional hierarchy of the hospital. The same characteristics were found in the graphs obtained from the actual hospital. The hospital is considered to be a building plan that has small and medium-sized departments and rooms that serve as hubs and are stacked in blocks.
In this block unit connection, there are rooms with a particularly high potential for location, and it is necessary to structure and design the elements to be considered around these rooms with high potential.

For further information, contact below.
Jogo BOKU, Yudai HONMA Lab, Yudai HONMA, TEL/FAX: +81-03-5452-6379 E-mail: jogo-boku@g.ecc.u-Tokyo.ac.jp
HP: http://www.honma-lab.iis.u-tokyo.ac.jp/

Computer – aided rock classification using python programming

Nartmongkhol Songserm[1]*(Presenter), Tanawoot Kongsung[1] and Ratchadakorn Chumkhiaoa[1]
[1]Graduated Students in Geotechnical & Earth resources Engineering, Asian Institute of Technology, Thailand,

ABSTRACT

Conventionally, people used the guideline instruction of rock classification to identify the rocks, but it might take a long time and make some confusion for people who are not familiar with it. Moreover, the use of the different criteria for rock identification can be misleading. This study aims to propose a computer-based classification for naming the rock identifications reducing human errors. The python coding was used to create a simple code for a visualization of the rock classification. Python is an open-source programming language and was designed to be highly extensible. Six main steps write the codes of the rock classification using python including 1) simplifying the workflow for rock visual classification, 2) identifying the required input data, 3) translating the workflow of the classification into the python code, 4) writing the python code, 5) testing the program, and 6) fixing the errors. The input data of rock type, texture, composition, and special characteristics as the variables were matched with the database. Then, the results display the identification of the rock types onto the screen. Finally, the study finding is very useful for fresh engineers and geologists, the computer-based classification provided a valuable technique to identify the rock type. In addition, the programming code of this study is useful to initiate a broad idea about the property identifications of the rock, the present study acts as a guide for future programming and code-developing of the rock classification and identification.

Objective

- To classify the rock sample by using Python code based on visual rock identification steps.

Scopes of Works

- Only basic or major names of rock that will be provided by using the program.
- No pre-fix name or special geological terms are included in this classification.
- The images using in this project are the rock that commonly found in geotechnical engineering works.
- The classification will be conducted in the way of showing questions and typing the answers.
- Using *PyCharm Integrated Development Environment* (IDE) for python programming.

Classification Criteria

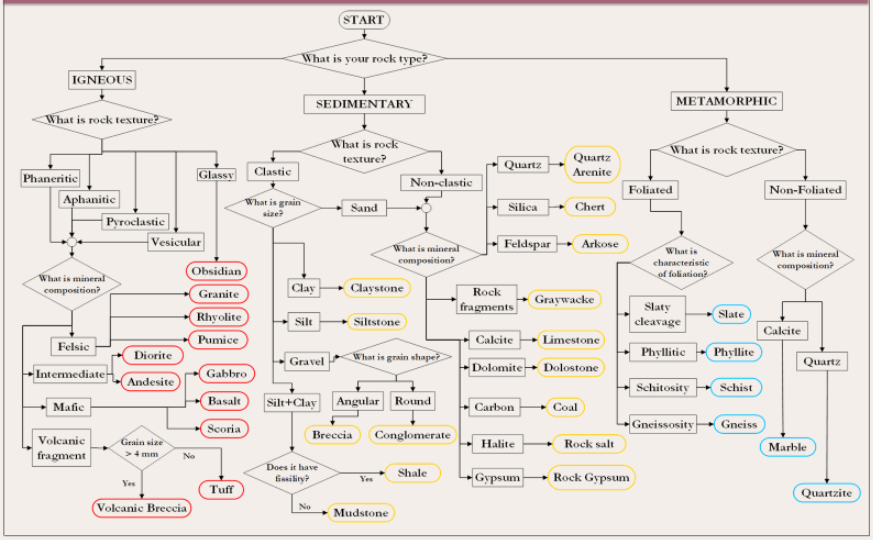

Methodology

- **Step 1** – Simplifying the workflow for rock visual classification.
- **Step 2** – Identifying the required input data;
- **Step 3** – Translating the workflow of the classification into the python code.
- **Step4** – Writing the python code.
- **Step 5** – Test running the program.
- **Step 6** – Debugging and Improving.

Results & Discussion

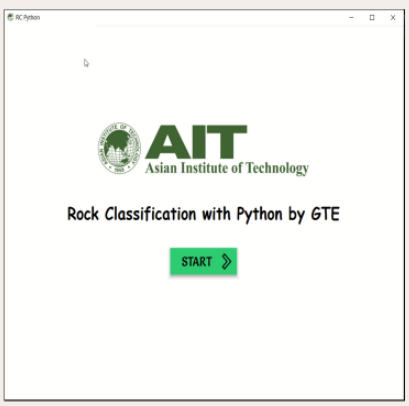

- There are some limitation such as restricted amount and types of rock image in the database, required knowledges about keywords or basic technical terms for answering, etc.
- For further development, some typical engineering properties should be included with the rock name.

Conclusions

- The program can classify the common rock name, and give a satisfactory result which may be useful for fresh engineers.
- It still has some limitation that should be improved further.
- This study acts as a guide for future code-developing of the rock classification

Acknowledgments

We thank Dr. Avirut Puttiwongrak for guidance on writing abstract for the presentation. We thank Dr. Geoff Chao for useful comment and discussion on the poster presentation. We thank Dr. Pham Huy Giao for useful comments and suggestions on python programming.

For further informati
Nartmongkhol Songs
E-mail: nartmongkho

Preliminary Analysis of Chiang Mai Earthquakes With Related To The Active Fault Zones of Thailand

Kornkanok Sangprasat[1], Avirut Puttiwongrak[2], and Passakorn Pananont[3]*

Abstract

Thailand consists of 16 active fault zones that almost active faults have located in the northern parts of Thailand where can trigger many earthquakes in northern Thailand. Previously, Mae Wang and Chom Thong districts, Chiang Mai, were not located in active fault zones and the earthquake was never recorded in these areas. However, these locations were subjected to record earthquakes frequently from 2016 to 2017. The purpose of this study is to collect and analyze earthquake data obtained from 20 seismic stations in Mae Wang and Chom Thong districts, Chiang Mai, during January 21, 2016 – February 7, 2017, using SEISAN for understanding the nature of these earthquake swarms. The result indicates that there were 120 earthquakes with magnitude (Ml) of 1.0-4.3 (26 earthquakes of Ml 1.0-1.4, 41 earthquakes of Ml 1.5-1.9, 36 earthquakes of Ml 2.0-2.4, 9 earthquakes of Ml 2.5-2.9, and 8 earthquakes of Ml greater than 3.0). The majority of these earthquakes were located in Mae Win subdistrict, Mae Wang District, Chiang Mai, while the biggest earthquake of Ml 4.3 located at latitude 18.59 ºN and longitude 98.55 ºE at 2.7 km depth. The locations of these earthquakes indicate that the distributions of earthquakes are clustered near the vicinity of the southwest of the Mae Tha Fault Zone. However, the relationship between these earthquakes and the active fault zones is supposed to consider carefully in further research, the site investigation is recommended to carry out in these locations for investigating the fault-related to the earthquake in the active zones.

Objective

The objectives of the study are collecting and analyzing seismic waveforms produced by recent earthquakes and defining their epicenters in Chom Thong and Mae Wang Districts, Chiang Mai Province.

Study Area

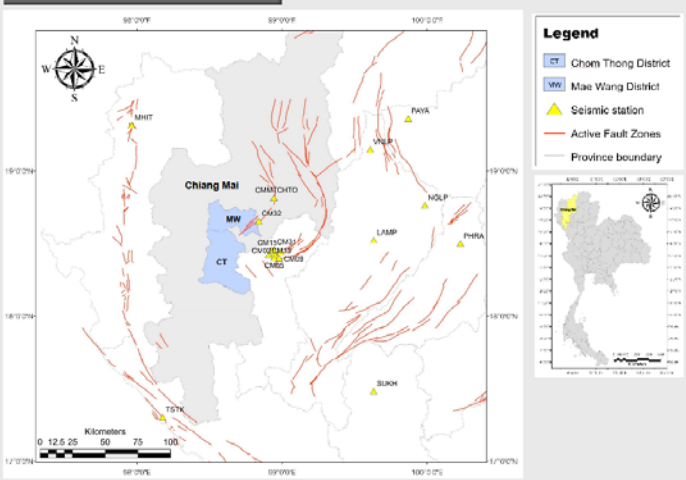

Methodology

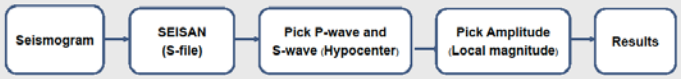

Waveforms collected from 20 seismic station is used to relocate epicenters by SEISAN. Moreover, the hypocenters of the earthquakes are calculated using the modified version of HYPOCENTER (Lienert et al., 1986; Lienert, 1991; Lienert and Havskov, 1995). The magnitude of the earthquake was computed by using a picked maximum amplitude on the Z-channel of the Wood-Anderson seismograph (Richter, C.F., 1935) using the updated seismic velocity model of Northern Thailand (TRF, 2014).

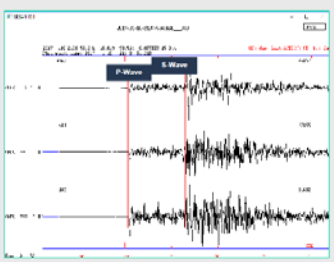

Result

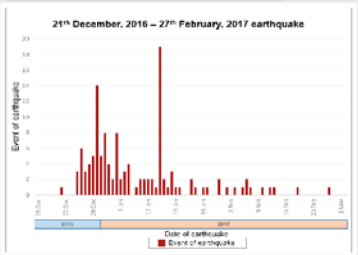

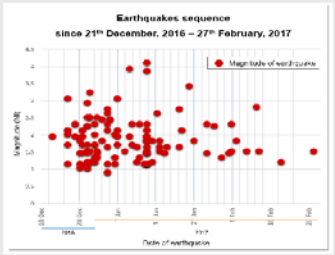

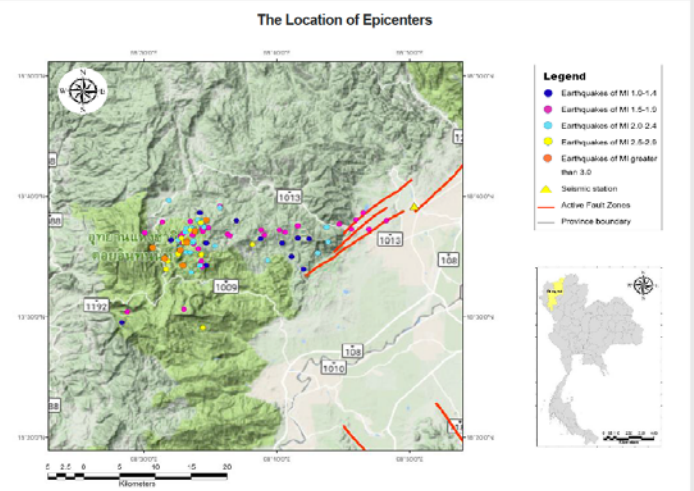

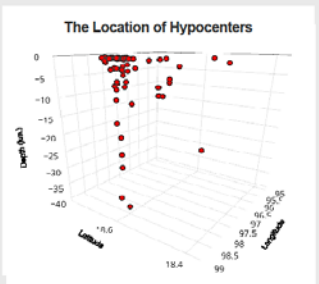

120 seismic events have been located using the IASP91 velocity model. Upper figure demonstrate amount and magnitude of earthquakes on each day, respectively. The results suggest that the magnitude (Ml) of these earthquakes ranges from 1 to 4.3. The distribution of relocated earthquakes which are between latitude 18.65˚ N to 18.67˚ N and longitude 98.46˚ E to 98.81˚ E.

Conclusion and Discussion

A sudden increase in recent earthquake activities has to lead to this more detailed study. The locations of these earthquakes suggest that the distributions of the earthquakes are clustered near the vicinity of the southwest of the Mae Tha Fault Zone. However, those detected earthquakes are small (Ml 1.0 to 4.3). They could be considered to be background earthquakes and not related to fault's activity. More extensive seismic wave data is required to examine the relationship between this earthquake swarm and the known fault location.

References

Department of Mineral Resources. 2016. **Active Fault Zones in Thailand.** Available Source: http://www.dmr.go.th/main.php?filename=Active _FAULTS_THAI, 15, January 2017.

L. OttemÖller, P. Voss and J. Havskov. 2016. **SEISAN EARTHQUAKE ANALYSIS SOFTWARE FOR WINDOWS, SOLARIS, LINUX and MACOSX.** Available Source: http://seis.geus.net/software/seisan/seisan.html, 6, January 2017

Acknowledgement

Thank you to Faculty of Science and Department of Earth Science for undergraduate research fund and seismic data from he Thai Meteorological Department. Especially, Asst. Prof. Dr. Passakorn Pananont and Asst. Prof. Dr. Avirut Puttiwongrak who provided the suggestion about this work and participants who supporting.

Influential Factors Affecting Travelers' Mode Choice Behavior on Mass Transit in Bangkok, Thailand

Phattarasuda Witchayaphong [1,*], Surachet Pravinvongvuth [1], Kunnawee Kanitpong [1], Kazushi Sano [2] and Suksun Horpibulsuk [3]

[1] Transportation Engineering, School of Engineering and Technology, Asian Institute of Technology, Bangkok 12120, Thailand
[2] Department of Civil and Environmental Engineering, Nagaoka University of Technology, Niigata 940-2188, Japan
[3] School of Civil Engineering, and Center of Excellence in Innovation for Sustainable Infrastructure Development, Suranaree University of Technology, Nakhon Ratchasima 30000, Thailand

ABSTRACT

Increasing use of single or fewer occupant vehicles has increased traffic congestion and transport-related emissions. Public transport as mass transit options are increasingly being encouraged amongst travelers to use, as this is an influential strategy to improve the transport network performance. This paper presents a study based on a revealed preference survey conducted on a random sample of 4,467 respondents to understand the influential factors affecting the users' choice of mass transit in Bangkok, Thailand. This study identified an inversely proportional relationship of socio-economic and spatial attributes on public transport mode choice. The binary logit model was employed to compare the utility of private vehicles and mass transit modes. The results showed that gender, age, average income, auto ownership, total travel cost in private transport, total travel time in public transport and distance range from home to mass transit station were the factors that influenced travelers' mode choice behavior. Moreover, to ascertain the effects of explanatory variables which influence the likelihood of Thai travelers, another binary logit model analysis was utilized by the four distance ranges condition. The studied results showed that there were few significant differences in the propensity to use mass transit. Due to the longer distance of the station, total travel time in public transport was not affected by the Thai travellers mode choice. This research will aid transport authorities and planners to gain knowledge on the impact of socio-economic and spatial behavior of public transport users on their mode choice, resulting in the development in sustainable transport in Bangkok, Thailand.

Problem Statement

Bangkok Traffic Congestion…
World rank # 2, Asian Rank # 1
Ref: *https://www.tomtom.com/en_gb/trafficindex/* ***Access Dated:*** *11/26/17*

How to balance…
"Private Cars" VS "Public Transportation"

Promote TH citizens…
"MODE SHIFT" and beneficial to the Policymakers and transport authorities

Research procedure

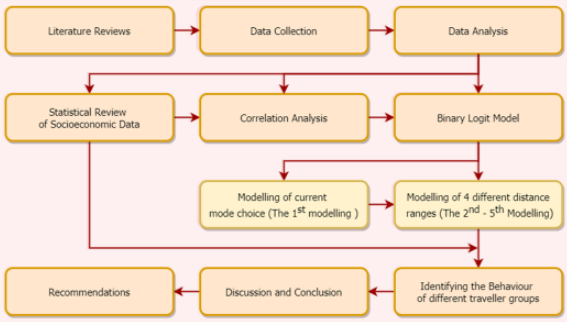

Study area in Bangkok (2 Main Mass Transits)

Legend:
4 distance ranges, which are indicated by circular shape are:
○ 0 – 400 m ○ 400 – 1,000 m ○ 1,000 – 10,000 m ** >10 km

Estimation results using binary logistics models (1st model)

	Variable Code	B	S.E.	Sig.	Exp(B)	95% C.I. Lower	95% C.I. Upper
Gender	G	0.381	0.067	0.000 **	1.463	1.282	1.670
Age (Range)	Age	−0.395	0.034	0.000 **	0.673	0.630	0.720
Average Individual Income	INC	−0.638	0.055	0.000 **	0.528	0.474	0.588
Household car ownership	Car	−0.675	0.061	0.000 **	0.509	0.451	0.574
Travel Cost of Private Vehicle	TC_{PRI}	0.009	0.001	0.000 **	1.009	1.007	1.011
Total travel time of Mass Transit	TT_{MT}	−0.004	0.002	0.022 *	0.996	0.992	0.999
Distance Range	$Dist_{Range}$	−0.228	0.031	0.000 **	0.796	0.749	0.847
Constant		2.012	0.198	0.000 **	7.478		
-2LL							5,207.479
Model chi-square							863.609
Cox & Snell R Square							0.176
Nagelkerke R Square							0.237
Hosmer and Lemeshow Chi-square							14.686
Number of observations							4,467

** significant at 1% level; * significant at 5% level.

$$U_{PUB} = 2.025 + (0.381 \times G) - (0.395 \times Age) - (0.638 \times INC) - (0.675 \times Car) + (0.009 \times TC_{PRI}) - (0.004 \times TT_{MassTransit}) - (0.228 \times Dist_{Range})$$

Summary model for each distance range (2nd – 5th Model)

	Dist. Range 1 (2nd Model) B	Dist. Range 1 (2nd Model) Sig.	Dist. Range 2 (3rd Model) B	Dist. Range 2 (3rd Model) Sig.	Dist. Range 3 (4th Model) B	Dist. Range 3 (4th Model) Sig.	Dist. Range 4 (5th Model) B	Dist. Range 4 (5th Model) Sig.
Gender	0.363	0.014 *	0.446	0.001 **	0.449	0.000 **	0.282	0.046 *
Age (Range)	−0.274	0.000 **	−0.352	0.000 **	−0.353	0.000 **	−0.606	0.000 **
Average Individual Income	−0.447	0.000 **	−0.681	0.000 **	−0.818	0.000 **	−0.644	0.000 **
Household car ownership	−0.736	0.000 **	−1.150	0.000 **	−0.460	0.000 **	−0.519	0.000 **
Travel Cost of Private Vehicle	0.007	0.000 **	0.016	0.000 **	0.008	0.000 **	0.008	0.000 **
Total travel time of Mass Transit	−0.008	0.045 *	−0.017	0.000 **	0.002	0.589	−0.001	0.730
Constant	1.322	0.001 **	1.760	0.000 **	1.321	0.000 **	1.545	0.000 **
-2LL		1081.662		1213.285		1600.169		1242.475
Model chi-square		138.236		241.168		214.919		226.543
Cox & Snell R Square		0.145		0.205		0.15		0.171
Nagelkerke R Square		0.194		0.273		0.201		0.243
Hosmer and Lemeshow Chi-square		13.881		6.371		11.921		12.571
Number of observations		880		1054		1324		1209

** significant at 1% level; * significant at 5% level.

Conclusion

- The influential factors affecting Thai travelers' mode choice behavior on mass transit was gender, age, average income, auto ownership, total travel cost in private transport, total travel time in public transport and distance range from home to mass transit station.
- Transport factors (Travel time and Travel cost) were considered less important towards the location and travel choice behavior.
- This indicated that householders who resided within 1 km distance to the public transport station, when given a choice, were less likely to commute even though the travel cost and time of public transport could be reduced.

Open Access Full-Text: https://www.mdpi.com/2071-1050/12/22/9522

Correspondent Author: Phattarasuda Witchayaphong (PhD Candidate), Transportation Engineering (TRE), School of Engineering and Technology (SET), Asian Institute of Technology (AIT), THAILAND. E-mail: p.Witchayaphong@gmail.com

Evaluation of crack-bridging strength degradation in SFRC structural beams under flexural fatigue

Mohamed ADEL, Post-doc Researcher, Egyptian

ABSTRACT: In this study, the degradation in crack-bridging strength of SFRC structural beams with 1.5% by volume of hooked-end steel fibers under different flexural fatigue stress levels is evaluated over the fatigue life using an inverse analysis method. The experimental flexural response is monitored during fatigue loading and compared with the calculated one from the section analysis calculations through the execution of the inverse analysis method. Based on the results, the crack-bridging strength is shown to degrade gradually at different flexural fatigue stress levels over the fatigue life. Further, the crack-bridging strength was degraded with a constant rate regarding the evolution of maximum rebar strain for all fatigue stress levels.

Background

Steel fiber reinforced concrete (SFRC) is a composite material reinforced with discrete, uniformly distributed, and randomly oriented steel fibers for bridging cracks. Therefore, SFRC has higher ductility, fracture energy, flexural strength, and durability.

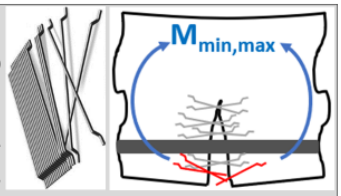

However, the crack-bridging strength induced by steel fibers of SFRC is continuously degrading as the loss mechanism of the bond strength at the fiber-matrix interface over the fatigue life. This leads to an increase in rebar strain levels and eventually shortens the fatigue life with a rupture failure of rebar of SFRC structural beams.

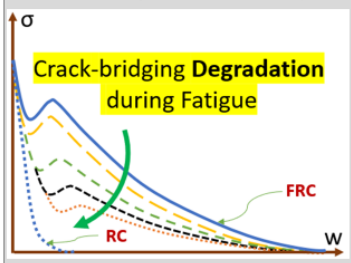

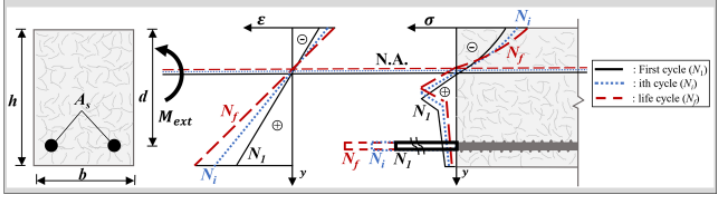

Inverse Analysis Method

The inverse analysis method aims for the derivation of the crack-bridging strength induced by double hooked-end steel fibers for SFRC beams under flexural cyclic loading. The inverse procedure was carried out based on the direct sectional analysis calculations over the fatigue life and limited by the experimentally measured response data of the tested SFRC beam.

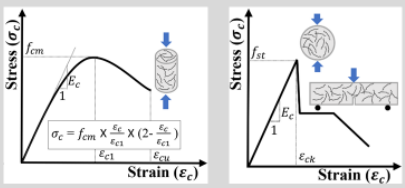

Constitutive laws of Concrete

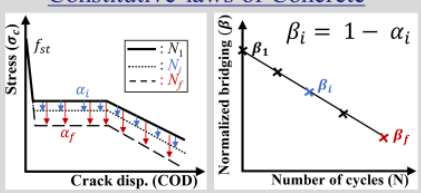

Crack-bridging strength degradation

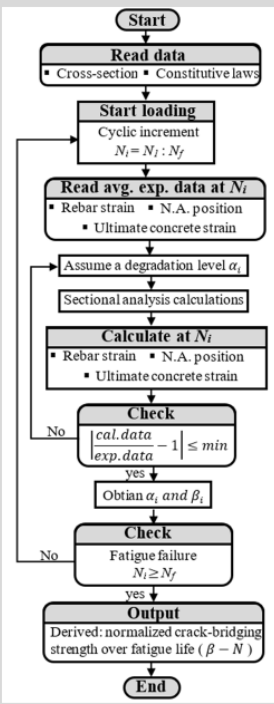

Experimental Program

Six structural-scale beams reinforced with conventional rebars (2D16) and made of normal and SRF concrete were tested under four-point flexural cyclic loading. The beams were designed with a dimension of 150 x 200 x 2000 mm and effective depth (d) of 170 mm, with a constant moment region of 300 mm.

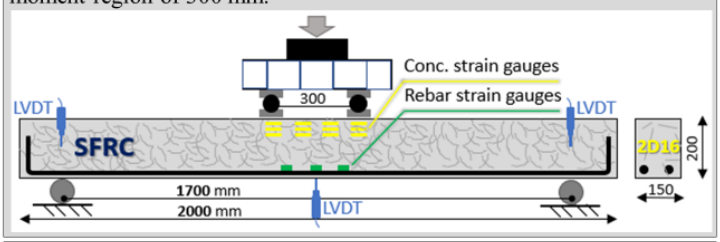

Discussion and Conclusion

- The higher evolution rate for experimental rebar strain of SFRC than NC structural beams confirmed the degradation of crack-bridging strength.

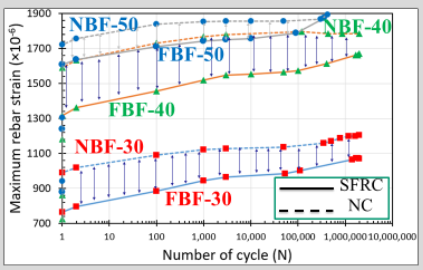

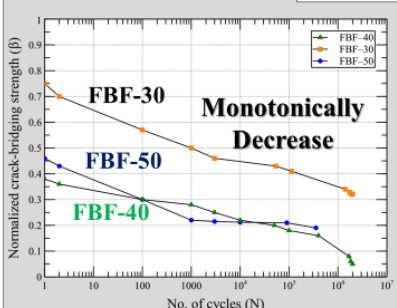

- The inverse analysis method successfully evaluates the degradation process of the crack-bridging strength based on sectional analysis calculations over fatigue life.

- The crack-bridging strength monotonically degraded over fatigue life and with a constant rate regarding the evolution of maximum rebar strain for all fatigue stress levels

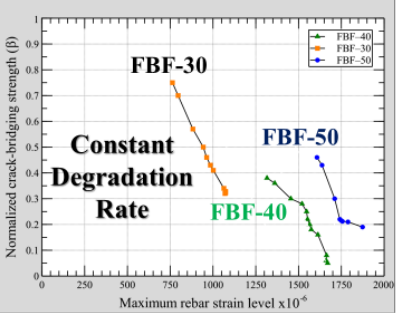

For further information, contact below.

Mohamed ADEL, Ph.D.

Kohei Nagai Lab, #Be-404. Institute of Industrial Science.

TEL: +81-3-5452-6655,

E-mail: adel@iis.u-tokyo.ac.jp

FAX: +81-3-5452-6395

HP: http://nagai.iis.u-tokyo.ac.jp/

Formation and Transformation of Informal Settlements from Historical Viewpoint in Yangon, Myanmar

Nyi Linn Maung, The University of Tokyo, Myanmar, M2 Student

Introduction

According to UN-Habitat, there are 432 informal settlements in Yangon nowadays, and most of them are the results of rural to urban migration due to economic development, disasters, and uncertain livelihoods in rural areas. However, it must be noted that these informal settlements are not simply the results of rural-urban migration, which is also related to profound economic policies adopted by successive governments after colonial government, which has its own roots in colonial city planning and economic legends. Therefore, the beginning of urban informality is worth to be examined to understand current problems.

Main Problem

There is a pressing need to understand the impacts of colonial city planning on indigenous race, Burmese, and the birth of urban poverty and urban informality to understand the persistence of this colonial legacy on later periods after Independence was granted.

Economic Aspects

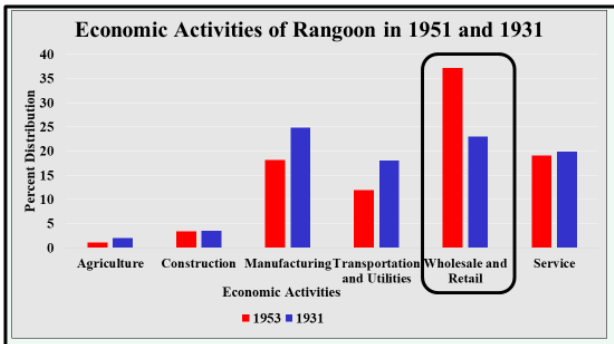

Major Economic Activity in Rangoon is Wholesale and Retail (Over 35%) , that is it is mainly consumer-service center without any substantial industrialization and in turn without substantial employment, manufacturing is negligible because of little contribution (Durable Goods – 20%) and (Non-Durable Goods – 63.3%)

City Planning in Dual Structure

- European were around cantonment, Indian were in proper town, and Burmese were in suburban without planning
- Since 1881, the city was changed in demographics into foreign city due to Indian immigration
- Burmese were excluded in planning and activities and modernism

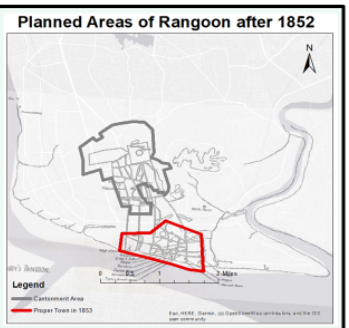

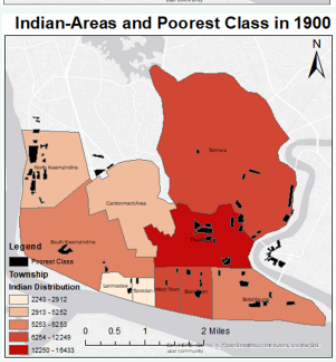

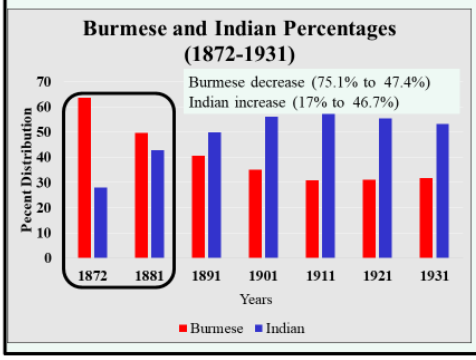

Housing Conditions

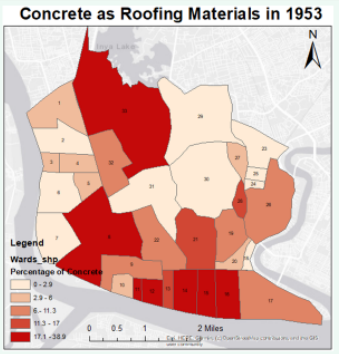

Household Size
- Central core – Average 4.8 persons per household

Tenure Status
- Rented – 81.5%
- Owned – 18.5%

% of Housings more than one story
- Central core – 38.2%

- The use of concrete as roof materials was prevalent in central core area and European areas, whereas Burmese used Bamboo or Thatch as roof materials, that is, rural characteristics
- Although the central core is in better condition by means of constructing materials, the area is extremely overcrowding

Occupation and Race Groups

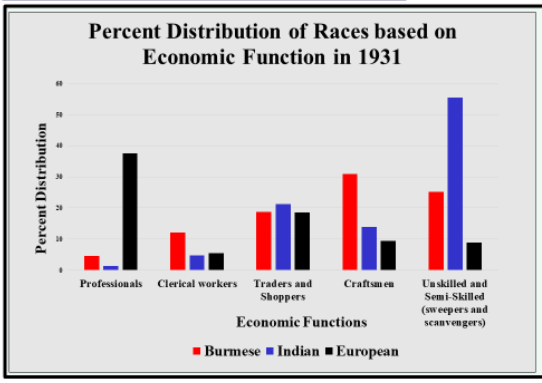

- Europeans in Professional-sectors
- Indians as skilled and unskilled labors
- Burmese in craftsmen-sectors, not related to modern activities

Conclusion

- European areas were restricted from central and suburban areas
- No incentives for private enterprises to provide substantial housings because Rangoon was not industrialized
- Burmese were racially excluded in terms of both employment and city planning
- Thus, historical development of Rangoon must be understood as an administrative city which has grown through tertiary low wage industries, sub-standard housings, people of rural-oriented abilities

For further information, contact below.
Nyi Linn Maung, River and Environmental Engineering Lab, TEL: +81-90-3577-6329, E-mail: nyilinnmaung@hydra.t.u-tokyo.ac.jp

Investigation of local bond behavior between corroded reinforcement and uncracked concrete using DIC

Kumar Avadh, Nagai Lab, Indian, D3

Abstract: This study proposes a new experimental scheme to directly observe and record the changes in local bond phenomenon due to change of shape of reinforcement after corrosion. The reinforcement was first corroded and then re-casted into a new specimen with an observation window. This specimen was subjected uniaxial tensile and bond interaction at interface is recorded simultaneous to application of load. Digital Image Correlation technique was then used to extract information regarding local crack opening and reinforcement slip behavior.

1. Background – Bond after Corrosion

Corrosion of reinforcement is major durability problem affecting structures worldwide. The steel damage and concrete damage modify reinforcement concrete interaction and degrades bond.

Steel Damage

Uncorroded Corroded

Steel Damage includes reduction in cross section, change in shape of ribs and addition of corrosion product layer

Concrete Damage

Cracking and spalling

Corrosion products induce expansive pressure which causes cover cracking

It is necessary to separate the influence of these damages on local bond interaction. A thorough understanding of bond phenomenon requires direct observation of real interaction and determination of local changes in stresses.

2. New Experimental Scheme

Accelerated Corrosion

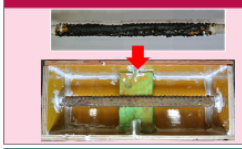

Remove corroded rebar and recast

Axial Tensile Loading

The reinforcement was first corroded using impressed current technique and then re-casted into a new specimen with 80 mm wide observation window in the center. Uniaxial test was then performed, and the local interaction was recorded through the window using a high-resolution camera.

The effect of concrete damage on bond was eliminated by recasting the corroded reinforcement.

3. Digital Image Correlation Analysis and Results

The recorded video was analysed using DIC technique. Changes in local stress conditions due to corrosion can be seen.

Strain Maps

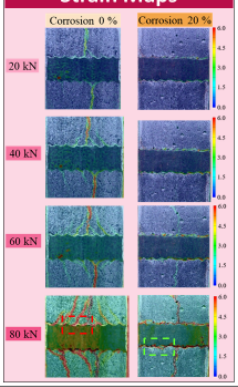

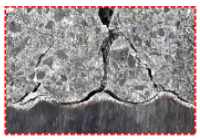

Angular Cracks

Slipping Failure

The strain maps shows clear changes in local stress conditions due reduction of rib height. Uncorroded specimen shows internal angular cracks indicating mechanical failure. In Corroded case, high strain is observed at the interface and the specimen failed primarily due to slipping.

4. Load-Slip and Opening-Sliding Relationships

DIC can be used to measure very local and small deformations.

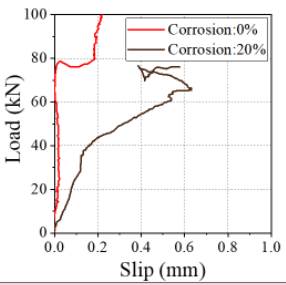

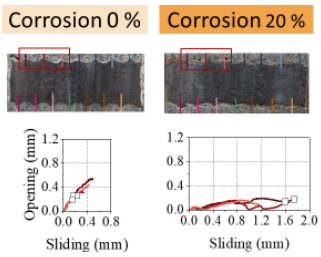

The load-slip behaviour computed using DIC showed that the stiffness decreases and slipping increases with increase in corrosion

The open-slide relation at the tip of ribs show that as the rib height reduces, the magnitude of crack opening reduces significantly and sliding of reinforcement increases.

Conclusion:

1. The strain distribution obtained using DIC clearly shows changes in local stress condition due to change in reinforcement rib height and shape.
2. The load slip curve shows decrease in stiffness and increase in sliding with increase in corrosion
3. The open-slide relations clearly show that as the rib height reduces, the crack opening reduces and sliding significantly increases.

For further information, contact below/本研究に関する担当者
Kumar Avadh, Nagai Lab, TEL: +81-3-5452-6437, FAX: +81-3-5452-6438
E-mail: kavadh@iis.u-Tokyo.ac.jp, HP: https://www.nagai.iis.u-tokyo.ac.jp/research.html

Development of Real-time Displacement Measurement Using Sampling Moiré Method in a Single Board Computer (a SBC)

Srikulnath Nilnoree* , Punchet Thammarak **

** Master student in Structural Engineering, Asian Institute of Technology (AIT), T*

*** Lecturer in Structural Engineering, Asian Institute of Technology (AIT), Thai*

Abstract

This poster presents the accuracy of displacement measurement based the real-time digital image processing by using sampling moiré method. The proposed system consists of a single board computer (Raspberry pi 3 Model B+ ; RPi) with Raspberry pi HQ camera and commercial lens. The sampling moiré method was written as a piece of code using Python 3 and embedded in RPi. The Raspberry pi HQ camera was used to capture digital images of a 2-D grating which was attached on the moving stage. In this study, the experiments were conducted under controlled conditions such as vibration control, lighting control and temperature control. The in plane displacement was successfully detected and reported by this proposed system. The results showed that the accuracy of the proposed system can achieve 1/100 of the grating pitch where the grating pitch was greater than 10 pixels and the sampling pitch was identical to its grating pitch. Moreover, this system also provided the compensation of misalignment between the camera and grating.

Background

Intensity of Digital image : Grayscale image

$$I(i) = I_a(i)cos[\emptyset(i)] + I_b(i) = I_a(i)cos\left[\emptyset_0 + 2\pi\frac{i}{P}\right] + I_b(i)$$

i = Direction of pixel array

P = Grating pitch (pixel)

$I(i)$ = Recorded intensity of the grating

$I_a(i)$ = The amplitude of the grating intensity

$I_b(i)$ = The background intensity in the image

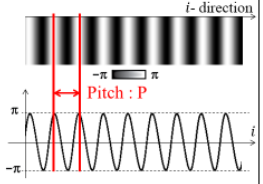

Fig. 1 Fringe pattern

Sampling Moiré Method

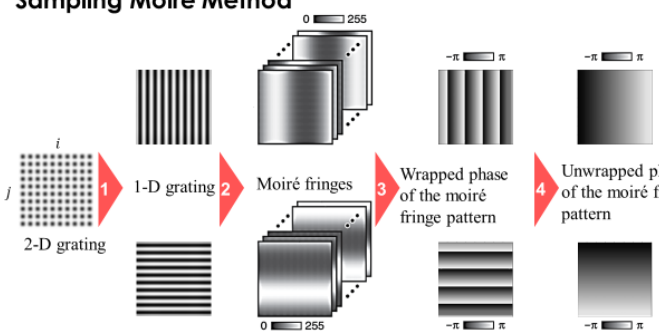

Fig. 2 Phase Shifting Diagram : 1. Low Pass Filter (LPF), 2. Phase shifting, 3. Wrapped phase distribution, 4. Unwrapped phase distribution

Displacement Calculation

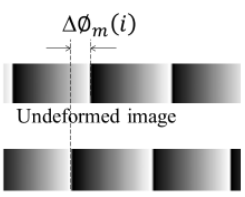

$$\delta(i) = p\frac{\Delta\emptyset_m}{2\pi} = p\frac{\Delta\emptyset}{2\pi}$$

$\delta(i)$ = Displacement of pixel (i)

p = Grating pitch (mm)

$\Delta\emptyset_m$ = Phase difference of the moiré fringe

$\Delta\emptyset$ = Phase difference of the moiré fringe

Fig. 3 Phase Difference

Results and Discussion

Distance	Conditions					Results		
	Grating (mm)	Spatial Resolution	Grating (pixel)	Sampling (pixel)	Misalignment angle	R-squared	RMSE (mm)	Frequency of Data (Hz)
2m	10 mm	360p	10 pixels	8 pixels	0 degree	0.99973	0.103	1.848
		360p			1 degree	0.99977	0.094	1.793
		360p			3 degree	0.99991	0.057	1.91
		360p			5 degree	0.99987	0.071	1.841
		360p		10 pixels	0 degree	0.99999	0.02	1.695
		360p			1 degree	0.99999	0.02	1.686
		360p			3 degree	0.99999	0.022	1.807
		360p			5 degree	0.99997	0.036	1.849
	20 mm	360p	20 pixels	18 pixels	0 degree	0.99997	0.064	0.97
		360p			1 degree	0.99995	0.09	1.039
		360p			3 degree	0.99997	0.073	0.914
		360p			5 degree	0.99996	0.075	0.911
5m	10 mm	360p	4 pixels	4 pixels	0 degree	0.99962	0.121	5.894
		360p			1 degree	0.99983	0.081	6.092
		360p			3 degree	0.99924	0.173	5.979
		360p			5 degree	0.99998	0.029	6.041
		720p	10 pixels	10 pixels	0 degree	0.99997	0.033	1.328
	20 mm	360p	8 pixels	8 pixels	0 degree	0.99997	0.064	3.284
		360p			1 degree	0.99999	0.047	3.613
		360p			3 degree	0.99995	0.084	3.536
		360p			5 degree	0.99982	0.164	3.675

Sampling pitch T=8 pixels vs T=10 pixels where P=10 pixels

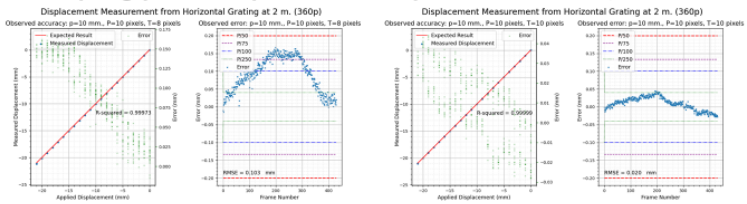

- The error decreases when sampling pitch (T) = grating pitch(P)

Camera Resolution 360p (P=T=4 pixels) **vs 720p** (P=T=10 pixels)

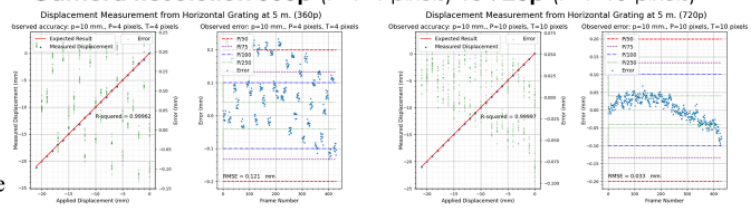

- Increasing the grating pitch can reduce the error.

Experimental Setup

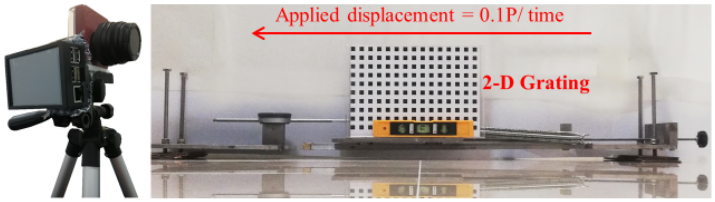

Fig. 4 Raspberry pi with 3.5 inch LCD connected to Raspberry pi HQ camera (left), Linear moving stage (right)

Conclusions

- Under controlled environment, the error of real-time displacement measurement using sampling moiré method is lower than p/100 (or less than 0.1 millimeters).
- The data frequency depends on the number of sampling pitch. To maintain the accuracy of the measurement, however, the sampling pitch and grating pitch should be identical.
- The uncontrolled conditions should be considered.

For further information, please contact : Punchet Thammarak, Research advisor, TEL: +66 81 930 5115, E-mail: punchet@ait.asia

ESTIMATION OF INTERNAL CORROSION LEVELS FROM SURFACE CRACKS OF CONCRETE USING MODEL PREDICTIVE CONTROL IN 3D RBSM

VIKAS SINGH KUNTAL, 特任研究員 NAGAI LAB IIS, INDIAN

ABSTRACT: Corrosion of the bars in concrete structures is one of the major maintenance problems. Effective maintenance requires the evaluation of residual performance based on estimates of spatially nonuniform levels of corrosion. The authors have developed a simulation system for estimating the levels of internal corrosion along the reinforcing bar length from surface crack information. This innovative system is produced by integrating the technique of Model Predictive Control (MPC) with Rigid-Body Spring Models (RBSM) of corrosion-induced cracking at the concrete mesoscale. The applicability of the system is verified crack data collected from in-house laboratory testing. In the laboratory testing, corrosion levels were quantified by 3D scanning of the extracted reinforcing bars. The simulation results agree with the corrosion measurements, demonstrating the potential of the MPCRBSM system for predicting the corrosion distribution along reinforcing bars using surface crack data.

BACKGROUND

Surface Observation Technology:

Image Capturing

Crack detection using AI

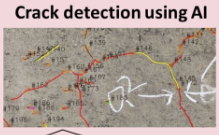

Precise surface info

Accurate value

Developed technology for precise surface observation

Precise surface crack info

Local Corrosion & Distribution

Precise corrosion is important.

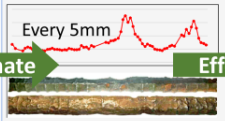

Estimate

Effect

Spalling Risk & Residual Capacity

OBJECTIVE AND SIMULATION BY 3D RBSM

3D analysis	Mesoscale analysis	Discrete analysis
Damage occurs in 3 Dimensions	Crack occurs at mesoscale	To predict the crack propagation and location

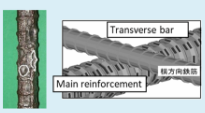

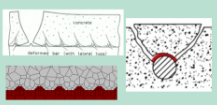

My Objective

Output

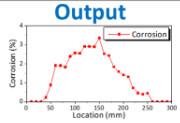

Corrosion distribution

Estimate by Simulation

Input

Precise Surface Crack

METHODOLOGY – Model Predictive Control

At each cross section (every 10 mm)

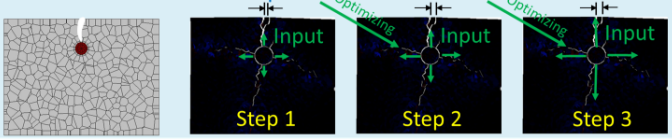

Optimizing equation

$$\Delta\varepsilon_{i+1} = \left(w^{t}_{i+1} - w^{s}_{i}\right) \times \left(\frac{\Delta\varepsilon_{i}}{w^{s}_{i} - w^{s}_{i-1}}\right)$$

(w^{t}_{i+1}: Target, w^{s}_{i}: Output)

$\Delta\varepsilon_i$, $\Delta\varepsilon_{i+1}$ - Incremental expansion at steps i and i+1, respectively.
w^{t}_{i+1} - Target crack width at step i+1.
w^{s}_{i-1} , w^{s}_{i} - Output surface crack width at steps i-1 and i, respectively

SIMULATION RESULS

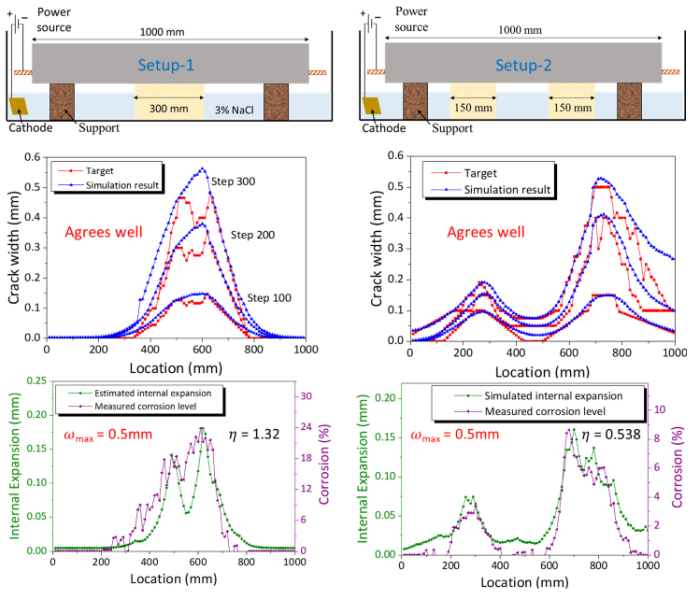

SURFACE CRACK COMPARISION

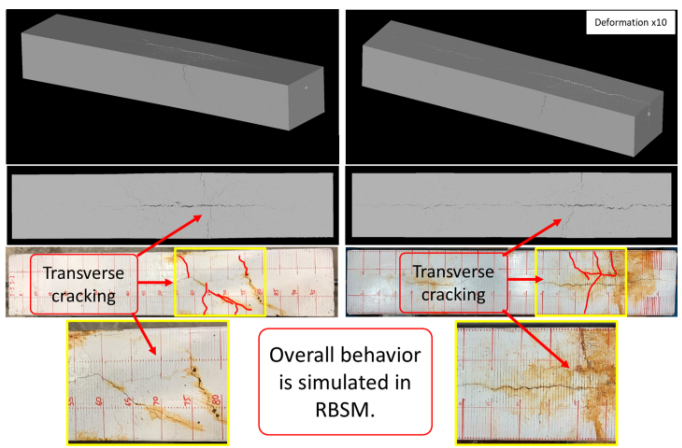

FRAMEWORK OF FULL SYSTEM

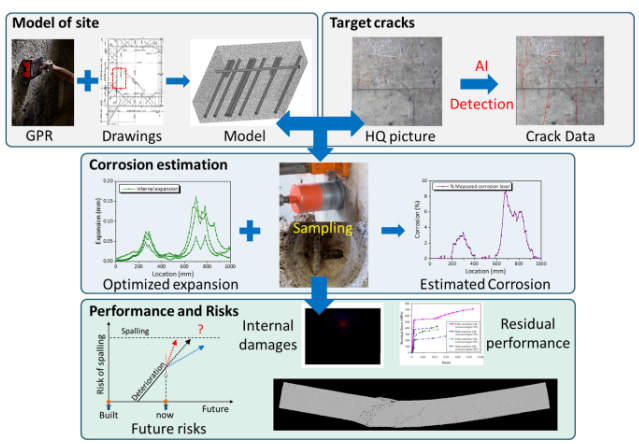

For further information, contact below.
Ass. Prof. Kohei Nagai, Dr. Eng , Be-404, Institute of Industrial Science
TEL: +81-3-5452-6655, FAX: +81-3-5452-6395 E-mail: nagai325@iis.u-tokyo.ac.jp HP: http://nagai.iis.u-tokyo.ac.jp/

Suppression of Wind Effects on Structures using Plasma Actuators

Saugat Shrestha*, Pennung Warnitchai**
*Graduate Student, Structural Engineering, AIT
**Professor, Structural Engineering, AIT

ABSTRACT

The interaction of wind with the structure creates regular occurring vortices in the wake region of the structure. This causes across wind oscillations. This with mean drag forces could be very critical to the safety and serviceability of a structure. So, plasma actuators is means of aerodynamic control to reduce the critical aerodynamic forces by manipulating the flow regime around the structure. The advantage of plasma actuator is that it is flush with the surface and the action is instantaneous (active control). So, the effect of plasma actuator is studied applying it to models of the most prolific shapes. Wind tunnel test is carried out in TU-AIT open type wind tunnel at different wind speeds. The flow is observed to have manipulated with the control measure (using actuators), suppressing the vortices. This manipulation leading to the reduction of the mean drag and the oscillations in the across wind direction, whose evidence has been provided by this research.

Interaction of the influent **wind** with the **structure,** induces **Vortex Induced Oscillations.**

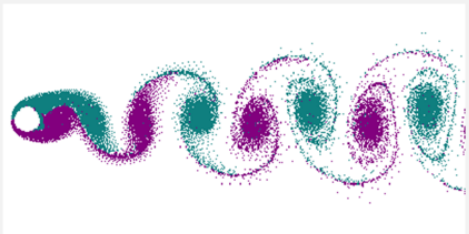

Problem
Uncontrolled oscillations

Safety and **Serviceability** Issues

Critical Aerodynamic Effects:
- **Mean Drag (Along wind)**
- **Oscillations (Across wind)**

Measures are taken to reduce the aerodynamic effects

Aerodynamic Approach: Changing the Flow Regime

Advantages:
- Flush with the surface
- Instantaneous action
- Minimum Power Use

Plasma Actuators

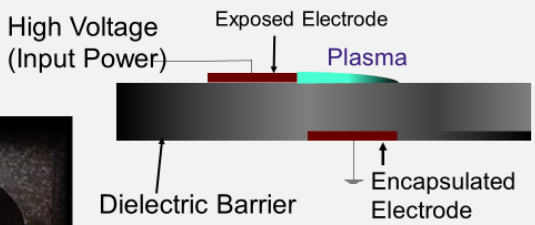

Collison of Ions with neutral air creates **Plasma**

Displace air around it creating **Electric Wind**

3m/s

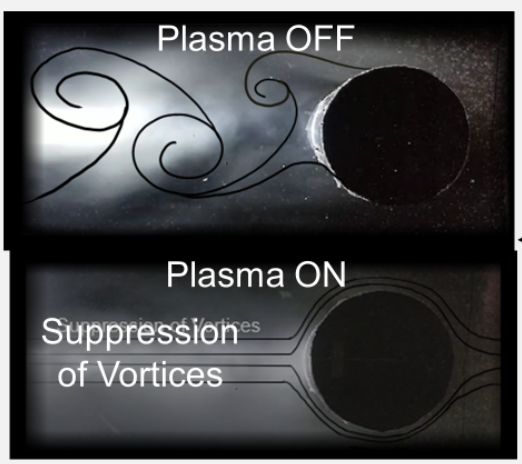

Main Parameter for aerodynamic control **Manipulates flow separation zone**

Wind Tunnel test (HFPI)

Mean Drag Force

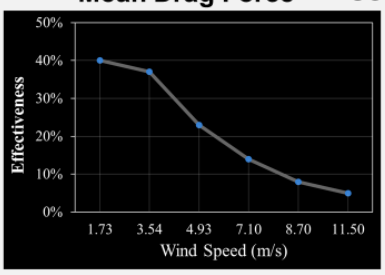

Oscillating Force (Across Wind) from PSD

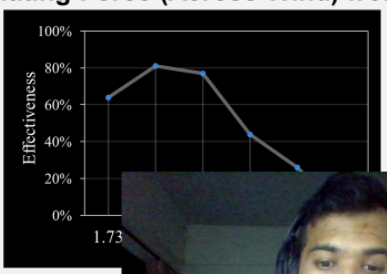

Circular model

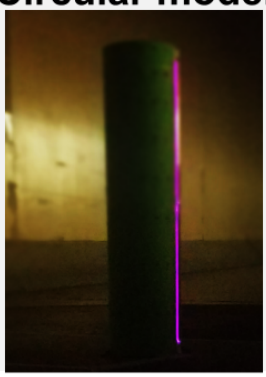

$$\text{Effectiveness} = \frac{BV - CV}{BV} \times 100$$

Where,
BV = Baseline Value of a parameter
CV = Control Value of a parameter

For further information, contact below.
Saugat Shrestha, Structural Engineering Department, CIE, Asian Institute of Technol
TEL: +66 0984943845 EMAIL: saugatshr4@gmail.com

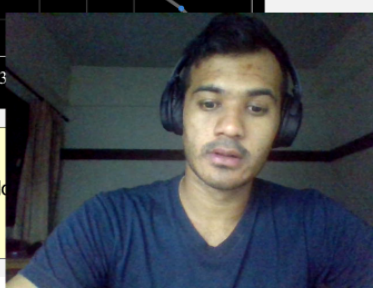

SIMULATION MODEL DEVELOPMENT FOR TRAFFIC SIGNAL LIGHT CONTROL WITH EMERGENCY VEHICLE PREFERENTIAL TREATMENT: A CASE STUDY OF BANGKOK

Isrrah Malabanan*, Dr. Kunnawee Kanitpong#, Dr. Ampol Karoonsoontawong+
*Master Student in Transportation Engineering, Asian Institute of Technology
#Associate Professor, Asian Institute of Technology
+Associate Professor, King Mongkut's University of Technology Thonburi

Abstract. Emergency vehicles (EVs) must reach their destinations within the shortest amount of time considering the importance of their service in saving lives and reducing property damage. One way of ensuring this is to provide preferential treatment to EVs at signalized intersections. Currently, most traffic light control systems in the country's capital are pre-timed and sometimes manually-operated by traffic enforcers. These conventional practices do not give preference to those providing crucial services to the public. Waiting time during red signal indication at signalized intersections have led to delays experienced by EVs. One way of reducing this lost time is through the alteration of traffic control signals that would give preferential treatment to EVs upon their detection. This study aims to develop the most efficient way of prioritizing EVs at a busy isolated intersection in Bangkok. Three options are presented which are traditional preemption, adaptive preemption, and proposed combined algorithm that adopts transit signal priority (TSP) strategies. Traffic simulation approach will be used to test the different algorithms via the VISSIM software and its COM interface. MATLAB programming language will also be used in scripting the custom algorithms that are not available in the software. This research aims to determine the best EV preferential treatment strategy among the three options through the measures of performance of average delay and queue length.

BACKGROUND & PROBLEM

DELAY is a major traffic problem especially for emergency vehicles.

AMERICAN HEART ASSOCIATION:
Chances of survival of cardiac arrest patients decrease by 7 to 10% for every minute that they are not given defibrillation.

NO PREFERENCE FOR EMERGENCY VEHICLES at signalized intersections.

If applied, there's NEGATIVE EFFECT to general traffic.

STUDY SITE

TUK CHAI INTERSECTION

Near
- Somdech Phra Debaratana Medical Centre
- Ramathibodi Hospital
- Queen Sirikit Medical Center
- Phramongkutklao Hospital
- Hospital for Tropical Diseases



ADVANCED TRAFFIC SIGNAL CONCEPTS

Emergency Vehicle Preemption (EVP)

Adaptive Traffic Signal Control (ATSC)

Transit Signal Priority (TSP)

TSP CONCEPTS

Early Green

Green indication is truncated

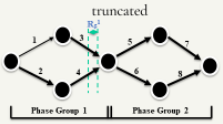

Green Extension

Green time is extended

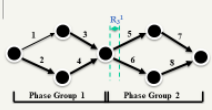

Phase Rotation

Phases are interchanged in the sequence

METHODOLOGY

DATA COLLECTION

Field Data Collection
Video Recording

MODEL DEVELOPMENT

Base Model Calibration
Proposed Models Development
Algorithm Scripting

SIMULATION

Traffic Simulation via VISSIM COM Interface

ANALYSIS

Hypothesis Testing
Model Comparison

THREE ALGORITHMS

Traditional Preemption

Base:
Fixed signal timing

Alteration:
Automatic green indication to approach with EV request

Adaptive Preemption

Base:
Adaptive traffic control Checks queue length

Alteration:
Automatic green indication to approach with EV request.

Proposed Combined

Base:
Fixed signal timing

Alteration:
Checks schedule and delay first before scheduling which to prioritize

MODEL DEVELOPMENT

- CURRENT CONDITION
  - CALIBRATION USING QUEUE LENGTH AND AVERAGE DELAY

Editing Parameter Settings
- Average standstill distance
- Additive part of safety distance
- Multiplicative part of safety distance
- Minimum headway
- Safety distance reduction factor

- PROPOSED MODELS
  - DETECTION DISTANCE
  - SCRIPTING ALGORITHMS USING MATLAB
  - INCORPORATE IN VISSIM USING COM INTERFACE

DATA COLLECTION

- TRAFFIC MOVEMENT COUNTS
- TRAVEL TIME AND SPEED
- VEHICLE DELAY
- SATURATION FLOW RATE
- POISSON DISTRIBUTION
- QUEUE LENGTH
- TRAFFIC SIGNAL TIMING

EXPECTED RESULTS AND CONCLUSION

For further information, please contact isrrahmalabanan@gmail.com.

Model of indirect physical contacts within social activities

Hiroki NOGAMI The University of Tokyo, Japan, B.A. in Eng.
Yudai HONMA The University of Tokyo, Japan, Ph.D. in Eng.

Abstract

We assume that during social activities a person contacts a great number of people indirectly via ones he/she has encountered directly and propose the model to calculate the probability of the multi-dimensional indirect contacts between people.

Background

The features of COVID-19:

- Secondary Infection
- Asymptomatic Patients

Many patients may be unconsciously caused by indirect contacts!

The purpose of this research:

Visualize the process of indirect physical contacts in daily social activities based on probability

The probabilities of indirect contacts

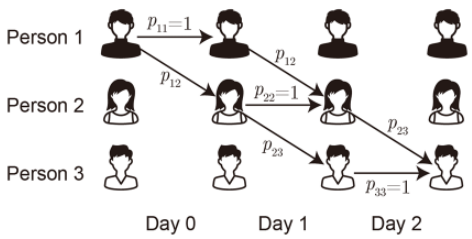

$\Psi\{p_1, p_2\}$= prob of p_1 or p_2
$= 1 - (1 - p_1)(1 - p_2)$

$P^2_{11}(2)=\Psi\{p_{11}p_{12}p_{23}, p_{12}p_{22}p_{23}, p_{12}p_{23}p_{33}\}$
$=\Psi\{P^2_{12}(1)p_{23}, P^2_{13}(1)p_{33}\}$

p_{ij} : prob of direct contact between i, j per day (input)

$P^s_{ij}(d)$: prob that i have experienced s-dimensional contact to j at day d

Note: i and j indirectly contact via $(s - 1)$ people

Indirect contacts have multiple routes, and each edge of routes has different probabilities.
Probabilities of indirect contacts can be calculated by multiplying probabilities of edges and subtracting complementary events.

Contact Matrix

Input: prob of direct contact per day

$p_{ij}=$
```
[[1.  , 0.29, 0.23, 0.55, 0.72],
 [0.29, 1.  , 0.68, 0.48, 0.39],
 [0.23, 0.68, 1.  , 0.06, 0.4 ],
 [0.55, 0.48, 0.06, 1.  , 0.53],
 [0.72, 0.39, 0.4 , 0.53, 1.  ]]
```

Algorithm

$$P^s_{ij}(d) = \Psi\{P^{s}_{ik}(d-1)p_{kj}, p^s_{ij}(d)\}$$

$$p^s_{ij}(d) = 1 - \prod_{k\neq i,j}^{n-2}(1 - P^{s-1}_{ik}(d-1)p_{kj})$$

Output:
prob pf contact experienced until day d

$P^1_{ij}(10)=$
```
[[0.   0.97 0.92 1.   1.  ]
 [0.97 0.   1.   1.   0.99]
 [0.92 1.   0.   0.46 0.99]
 [1.   1.   0.46 0.   1.  ]
 [1.   0.99 0.99 1.   0.  ]]
```

$P^2_{ij}(10)=$
```
[[0. 1. 1. 1. 1.]
 [1. 0. 1. 1. 1.]
 [1. 1. 0. 1. 1.]
 [1. 1. 1. 0. 1.]
 [1. 1. 1. 1. 0.]]
```

$P^{10}_{ij}(10)=$
```
[[0.   0.66 0.59 0.55 0.59]
 [0.71 0.   0.42 0.63 0.73]
 [0.81 0.67 0.   0.78 0.82]
 [0.66 0.68 0.67 0.   0.71]
 [0.41 0.51 0.43 0.43 0.  ]]
```

Indirect contact

It takes much computing cost to find all routes of indirect contacts, so we make "contact matrix", a set of probabilities of direct contact as input data and the algorithm to process it easier. Outputs are probability of experienced contact.
This method can approximately calculate contact probabilities for all pairs, dimension and day.

Trial: A group of 15 people

Pattern 0:
Each pair has randomly different probabilities

```
[[1.   0.29 0.23 0.55 0.72 0.42 0.98 0.68 0.4
 [0.29 1.   0.18 0.53 0.53 0.63 0.85 0.72 0.6
 [0.23 0.18 1.   0.49 0.43 0.31 0.43 0.89 0.5
 [0.55 0.53 0.49 1.   0.61 0.12 0.83 0.6  0.5
 [0.72 0.53 0.43 0.61 1.   0.08 0.76 0.24 0.1
 [0.42 0.63 0.31 0.12 0.08 1.   0.69 0.55 0.1
 [0.98 0.85 0.43 0.83 0.76 0.69 1.   0.4  0.
```

Pattern 1:
One contacts specific people frequently and never others

```
[[1.  0.5 0.5 0.  0.  0.  0.  0.  0.  0.
 [0.5 1.  0.5 0.5 0.  0.  0.  0.  0.  0.
 [0.5 0.5 1.  0.5 0.5 0.  0.  0.  0.  0.
 [0.  0.5 0.5 1.  0.5 0.5 0.  0.  0.  0.
 [0.  0.  0.5 0.5 1.  0.5 0.5 0.  0.  0.
 [0.  0.  0.  0.5 0.5 1.  0.5 0.5 0.  0.
 [0.  0.  0.  0.  0.5 0.5 1.  0.5 0.5 0.
 [0.  0.  0.  0.  0.  0.5 0.5 1.  0.5 0.
```

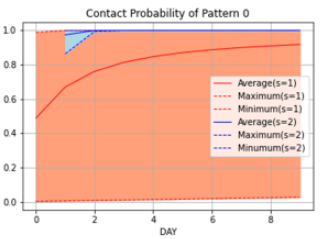

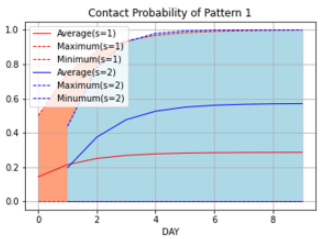

Pattern 2:
One contacts specific people frequently and less others

```
[0.32 0.32 1.   0.32 0.32 0.07 0.07 0.07 0.
 [0.07 0.32 0.32 1.   0.32 0.32 0.07 0.07 0.
 [0.07 0.07 0.32 0.32 1.   0.32 0.32 0.07 0.
 [0.07 0.07 0.07 0.32 0.32 1.   0.32 0.32 0.
 [0.07 0.07 0.07 0.07 0.32 0.32 1.   0.32 0.
 [0.07 0.07 0.07 0.07 0.07 0.32 0.32 1.   0.
```

Pattern 3:
One contacts all the others infrequently

```
[0.14 0.14 1.   0.14 0.14 0.14 0.14 0.14 0.
 [0.14 0.14 0.14 1.   0.14 0.14 0.14 0.14 0.
 [0.14 0.14 0.14 0.14 1.   0.14 0.14 0.14 0.
 [0.14 0.14 0.14 0.14 0.14 1.   0.14 0.14 0.
 [0.14 0.14 0.14 0.14 0.14 0.14 1.   0.14 0.
 [0.14 0.14 0.14 0.14 0.14 0.14 0.14 1.   0.
```

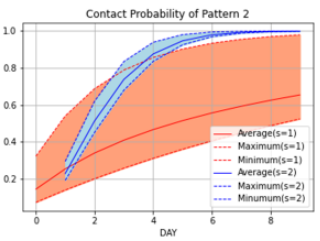

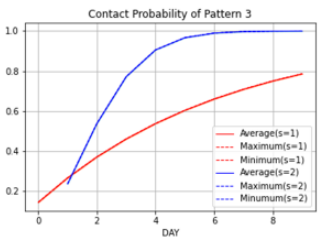

In the inputs of Pattern 1 to 3, the expected value of the number of people one meets per day is limited to 2, that reflects restriction of meeting at pandemic situation.
Though Pattern 3 results high probability of contacts in all pairs, Pattern 1 keeps zero in most of the pairs. Pattern 2 shows that it is difficult to prevent secondary contacts.

Now trying: Contacts Rate in Railway

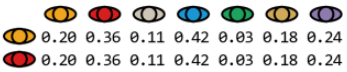

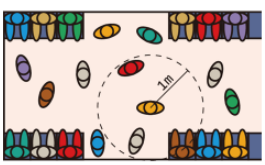

This method can also apply on contact between communities. In order to simulate spread in railway, we are creating the probabilities of direct contacts in train based on OD trip data in Tokyo. This study will give hints why there are differences of distribution of COVID-19 patients in regions.

For further information, contact below.
Hiroki NOGAMI, Yudai Honma Lab. TEL/FAX: +81-3-5452-6379 E-mail: nogami@iis.u-tokyo.ac.jp
HP: http://www.honma-lab.iis.u-tokyo.ac.jp/

Numerical study on dynamic behavior of surface ground near the long-distance ground-flow area caused by the 2018 Sulawesi earthquake, Indonesia

Taichi Kumagai, Nagaoka University Of Technology, Japan, M1

Background

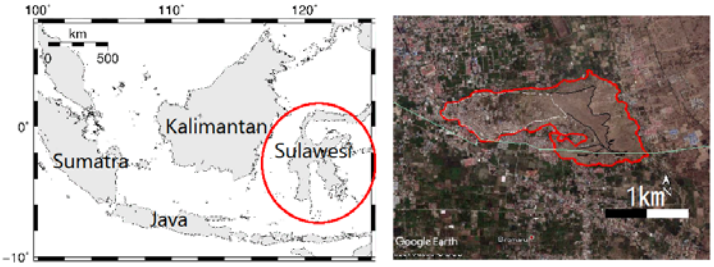

- In 2018, a strong earthquake struck Palu city.
- Large-scale ground flow on the deposit ground with gentle slope(About 1.9%)

Objective

Final Goal — We clarify mechanism of large-scale lateral flow from geotechnical earthquake

Preliminary Study — We evaluate dynamic ground behavior of surface layer during the earthquake using numerical calculation method

This Paper — We describe relationship between the input ground motion level and the behavior of surface ground during earthquakes

Method

Equivalent linear analysis method considering the frequency characteristics

Selection Area

Red line areas are ground flow

These marks are Boring Site

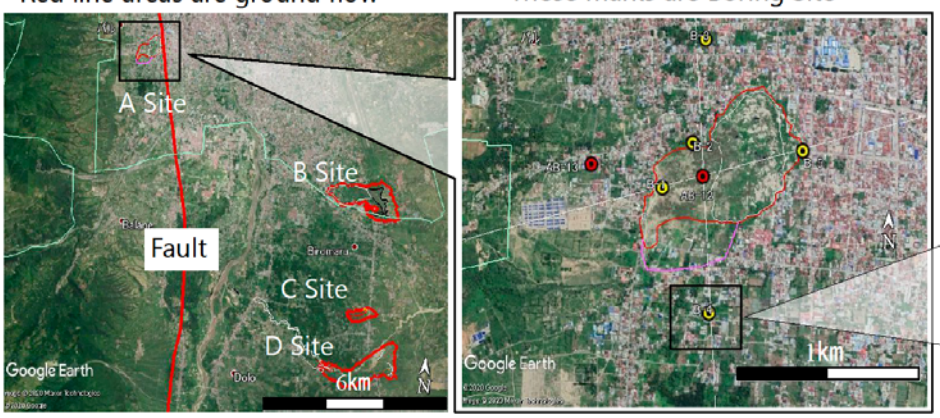

Ground Model

- Soil parameters were determined by a standard value or empirical relationship
- Make a model Based on N value

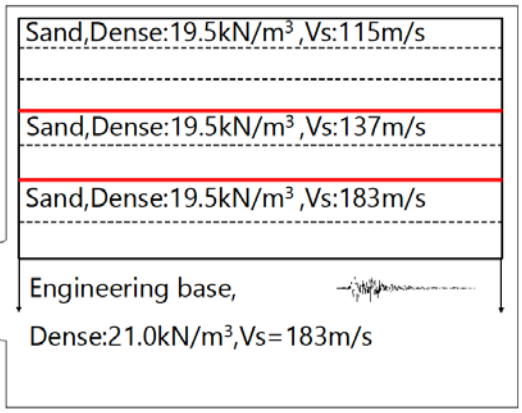

Input Waveform

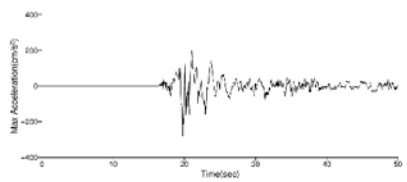

Observed record of Palu City

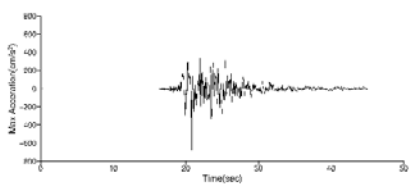

Observation record of 1995 Kobe earthquake

- Digital data still hasn't released in Palu city
- Used observation record of 1995 Kobe earthquake similar characteristics

Result

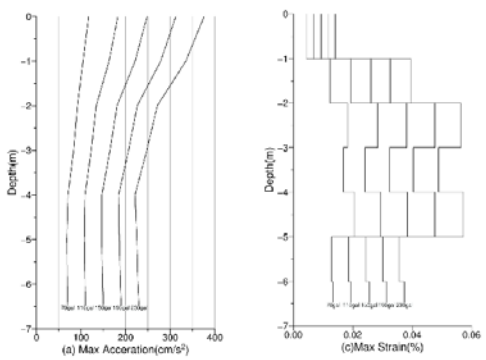

About Max Acceleration

- Shallow layer
→ Response increase

About Max shear strain

- Small input level
→Shear strain of the second layer is large
- Large input level
→Shear strain of the first layer is large too

According to analysis , the surface ground motion is no specific characteristic

⇩

The large-scale flow is caused by a combination of other causes in addition to the seismic behavior of the ground

For further information, contact below.
Taichi Kumagai, Earth quake lab, name, TEL: +81-9443-5552, E-mail: s161024@stn.nagaokaut.ac.jp HP: https://whs.nagaokaut.ac.jp/gee-l/

Estimating the ground characteristics of Koiwagawa area which caused house damages by the 2019 Off the Yamagata prefecture earthquake

HARUKI Suzuki , Nagaoka University Of Technology , Japan M2

Background (2019 Off the Yamagata prefecture earthquake)

Earthquake：Yamagata Prefecture Offshore Earthquake (Yamagata Earthquake)
Date and time：June 18, 2019 22:22
Scale：Mw6.2
Epicenter：Offshore Yamagata Prefecture（38°36.4'N　139°28.7'E）
Depth：About 15km
Maximum seismic intensity：6＋
Fuya, Murakami City, Niigata Prefecture
Residential damage：

Yamagata Prefecture
Complete destruction　0 building
Partial damage　667 building

Niigata Prefecture
Complete destruction　0 building
Partial damage　613 building

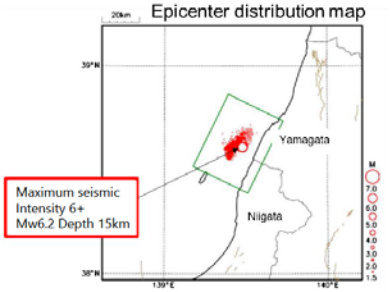

Introduction

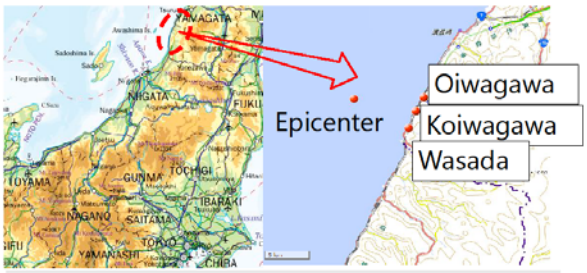

・The Koiwagawa area was heavily damaged by the roof tiles, but the adjacent Oiwagawa and Wasada areas were no damage.
→The ground characteristics of the Koiwagawa area may be vulnerable to damage.

Field survey result

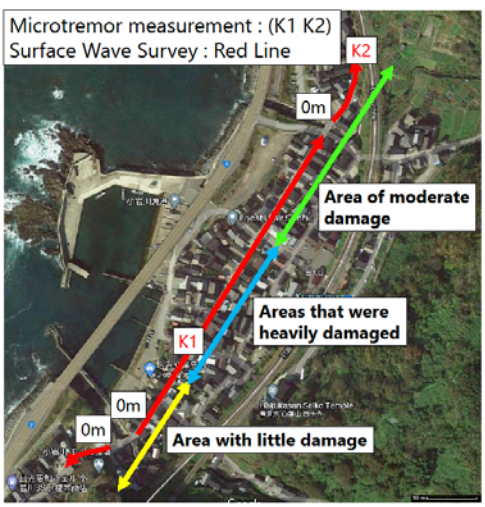

Field survey points in the Koiwagawa area

Area of moderate damage

Areas that were heavily damaged

Area with little damage

Result (Microtremor Measurement)

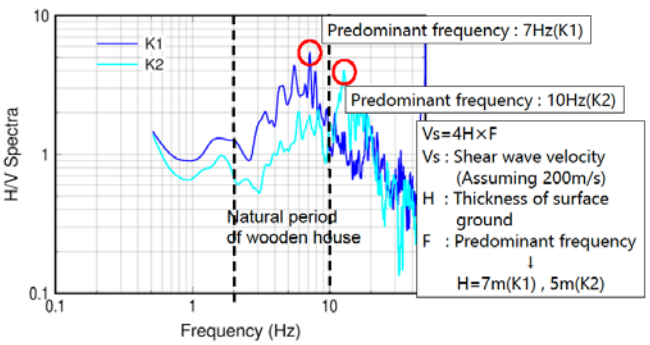

Consideration

・The Predominant frequency in the Koiwagawa area is in the natural period of wooden houses
・Therefore, it is considered that a resonance phenomenon occurred in the Koiwagawa area.
・It is estimated that the Koiwagawa area has a deep surface layer.

Result (Surface Wave Survey)

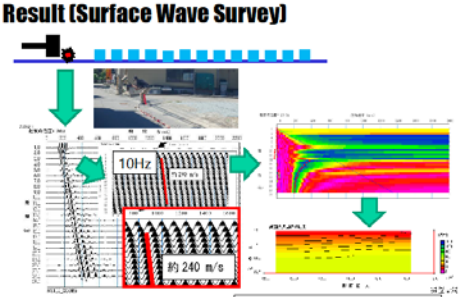

Consideration

・It is possible that the area with less damage has a shallow surface layer thickness, and the area with a lot of damage has a deeper surface layer thickness.
・Koiwagawa area can be estimated to be relatively hard ground.

Summary

・It can be said that there is a correlation between house damage and surface thickness.
・It is estimated that the surface layer thickness exists near Vs = 400 m/s from the microtremor measurement and SWS.

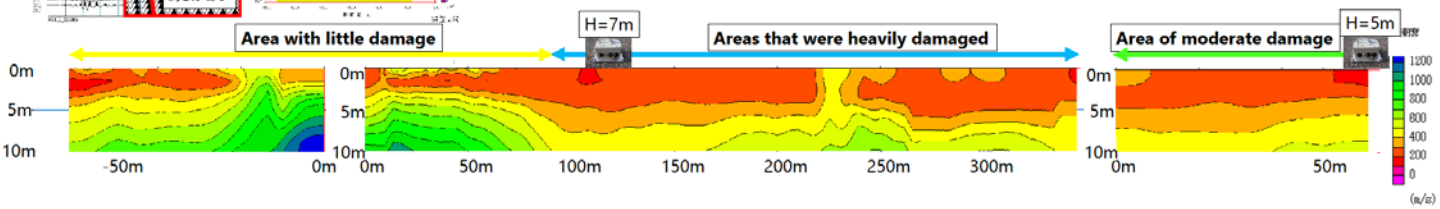

For further information, contact below.
Name: HARUKI Suzuki　TEL：+8190-5543-30814　E-mail: 173253@stn.nagaokaut.ac.jp
Labo: Earthquake engineering　HP: https://whs.nagaokaut.ac.jp/gee-l/index.html

Experimental study on simple retrofitting method for hollow blocks masonry walls

Zamzam Multazam, The University of Tokyo, Indonesia, Graduate Student (M2)

Abstract: Collapse of the unreinforced Masonry (URM) building is the most significant cause of human casualties during the earthquake. This type of building is mostly found in developing countries where construction code is often neglected. Recently, the Concrete Hollow Block (CHB) has become a popular material for residential masonry buildings in Southeast Asia, mainly in Philippine. Most of the CHBs manufactured and used there have low compressive strength and weak against the lateral load. Therefore, increasing seismic capacity for existing and new masonry houses has been one of the most urgent missions for earthquake disaster mitigation in recent years. We developed a new retrofitting method, which is on paint-form, by using fiber as the primary reinforcing material. This method is easy to apply, and commonly used to make the house look fine. This study discusses the dynamic response on 1:4 scaled unreinforced masonry and fiber-reinforced paint house models under the shake table tests. Simple and easy-to-use sinusoidal motion whose frequencies ranging from 2 to 35 Hz and amplitudes ranging from 0.05 to 1.4 g is applied to the structures to obtain the dynamic responses. We found this method enabled to enhanced the deformation capacity of a CHB building.

Specimen

Shake table test were caried out to obtain an understanding of the dynamic response, failure behavior, and cracks pattern of CHB masonry house with and without fiber-reinforced paint. Two identical 1/4 scaled house models were constructed using CHB with compressive strength 0.28 MPa as masonry. The mortar was prepared by mixing cement and sand with ratio 1:6. The mixture was specially designed to obtain mechanical properties similar to CHB houses in developing countries.

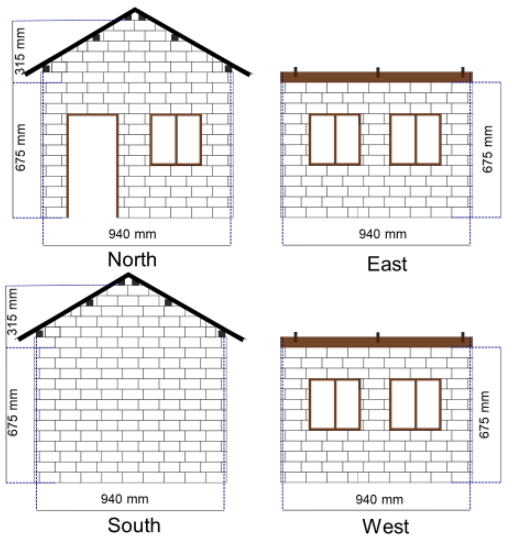

Model dimension

Retrofitting Procedure

URM house model

Fiber-reinforced paint house model

- The fiber ratio of paint is 1 % (by weight)
- The specimen is painted inside and outside (including door, windows, and roof part that touch the wall)
- The thickness of the coating is 1 mm.

The wood that touches the wall is painted.

Input motion

We installed 24 unit of 1-dimensional accelerometers and five laser displacement measuring devices. 54 runs sinusoidal motions of frequencies ranging from 2 to 35 Hz and amplitudes ranging from 0.05 to 1.4 g were applied to obtain the structures' dynamic response. The URM house model was tested on November 25th, 2020, and the retrofitted house model is on December 3rd, 2020.

The following table shows the loading sequence for the shake table test.

Amplitude (g)	Frequency (Hz)							
	2	5	10	15	20	25	30	35
1.4		50						
1.2	54	49						
1		48						
0.8	53	47	43	40	37	34	31	28
0.6	52	45	42	39	36	33	30	27
0.4	51	44	41	38	35	32	29	26
0.2	46	25	24	23	22	21	20	19
0.1	18	17	16	15	14	13	12	11
0.05	10	9	8	7	6	5	4	3
Sweep	1,2							

Loading sequence

Failure behaviour

No	Description	Image
Run 20-24	• Input motion: Sinusoidal wave, f=10-30Hz, amp= 0.2g • Damage level: Moderate • Minor cracks appear on the wall	
Run 25	• Input motion: Sinusoidal wave, f=5 Hz, amp= 0.2g • Damage level: Heavy • Gable walls (North and South) collapsed fell) • Large displacement, wall separation is developed	
Run 43	• Input motion: Sinusoidal wave, f=10 Hz, amp= 0.8g • Damage level: Destruction • The model was totally collapsed	

Damage status of URM house model

For further information, contact below.

Zamzam Multazam, Meguro Lab, TEL: +81-80 7499 7835, E-mail: zamzammultazam@g.ecc.u-Tokyo.ac.jp

Effects of surface ground characteristics on earthquake damage of wooden houses

Hikaru TAKADA, Nagaoka University of Technology , JAPAN, M1

Background

The Mid Niigata prefecture Earthquake in 2004 caused extensive damage of wooden houses.

↓

The damage degree varied over a radius of about 500 m.

⋮

The cause of the damage is likely to be the magnitude of the earthquake motion ?

Kawaguchi Budokubo, Nagaoka city, Niigata prefecture

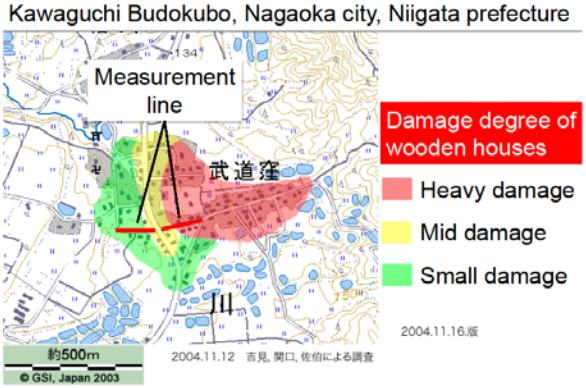

Objective

Examining Vs Distribution in Surface ground

Vs Distribution indicates the extent of the firmness of the Surface ground

What is Vs?

Vs is secondary wave velocity.
Large Vs value is Hard ground. → Small amplitude
Small Vs value is Soft ground. → Large amplitude

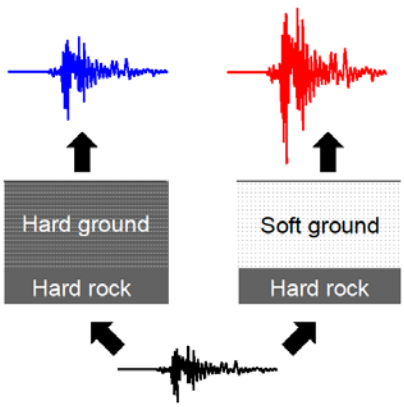

Method

Use Surface Wave Survey

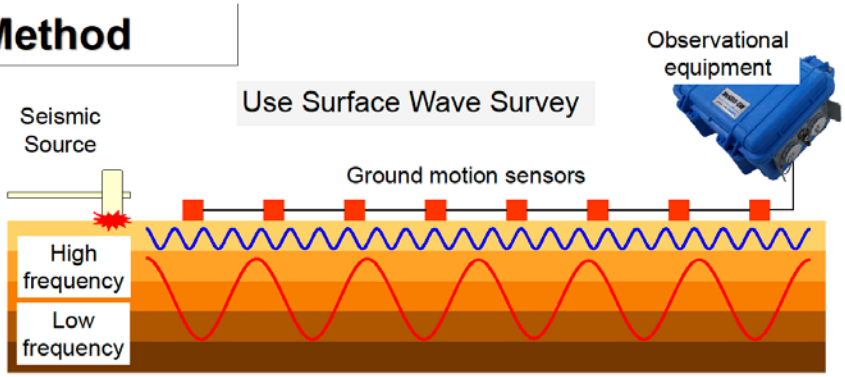

Result

- In the Heavy and mid damage area were small Vs values distributed → Soft ground → Large amplitude
- In the Small damage area were large Vs values distributed → Hard ground → Small amplitude

∴ The cause of the damage is likely to be the magnitude of the earthquake motion

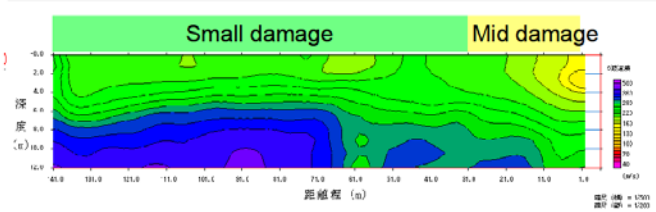

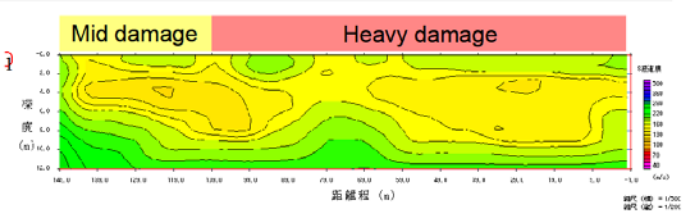

For further information, contact below.
Hikaru TAKADA, Earthquake Engineering Laboratory TEL: +81-258-46-6000, E-mail: s205037@stn.nagaokaut.ac.jp
HP: https://whs.nagaokaut.ac.jp/gee-l/index-e.html

Risk assessment of Rail Infrastructure in India to support business continuity plan

Dheeraj Joshi*, Wataru Takeuchi

Institute of Industrial Science, The University of Tokyo (*India)

Abstract: History of major developed geographies such as Japan, Western Europe and the United States shows that the period of construction of transport infrastructure like railroads harmonize with the period of rapid economic growth. Rail infrastructure in India is also the backbone of economy in India and is the main transport mode for passenger including newly planned High Speed Rail corridors and freight transportation. But rail infrastructure assets are frequently exposed to multi-hazards which sometimes cause disruptions in safe operations. Disruptions like disasters have the potential to interrupt the organization's entire operations and its ability to deliver products and services, that is, preventing them from continuing in a normal way. Even the powerful Roman empire due to high costs on maintenance of infrastructure owing to hazards and other safety standards had to shift the capital to Constantinople but this enormous cost on maintenance of assets ultimately ruined the Roman empire (ICUS, 2020).

India being a developing country, it is highly necessary to develop rail infrastructure including High Speed Rail projects in a sustainable manner so that they can be well assimilated in and supported by the developing economy of India. Sustainable Development Goals of the United Nations identifies sustainable transport systems as a key driver in sustainable development besides reliable transport infrastructure also improves socio-economic profile of any country.

The SDG 11 and the Sendai Framework for Disaster Risk Reduction calls for understanding risks through risk assessments towards avoiding losses due to disasters. This study try to do integrated spatio-temporal study of local socio-economic-environmental vulnerability factors with hazards for national rail infrastructure risk assessment to identify vulnerable rail infrastructure in India for disaster risk informed investment and planning towards business continuity for safe rail operations.

Keywords: Multi-hazards, vulnerability, exposure, sustainability.

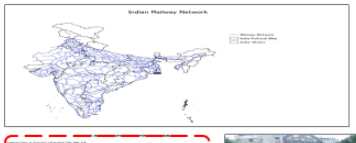

Indian Railway network

Hazard snapshots of Vadodara-Surat section of Indian Railways during floods of 2019.

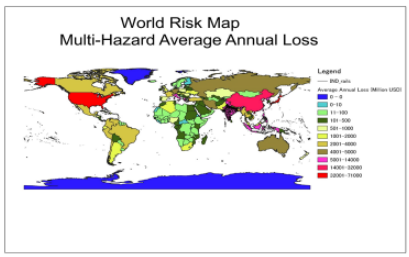

World Risk map (UNDRR) superimposed with railroad shape file of India on QGIS

BACKGROUND

India: (>) billion population + spatially distributed transport network and energy inefficient transport network.

- Large potential to invest in sustainable transport systems like HSR corridors.
- Spatially distributed rail infrastructure + multi-hazards in India + vulnerability = frequent disruptions in train operations and loss to rail business.

Resilience of existing and planned infrastructure important towards business continuity for safe operations.

Hazard type and associated loss in India (Koks et al, 2019)

Hazard Type	Potential Annual Loss in India (Million USD)
Earthquake	101-500
Tropical Cyclones	1001-2000
Tsunami	15.01-30
Floods	5001-14000
Volcano	No Data

Manish Ramaiah, Ram Avatar, 2019

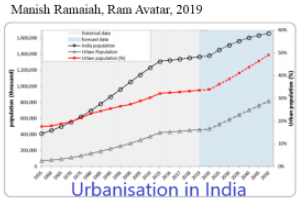

Risks associated with Urban Areas & loss of Green Space

Kalinga Utkal Express accident at Khatauli in 2017

Understanding risks through inclusion of ground truth case studies which caused accidents

OBJECTIVE

- The ground realities and challenge to move from managing disaster to managing risk for railways infrastructure are the main motivators of this study.
- Analysing local compounding vulnerability factors including those risks due to urbanization and ground case studies.
- Risk assessment under multi-hazards to identify critical infrastructure in Indian Railways.

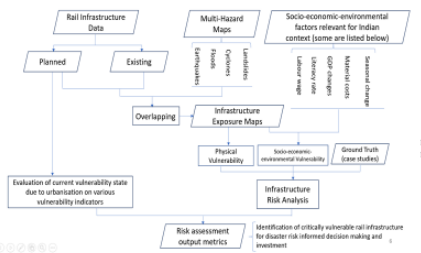

Process flow for the study

Remote sensing dataset description

Data	Data Description	Year
DMSP-OLS NTL	Annual product – stable lights composite	2001-2013
NPP-VIIRS DNB	Monthly product – "vcmcfg"	2013-2019
LANDSAT-7	Landsat 7 ETM+ sensor – SR product	2001-2019

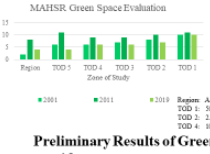

Remote sensing images for NDVI and Nightlights

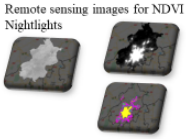

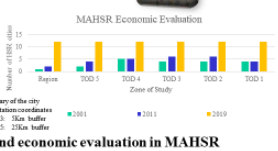

Preliminary Results of Green Space and economic evaluation in MAHSR corridor

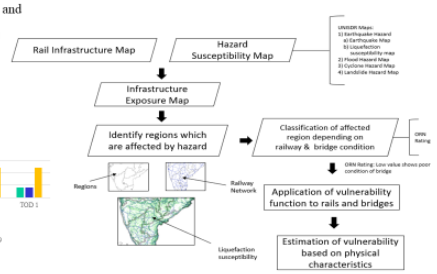

Physical vulnerability assessment

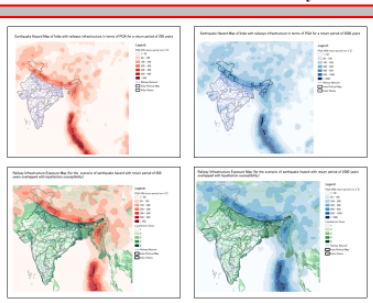

Physical Vulnerability Assessment Results

(in top two figures on left) Result of physical vulnerability assessment in case of different earthquake hazard scenarios.

(in bottom images on left) Result of physical vulnerability in case of earthquake hazard scenarios overlapped with liquefaction susceptibility.

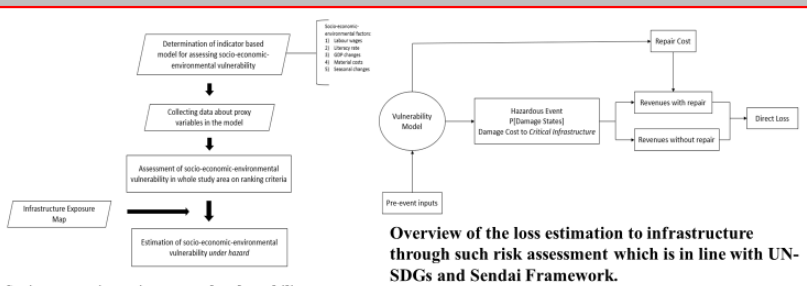

Socio-economic-environmental vulnerability assessment

Overview of the loss estimation to infrastructure through such risk assessment which is in line with UN-SDGs and Sendai Framework.

CONCLUSION AND FUTURE TASK

- Scope for cohesive strategy by urban and transport planners for risk informed development for increasing green space around planned HSR stations.
- Rail infrastructure is critical in Gujarat, north-eastern states and northern states in India in terms of seismic and liquefaction hazard.
- Future task is work on fragility curves for damage assessment under hazards, local vulnerability assessment under hazard scenarios and mapping ground emergency case studies for risk mapping of rail infrastructure in India.

For further information, contact below.

Dheeraj Joshi, M-2, W.TAKEUCHI Lab, TEL: +81-08073681698, FAX: 03-5452-6410, E-mail: dheeraj-joshi@g.ecc.u-tokyo.ac.jp

HP: http://wtlab.iis.u-tokyo.ac.jp/en/member_e.html

Tsunami Evacuation Simulation using Agent-based Modeling

Nattapon Trumikaborworn[1] ,Panon Latcharote[2], Pennung Warnitchai[3]
(1) Graduate student, Dept. of Development and Sustainability, Asian Institute of Technology, (2) Lecturer, Faculty of Engineering, Mahidol University,
(3) Professor, Dept. of Civil and Infrastructure Engineering, Asian Institute of Technology

Abstract: In Thailand, tabletop exercises and evacuation drills are the main tools for raising tsunami awareness of stakeholders such as practitioners and people. Today, tsunami evacuation simulation can play an important role to help practitioners with risk assessment. This research aims to develop a computer simulation using agent-based modeling and a game engine that is very useful in studying a complex system. The simulation is composed of a large number of interacting entities (i.e., agents) with each other and the environment (e.g., building, road network, signage). The interaction (i.e., logics) of the agents is based on physics and decisions of the evacuation process. Tsunami risk assessment derives from the simulation results such as casualty estimation, bottleneck identification, and so on.

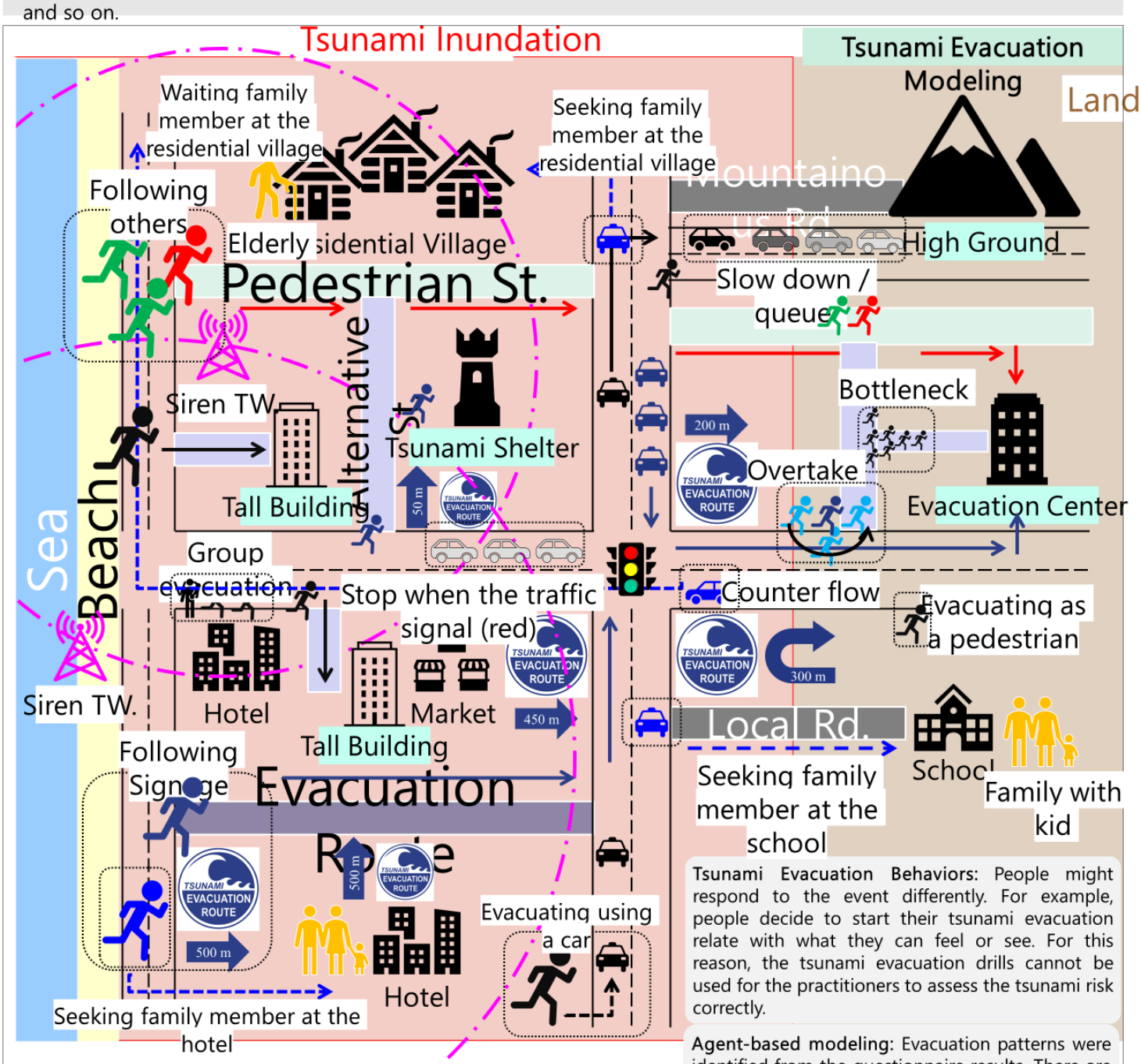

Tsunami Evacuation Behaviors: People might respond to the event differently. For example, people decide to start their tsunami evacuation relate with what they can feel or see. For this reason, the tsunami evacuation drills cannot be used for the practitioners to assess the tsunami risk correctly.

Agent-based modeling: Evacuation patterns were identified from the questionnaire results. There are two main patterns known as not gathering and gathering. Moreover, the gathering pattern can be divided into waiting or seeking. One decision can be associated with another decision or agent characteristics. This can be modeled using conditional probability.

Discussion: 1) Decisions of local and visitor agents are different. These differences can lead to differ number of victims. 2) Higher number of victims of one agent type might be caused by the higher number of agents who decided to go to the gathering place comparing with another type. 3) Having evacuation signs can be a positive factor reducing the number of victims.

For further information, contact - Name: Nattapon Trumikaborworn, Email: nattapon.trum@gmail.com

Investigation of Seawater Intrusion Using Geoelectrical Survey in Coastal Aquifer of Phuket Island, Thailand

Sakanann Vann, Cambodian

Faculty of Technology and Environment, Prince of Songkla University, Phuket Campus, Ph.D in Earth System Science

Abstract: The main purpose of this study is to investigate the seawater intrusion problem in the coastal area of Phuket. The average groundwater data of chloride (Cl-) and Total dissolved solids (TDS) concentrations were done the qualitative assessment in 8 coastal subdistricts, when seawater intrusion is associated with high salinity groundwater, analysis of the groundwater generally indicates a high concentration of major anions, i.e., chlorides (Cl), as well as a high TDS content. Therefore, the risk areas with seawater intrusion problem were identified by these levels of Cl- and TDS exceeding threshold numbers. The geo-electrical method of 4 survey lines were successfully conducted in the study area for a quantitative assessment of the seawater intrusion. 2D inversion models from the resistivity data showed high-resolution subsurface resistivity anomalies of seawater intrusion zones. Furthermore, the artificial seawater intrusion was mixed by Andaman seawater and tap water with the different proportions of the Andaman sea by volume. Each artificial seawater intrusion was measured the fluid electrical conductivity and TDS in order to determine the fluid resistivity ($\rho f luid$). The resistivity decreases when the formation is mixed up with seawater. Likewise, the correlations between formation and fluid resistivities were done. Then, the formation factor of geological material in the study area would be defined by the above information. Time-lapse Electrical Resistivity Imaging (time-lapse ERI) were conducted to prove that the low resistivity plumes are scientifically interpreted as being seawater intrusion. Finally, the research results indicate the coastal areas of Mai-Khao, Kamala, Rawai, and Chalong have been encountered by the seawater intrusion.

Problem Statement

Sea level rising, high over-pumping and so on

↓

Do they induce seawater intrusion problem in Phuket?

↓

Where are the risk areas of seawater intrusion in Phuket?

↓

How far does the seawater intrude inland in the study areas? How depth is it?

Research Objectives

- **To assess seawater intrusion** problem in underground freshwater aquifers in Phuket coastal area.
- **To map the risk areas of seawater intrusion** in Phuket Island
- To know the **spatial distance and depth of seawater intrusion** in the aquifer in the risk area of seawater intrusion

Introduction

Seawater intrusion can gradually cause a severe problem by contaminating freshwater aquifers and causing a lack of freshwater. Coastal areas of Phuket Island are likely to be at risk of seawater intrusion due to many factors, e.g., sea-level rise, over-use of groundwater, and so on. The main purpose of this study was to assess the seawater intrusion problem, which refers to the encroachment of seawater into underground freshwater aquifers, in the coastal area of Phuket.

Site Description

Phuket (Fig 1), the biggest island in Thailand, located in the Andaman Sea of southern Thailand, is a place that has been developed significantly: economic improvement, social integration, industrialization, especially the expansion of tourism vision. 70% of the total area of Phuket (543 Km2) is covered by mountains stretching from North to South, and 30% of flat plain areas, mainly in the middle and eastern parts of the island. Phuket Island is geologically composed of igneous rock (granite and granodiorite) in the western part, and of sedimentary rock(mudstone and conglomerate) in the central part.

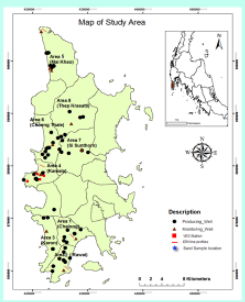

Fig. 1 The map of study area

Research Methodology

- An analysis of existed groundwater chemical data including Chloride concentration (Cl) and Total Dissolved Solids (TDS) from 2003 to 2016, obtained from groundwater producing and monitoring wells was carried out to map the seawater intrusion in the coastal areas of Phuket.
- Four lines of Electrical Resistivity Imaging (ERI) were successfully conducted in the coastal areas of Phuket to delineate the extent and depth of seawater intrusion which was validated with time-lapse ERI to confirm that there is no present of clay instead of seawater intrusion in the study area. The relationship between the formation of resistivity versus TDS and formation and fluid resistivity demonstrated by laboratory testing was done to confirm the value of resistivity for seawater intrusion in the study area. The flow chart of the research methodology is shown in Fig 2.

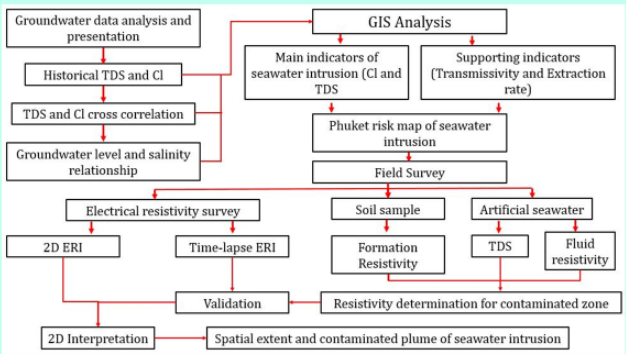

Fig. 2 The flowchart of research methodology

Results and discussions

Assessment of Phuket Seawater Intrusion using groundwater data analysis

The maximum average Cl and TDS (in Mai Khoa) are approximately 7,000 mg/L and 12,000 mg/L (Fig. 3f). Therefore, it can be evaluated that the area where has a severe seawater intrusion problem is Mai-Khao. Other three areas- Chalong, Rawai, and Kamala- are likely to meet seawater intrusion because their correlation between Cl concentration and TDS show high (Fig. 3b, 3c, and 3e, respectively), and the average Cl and TDS are also higher than the thresholds (Cl: 600 mg/L and TDS: 1,500 mg/L). Mapping of TDS, Cl, transmissivity, and groundwater extraction in single maps was done by GIS techniques. The map shows that the coastal areas of Mai-Khao are the most risk area for seawater intrusion, while Kamala, Chalong, and Rawai are risked to be moderate seawater problems, as shown in Fig. 4.

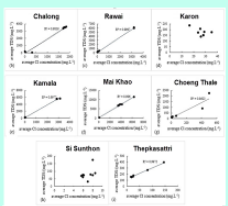

Fig. 3 Cross-plots of average TDS versus Cl in all 8 areas

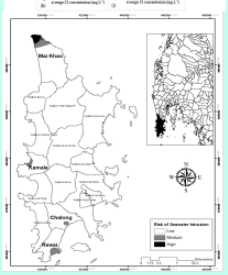

Fig. 4 Map of seawater intrusion risk in Phuket

An effect of Seawater Intrusion on Electrical Resistivity

The formation resistivity decreases with an increase in the volume of seawater in saturated beach sand. The resistivity with 100% of the artificial seawater intrusion was lower than 4 Ohm-m (TDS > 2000 mg/L), compared to approximately 150 Ohm-m (around 121 mg/L of TDS) in 0% seawater. The resistivity increases from 4 up to 22 Ohm-m (1930 mg/L of TDS) when the artificial seawater was added into the sample at 20%. The seawater intrusion is indicated by TDS is higher than 1500 mg/L. The groundwater in the study areas is interpreted as being contaminated with seawater when its resistivity is lower than 30 Ohm-m (TDS > 1500 mg/L), as shown in Fig. 5.

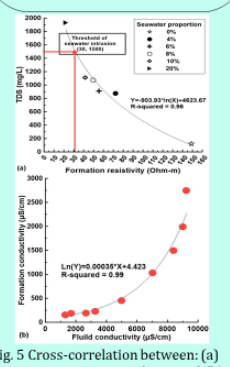

Fig. 5 Cross-correlation between: (a) formation resistivity and TDS and (b) formation and fluid resistivity

Delineation of Seawater Intrusion Zone Using 2D ERI

A low resistivity zone (lower than 30 Ohm-m) can be interpreted as the presence of a seawater intrusion because freshwater has a resistivity of between 50 and 100 Ohm-m with a resistivity of 10 to 50 Ohm-m corresponding to the transition, or brackish water zone. Seawater intrusion in Kamala (Fig. 6a) can be seen to intrude in a freshwater aquifer with the expansion approximately 400 m inland and in the depth around 4 m below the land surface while seawater in Chalong (Fig. 6b) intrudes in a freshwater aquifer with the expansion approximately 150 m (3 m in depth). In terms of Rawai (Fig. 6c), the bedrock zone has been found in the shallow depth around 3 m above mean sea level and the saline zone has been found near the bedrock zone in shallow depth as well. Regarding Mai Khao (Fig. 6d), the area which is located around 500 m from the beach is completely covered by seawater intrusion.

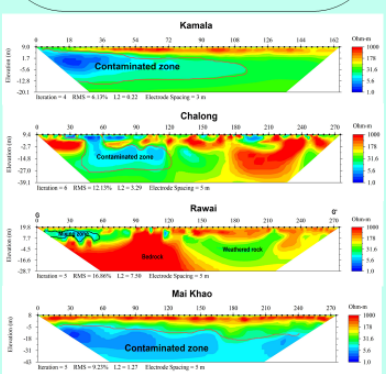

Fig. 6 ERI results: (a) Kamala, (b) Chalong, (c) Rawai and (d) Mai Khao

Validation of Seawater Intrusion Using Time-Lapse ER

The resistivity interpretation of the seawater intrusion is not straightforward, due to the presence of the clay layers in the area which are also conductive, like seawater. Therefore, a time-lapse ERI has been employed for the seasonal monitoring of seawater intrusion and groundwater dynamics in the coastal aquifer, Phuket, since it is possible to prove that low resistivity value (smaller than 30 Ohm-m) should be confirmed as seawater intrusion, not clay layers. The rise of resistivity (percentage change from 20% to 100%), as shown in Fig. 7, is shown in the zone locating the western part of the inversion model. This zone is highly conductive during the dry season (February 2018). However, the resistivity value of this zone is higher in the rainy month (June 2019), compared to that of the dry season. For this profile, it indicates clearly that the reduction in resistivity presents near the ground surface (approximately 4 m in thickness) owing to freshwater recharge. According to the is evidence, the low resistivity plumes (smaller than 30 Ohm m) are confirmed as indicating the presence of seawater intrusion, not clay layer.

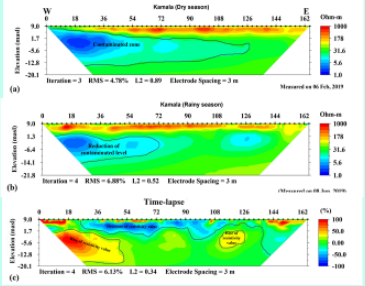

Fig. 7 Time-lapse ERI result: (a) ERI in dry season, (b) ERI in rainy season, (c) Time-lapse ERI in Kamala

Conclusion

An integration between geo-electrical surveys (electrical resistivity imaging) and groundwater chemistry data has proved to be an effective tool for delineating the spatial extent and interface between freshwater and seawater of seawater intrusion. This study will be worthwhile for further research in this study area to study a modelling of seawater intrusion in order to determine and predict the effects of different pumping scenarios

Further works

The further research will be answered to the following questions:

(1) What is the situation of seawater intrusion in Kamala coastal aquifer, Phuket, in next 15 years?

(2) What is the impact of groundwater recharge and discharge on seawater intrusion in Kamala coastal aquifer?

(3) What are the proper mitigation and management scenarios to control seawater intrusion in Kamala aquifer?

Detection of drainage canals in Indonesian peatland and scenario evaluation of peatland restoration measures

Daiki Shimizu, Wataru Takeuchi
Institute of Industrial Science, The University of Tokyo, Japan

Abstract: *Carbon dioxide accounts for about 70% of the world's greenhouse gas emissions and its reduction is required to mitigate global warming (IPCC AR5, 2014; IPCC, 2018). On the other hand, the importance of peatlands, which are widely distributed around the world in high latitudes and tropics, has been pointed out in recent years since the peat soils were formed by thousands of years of sedimentation of plant remains without decomposition and store 500-700 Gt of carbon. The peat distributed in the tropics, in particular, accounts for more than 54% of the world's total peat area and is called "tropical peatland" (Page et al., 2011).Indonesia, which has the largest tropical peat in Southeast Asian countries, is said to have the largest carbon storage capacity on earth, with 55 Gt of carbon stored in its peat (Jaenicke et al., 2008). However, Indonesia's peatland has been threatened by anthropogenic development since the early 1990s. The construction of artificial drainage canals mainly associated with the Mega Rice Project by the government or plantation development has led to the lowering of the groundwater table, leading to peat decomposition, carbon dioxide release, and increased fire risk. Thus, although the distribution of drainage canals can cause carbon dioxide release and peat fires, studies on the spatial distribution of drainage canals haven't conducted yet and, therefore, studies on evaluation of restoration measures which take the distribution into account haven't conducted (Dohong et al., 2017). Therefore, this study try to detect the drainage canal distribution which has been constructed in Indonesia and evaluate scenarios for peat restoration policies considering the increased ecological respiration and fire risk associated with drainage canal distribution.*

1. Background

The United Nations has set 2021-2030 as the "UN Decade on Ecosystem Restoration" recently. Among ecosystems around the world, restoration of Indonesian peatland has been said to be the most important aspect for climate change mitigation. Indonesia has the largest peatland (Figure 1) and is assumed to be the largest carbon reservoir on earth, with as much as 55 Gt of carbon stored in peat. However, Indonesian tropical peatland has been threatened by anthropogenic development since the early 1990s, and peat degradation has been progressing. Recent studies also pointed out that Indonesian peatland is estimated to be one of the highest priority areas (Strassburg et al., 2020).

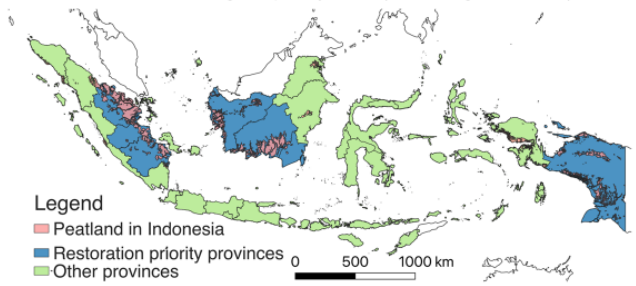

Figure 1. Peatland distribution map in Indonesia

The construction of artificial drainage canals associated with the Mega Rice Project ,which had been aimed to convert peatland to farmland by the government, or plantation development has led to the lowering of the groundwater table, leading to peat decomposition, carbon dioxide release, and increased fire risk. Thus, although the drainage canals lead to carbon dioxide release and peat fires, studies on the spatial distribution of drainage canals haven't conducted yet and, therefore, studies on evaluation of restoration measures which take the distribution into account haven't been conducted (Dohong et al., 2017). The need to identify the distribution of drainage canals has been pointed out also by other previous studies (Sinclair et al., 2020; Ritzma et al., 2014; Leng et al., 2019).

In this study, we try to detect the drainage canal distribution which has been constructed in Indonesia and evaluate scenarios for peat restoration measures. In measure evaluation, we consider the ecological respiration and fire risk associated with groundwater level change caused by the existence of drainage canals.

Since this study is ongoing, the progress at this point; a result of drainage canal detection part is shown here.

2. Objective

1)To identify the distribution of drainage canals in Indonesian peatland

2)To assess the effectiveness of rewetting measures in some simple scenarios based on assumptions such as water level recovery effect

3. Methodology

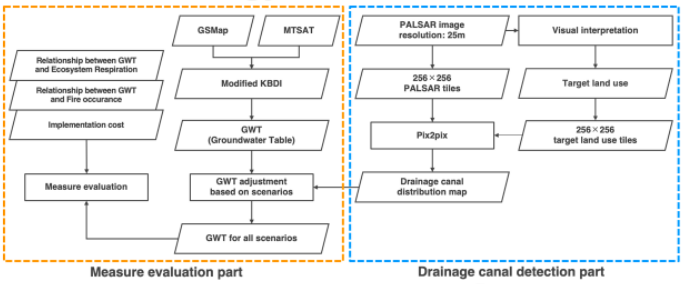

Figure 2. Overall research flowchart

•Drainage canal detection

We try to detect the drainage canal distribution map in Indonesian peatland using PALSAR image and Pix2pix for data and detection method each. Pix2pix is one of GAN (Generative Adversarial Networks) and has been applied well in the context of remote sensing.

•Measure evaluation

With obtained drainage canal distribution map and GWT distribution, which is derived from GSMaP and MTSAT, GWT distribution for each measure scenario is estimated. Drainage canal detection part is followed by measure evaluation part using relationships between GWT and Ecosystem Respiration, GWT and Fire Occurrence (Figure 3 & 4), measure evaluation part based on some assumptions.

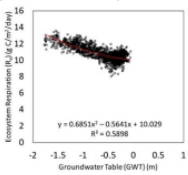

Figure 3. Relationship between GWT and Ecosystem Respiration in drained forest

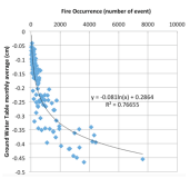

Figure 4. Relationship between GWT and Fire Occurrence

4. Result and Discussion

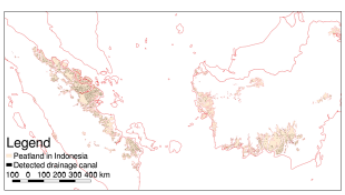

Figure 5. Detection result in Sumatra and Kalimantan

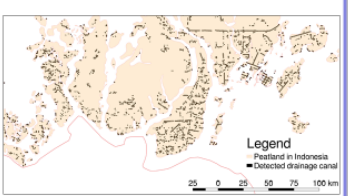

Figure 6. Detailed detection result in South Kalimantan

As mentioned above, we only show a result of drainage canal detection part here. Figure 5. is for Sumatra and Kalimantan, and Figure 6 is for particularly South Kalimantan where a large number of drainage canals had been constructed over several decades. Although we can't precisely assess the detection precision since we have no validation data, we were able to detect the drainage canals all over the peatland in Indonesia. Since thick drainage canals are likely to be more easily detected on SAR images, and the larger the canal, the greater the environmental impact on the surroundings, we can say we were able to detect the drainage canals mainly in high priority area.

5. Conclusion and Next step

- Drainage canals were detected all over the peatland in Indonesia
- We will enhance the accuracy of this model by building a different model for each province using different training dataset
- Measure evaluation will be conducted after improving the drainage canal detection model

References
- Strassburg, B.B.N., Iribarrem, A., Beyer, H.L. et al. Global priority areas for ecosystem restoration. Nature 586, 724–729 (2020). https://doi.org/10.1038/s41586-020-2784-9
- Aziz, Ammar & Dohong, Alue & Dargusch, Paul. (2017). A review of the drivers of tropical peatland degradation in South-East Asia. Land Use Policy. 69. 10.1016/j.landusepol.2017.09.035.
- Sinclair, Amanda & Graham, Laura & Putra, Erianto & Saharjo, Bambang & Applegate, Grahame & Grover, Samantha & Cochrane, Mark. (2019). Effects of distance from canal and degradation history on peat bulk density in a degraded tropical peatland. Science of The Total Environment. 699. 134199. 10.1016/j.scitotenv.2019.134199.
- Ritzema, Henk & Limin, Suwido & Kusin, Kitso & Jauhiainen, Jyrki & Wösten, H.. (2014). Canal blocking strategies for hydrological restoration of degraded tropical peatlands in Central Kalimantan, Indonesia. CATENA. 114. 11–20. 10.1016/j.catena.2013.10.009.
- Leng, Lee & Ahmed, Osumanu & Jalloh, Mohamadu Boyie. (2018). Brief review on climate change and tropical Peatlands. Geoscience Frontiers. 10. 10.1016/j.gsf.2017.12.018.

For further information, contact:

Daiki Shimizu, Bw-601, 6-1, Komaba 4-chome, Meguro, Tokyo 153-8505 JAPAN (URL: http://wtlab.iis.u-tokyo.ac.jp/ E-mail: shimizu-daiki974@g.ecc.u-tokyo.ac.jp)

Empirical Model Of Thailand Shale Compaction Based On Geological Age Classification

Syukratun Nufus[1], and Avirut Puttiwongrak[2]

1 Master Student, Faculty of Technology and Environment, Prince of Songkla University Phuket Campus, Phuket, Thailand
2 Assistant Professor, Geotechnical and Earth Resources Engineering, Asian Institute of Technology, Pathumthani, Thailand, avirut@ait.ac.th
Indonesian, Master Student

ABSTRACT

Shale is a clastic rock formed from tiny particles of clay, the compaction can be defined as a process related to the pressure and burial depth of sedimentary. Shale compaction has been studied for many years. However, curves graphically showing relationships between shale porosity and burial depths are normally widely scattered. The variation in shale porosity decreases as the burial depth increases, this is known as the conventional compaction trend. This study aims to be refined the variation of the Thailand shale compaction, the research findings have revealed that mechanical compaction or burial depth is certainly one of the main controlling factors of compaction of shale, but it cannot be a single factor to explain the compaction curves. The Thailand shale compaction data classifying with the geological ages (Paleozoic, Mesozoic, and Cenozoic) were collected and plotted as the conventional compaction curve, the graph clearly showed that the data scatters are due to the geological ages (the older geological age gives the lower porosity). Numerical analysis was conducted in this study to estimate the time (geological ages) of shale compaction from the burial depth using the velocity function. Then, the empirical models of each geological age were established by the numerical methods. Finally, the three-dimension (3D) plot was carried out to demonstrate the compaction trends in each age. The findings in this study act as a guide for future study of the standard curve of shale compaction. The reconstructed data plots on porosity-depth graph of Thailand shales might be studied with compaction curves varying with time.

INTRODUCTION

Thailand Geological Information

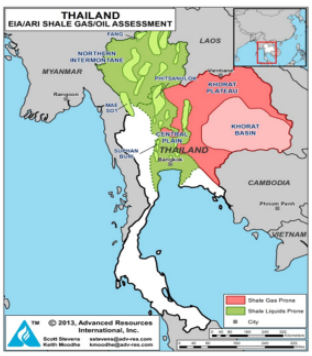

Fig. 1. Thailand Shale Assessment

The geological setting of Thailand is divided into several regions with different geological and lithological histories. Central Thailand contains Quaternary sediments. The northern, western, and peninsula of Thailand are abundant with Paleozoic rocks with small, deformed Mesozoic strata outliers, and sometimes small Tertiary basins. In Northeast Thailand, extensive Mesozoic rocks are found in the Khorat Plateau. Thailand has significant shale potential, mostly located in Northeast Thailand, in the Khorat Basin, the North Intermontane, and the Central Plains (Fig. 1).

Objective

- To determine the compaction trend ranges of Thailand shale for each geological age.
- To estimate the geological age based on numerical analysis.
- To obtain the mathematical function of the relationship among the geological age, depth, and porosity for Thailand shale based on numerical analysis.

METHODOLOGY

Data Collection

Shale compaction data used in this study is the Thailand shale data obtained by the Department of Mineral and Fuel (DMF) of Thailand. The data categorized by three eras of geological age, i.e., there are Cenozoic, Mesozoic, and Paleozoic.

Geological Age Estimation

The estimation of geological age is analyzed in this study by examining the relationship among velocity, depth, and geological age as suggested by Faust, 1951, where velocity is a function of depth:

$$v = \alpha_m Z^{1/6} \quad (1)$$

$$\alpha_m = \alpha(T)^{1/6} \quad (2)$$

And the relationship of velocity, depth and geological age in years:

$$v = \alpha\,(TZ)^{1/6} \quad (3)$$

Where v is the velocity in m/s, Z is depth in m, T is geological age (time) in years, and α is given presently the value of 46.55 and is numerically equal to velocity in meter per second when TZ = 1. From those equation suggested by Faust, 1951, we can calculate the geological time using this equation:

$$T = \left(\frac{v}{\alpha}\right)^6 \times \frac{1}{Z} \quad (4)$$

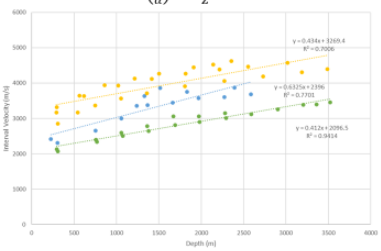

Fig. 2. Modified plots from Faust (1951) velocity as a linear function for each geological time era, Cenozoic (green), Mesozoic (blue), Paleozoic (yellow)

RESULT AND DISCUSSIONS

Empirical Thailand Shale Compaction Model

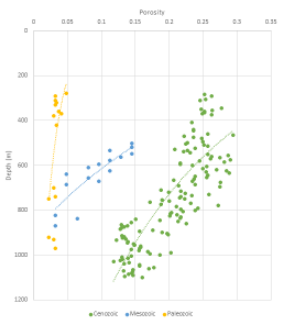

Fig. 3 Thailand shale porosity-burial depth graph for each geological age eras, Cenozoic (green), Mesozoic (blue), Paleozoic (yellow).

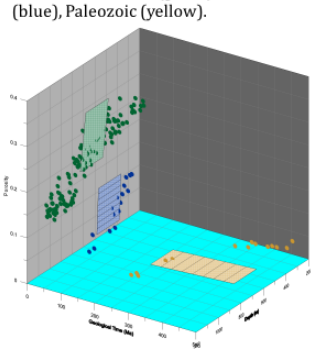

Fig. 5 3D plot of porosity-depth-geological age

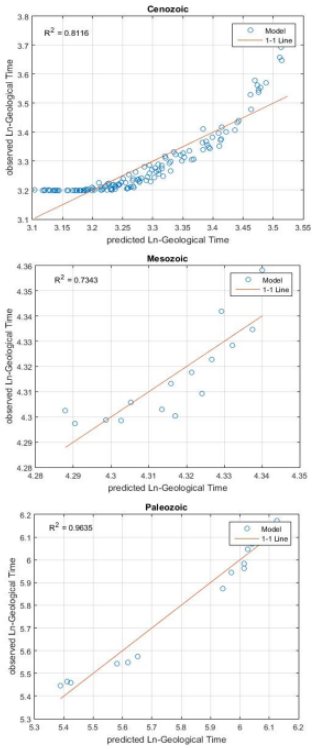

Fig. 4 Validation of empirical model in each geological eras

The empirical models of each geological ages were found by the multi-linear regression (Fig. 4), the porosity functions with geological age and depth are expressed:

- Cenozoic Era (T < 65M years ago):

$$\phi_C = -1.31 \ln T - 0.00078z + 5.1 \quad (5)$$

- Mesozoic Era (65M < T < 250M years ago):

$$\phi_M = 3.54 \ln T + 0.00035z - 15.3 \quad (6)$$

- Paleozoic Era (T > 250M years ago):

$$\phi_P = 0.32 \ln T + 0.00032z - 2.03 \quad (7)$$

CONCLUSIONS

The scatters of porosity for Thailand shales show that the porosity decreases with the increasing burial depth of the shale and also affects the geological ages, at the shallow depth. The empirical function of porosity and depth only cannot represent the compaction curve of the Thailand shales, the geological age (or time) need to be taken into account in the shale compaction function. The finds in this study show that the empirical function of Thailand shales is supposed to establish based on the difference of the geological ages including Cenozoic, Mesozoic, and Paleozoic. The empirical models of Thailand shale in each geological age among porosity, depth, and geological time using multiple linear regression were established.

ACKNOWLEDGEMENT

The authors would like to thanks the Department of Mineral and Fuel (DMF) of Thailand for providing the Thailand shale data that used in this study.

For further information, contact below.
Syukratun Nufus, Master Student, Faculty of Technological and Environment,
Earth System Science Program, Prince of Songkla University, Phuket campus, Thailand
email: nsyukratun@gmail.com, Phone: +6285270303226

REFERENCES

Faust, L. Y., (1951), Seismic Velocity as a functi
Vol. 16, Issue 2, pp. 192–206.

Puttiwongrak, A., Vann, S., Giao, P. H., (2020), A
Change With Depth And Geologic Time In Deep
Vol.19, Issue 73, pp. 108–115.

U.S Energy Information Administration, (2015
Gas Resources: Thailand, U.S. Department of E

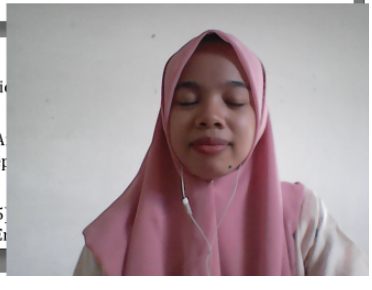

Evaluation of CMIP5 General Circulation Model (GCMs) for Simulating Precipitation and Temperature of Koshi river basin of Nepal

Pragya Pradhan, Sangam Shrestha
Doctoral student in Water Engineering and Management , Asian Institute of Technology
Professor in Water Engineering and Management, Asian Institute of Technology

9th International Joint Student Seminar on Civil Infrastructures
8-10 December 2020
Asian Institute of Technology, Thailand

Abstract

The performance of General circulation model (GCMs) in a region is generally assessed according to their capability to simulate the historical precipitation and temperature. This study evaluates the performance of 12 different Coupled Model Intercomparison Project Phase 5 (CMIP5) General circulation model (GCMs) for Koshi river basin of Nepal .The Koshi river basin is a transboundary river basin which is from Himalayan region to Terai region of Nepal. The evaluation of performance of GCMs in such river basin which includes the climate patterns from snow cover to flood is quite challenging because of low data availability. The performance of GCMs are evaluated depending upon seven different climate indices (SDII, FD, R95P, WSDI, CSDI, CDD, CWD) using Entropy method and Ranking technique i.e., Compromise programming. Hence, performance of GCMs vary with each climate indices as climate indices define different characteristics of precipitation and temperature. The GCMs: ACESS1.0, CanESM2 performs better for Simple daily intensity index (SDII), Very wet days (R95P) and Warm spell duration index (WSDI). Similarly, BCCCSMI, MIROC-ESM performs better for Consecutive dry days (CDD), Consecutive wet days (CWD). CNRM-CM5, NorESM1-M performance is better for Cold spell duration index (CSDI). MIROC5, IPSL-CM5A-MR, MPI-ESM-LR performance is better for Frost days (FD).

Study area

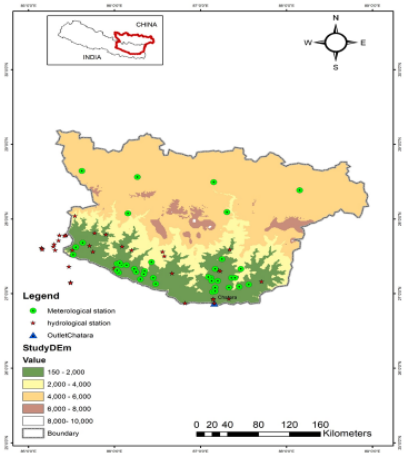

Fig 1: Location Map of Koshi river basin, Nepal

Methodology

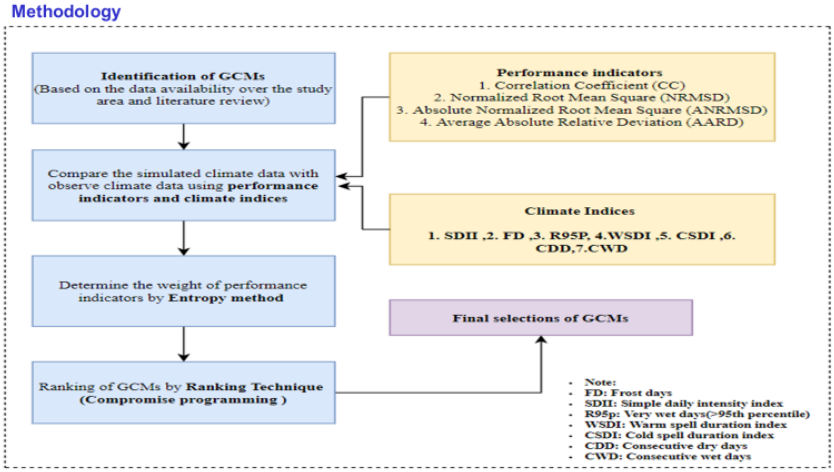

Fig 2: Research Framework

Entropy Method

Step 1: Formation of decision matrix which shows the performances of different GCMs (m) with respect to various performance indicators (n).

$$X = [X_{ij}]_{matrix} = \begin{bmatrix} X_{11} & \cdots & X_{1n} \\ \vdots & \ddots & \vdots \\ X_{m1} & \cdots & X_{mn} \end{bmatrix}$$ where, i = 1, 2…., m; j = 1, 2…, (eq 1)

Where, X_{ij} presents the performance value of i^{th} GCM on j^{th} criteria

Step 2: Normalization of the decision matrix

$r_{ij} = \frac{X_{ij} - min(X_{ij})}{max(X_{ij}) - min(X_{ij})}$ where, i = 1, 2…., m; j = 1, 2…, n (eq 2)

$r_{ij} = \frac{max(X_{ij}) - X_{ij}}{max(X_{ij}) - min(X_{ij})}$ where, i = 1, 2…., m; j = 1, 2…, n (eq 3)

Step 3: Determination of Entropy value (e_j)

$e_j = \frac{-1}{\ln(m)} \sum_{i=1}^{m} K_{ij} * \ln K_{ij}$ where, i = 1, 2…., m; j = 1, 2…, n (eq 4)

$K_{ij} = \frac{r_{ij}}{\sum_{i=1}^{m} r_{ij}}$ where, i = 1, 2…., m; j = 1, 2…, n and $0 < e_j < 1$ (eq 5)

k_{ij} is normalize payoff matrix

Step 4: Calculation of Entropy weights (W_j) based on degree of diversification (Dd_j).

$$Dd_j = 1 - e_j \quad \text{(eq 6)}$$

$$W_j = \frac{Dd_j}{\sum_{j=1}^{j} Dd_j}, \sum_{j=1}^{j} W_j = 1 \quad \text{(eq 7)}$$

Ranking Technique (Compromise Programming)

The compromise programming is based on the Euclidean distant theory and if the value of $L_p(a)$ is low then the GCMs model has better performance

$$L_p(a) = \left[\sum_{j=1}^{J} w_j^p \left| f_j^* - f_j(a) \right|^p \right]^{\frac{1}{p}}$$

$L_p(a)$ = Lp metric for GCM a for the chosen value of parameter p;

Results and Discussion

Rectangular matrix of performance indicators obtained for 12 chosen GCMs for *Very wet days (R95P)*

R95P SN	GCM	CC	NRMSD	ANRMSD	AARD
1	ACESS1.0	0.072	1.988	1.573	0.164
2	BCCCSM1	-0.095	3.143	2.396	0.100
3	CANESM2	0.197	2.805	1.838	0.070
4	CNRMCM5	0.086	3.740	3.228	0.091
5	CSIRO	-0.074	1.779	1.299	0.093
6	IPSL	0.014	2.259	1.702	0.225
7	MIROC	-0.012	3.990	3.237	0.422
8	MIROESM	-0.094	3.678	2.962	0.065
9	MPIESMLR	-0.022	3.892	3.327	0.359
10	MPIESMMR	0.019	4.086	3.641	0.306
11	MRICGM3	0.087	3.205	2.475	0.079
12	NORESM1	-0.034	3.985	3.323	0.410
	max	0.197	4.086	3.641	0.422
	min	-0.095	1.779	1.299	0.065
	max-min	0.292	2.307	2.343	0.357

Rectangular matrix of normalized performance indicators for 12 GCMs for *Very wet days (R95P)*

R95P SN	GCM	CC	NRMSD	ANRMSD	AARD
1	ACESS1.0	-0.162	-0.054	-0.072	-0.172
2	BCCCSM1	-0.267	-0.201	-0.188	-0.083
3	CANESM2	0.000	-0.168	-0.117	-0.017
4	CNRMCM5	-0.149	-0.248	-0.260	-0.067
5	CSIRO	-0.257	0.000	0.000	-0.071
6	IPSL	-0.206	-0.100	-0.095	-0.230
7	MIROC	-0.222	-0.264	-0.261	-0.335
8	MIROESM	-0.266	-0.243	-0.240	0.000
9	MPIESMLR	-0.229	-0.258	-0.267	-0.311
10	MPIESMMR	-0.203	-0.269	-0.286	-0.285
11	MRICGM3	-0.149	-0.206	-0.196	-0.040
12	NORESM1	-0.235	-0.263	-0.267	-0.331
	Sum	**-2.345**	**-2.274**	**-2.249**	**-1.940**
	ej (Eq. 8)	**0.944**	**0.915**	**0.905**	**0.781**
	Ddj (Eq. 10)	**0.056**	**0.085**	**0.095**	**0.219**
	Wj (Eq.11)	**0.124**	**0.186**	**0.208**	**0.482**

GCM model	R95P Lpa	R95P Rank
ACESS1.0	1.065	2
BCCCSM1	1.461	6
CanESM2	1.258	4
CNRM-CM5	1.664	8
CSIRO-Mk3.6.0	1.032	1
IPSL-CM5A-MR	1.158	3
MIROC5	1.774	10
MIROC-ESM	1.650	7
MPI-ESM-LR	1.758	9
MPI-ESM-MR	1.826	12
MRI-CGM3	1.438	5
NorESM1-M	1.789	11

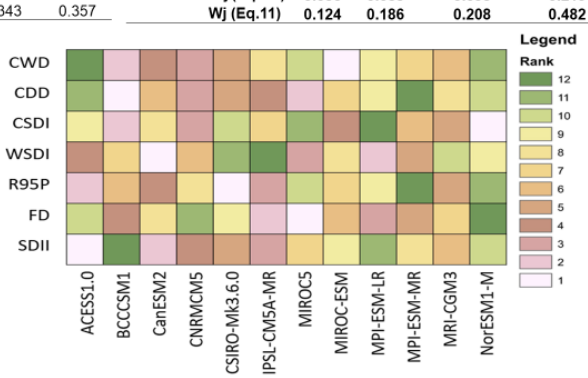

Fig 3:Grid showing the rank value for all 12 GCMs and climate indices in Koshi river basin, Nepal

Conclusions

- IPSL-CM5A-MR, BCCCSM1, CNRM-CM5,MIROC5 ,ACESS 1.0 and CanESM2 are the over all best model for the study of future climate patterns in Koshi river basin.
- BCCCSM1 and CNRM-CM5 both performs better in Consecutive wet days (CWD) ,Consecutive dry day (CDD), Cold spell duration index (CSDI) . It means these models prefer estimating the rainfall and minimum temperature of the river basin.
- Each GCMs model performance is different in each climate indices

Name: Pragya Pradhan
Email: pradhanpragya0.327@gmail.com
st120872@ait.asia

Evaluating Factors of Severe Injuries on Motorcycle Rear-end Collision in Thailand

Mr. Phanuphong Prajongkha, Doctoral Student in Transportation Engineering, AIT, Thailand.
Associate Professor Dr.Kunnawee Kanitpong, Transportation Engineering, AIT, Thailand.

Abstract The study aims to evaluate severe injuries of rear-end collisions, in Thailand between 2016 to 2019. The rear-end collisions comprise four models, and these can determine the likelihood of severe outcomes. M1 is all types of rear-end collisions to MC, and M2 is the MC's rear-end collisions. M3 is the MC's rear-end collisions with traveling OV, and M4 is the MC's rear-end collision with hitting parking OV. The results found that the significant factors depend on various conditions related to light condition, impact speed, suburban, rural, not wearing a helmet, transmission auto, brake systems, attention failure.

Introduction

- **Why this study needs to be conducted?**

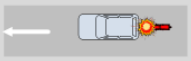

The rear-end collision is highest severe injuries all types of road accident in Thailand.

- **Objective**

To find factors that lead to the increase in severe injuries to the motorcyclists and passengers.

Methodology

This study is analyzed by ordered logit model as below

$$\text{Logit}\,[P(Y \geq j)] = \alpha j + \beta' x_1 = \alpha j + \beta_1 x_1 + \beta_2 x_2 + ..i = 1,2,3..,k$$

Y is dependent variable related to level of injury,
X is independent variables related to various variables,
B(beta) is coefficient matrix related to endogenous variables.

- **Framework**

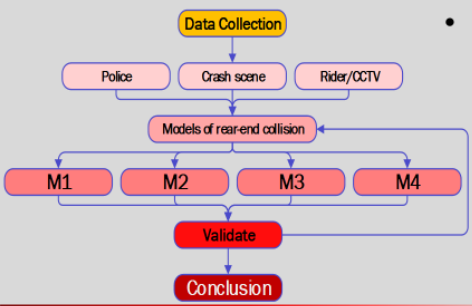

- **Definition of model**

M1: MC hits Car & Car hits MC
M2: MC hits Car
M3: MC hits Car running
M4: MC hits Car parking

Results

- **Descriptive Data**

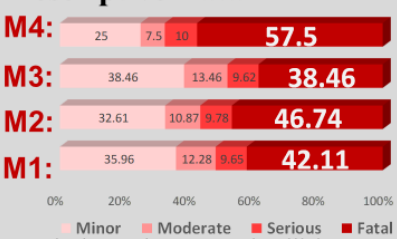

The graph shows that rear-end collision can lead to the high percentage in fatalities in particular case of MC hitting car parking. If riders run at high speed, they have the high percentage to death.

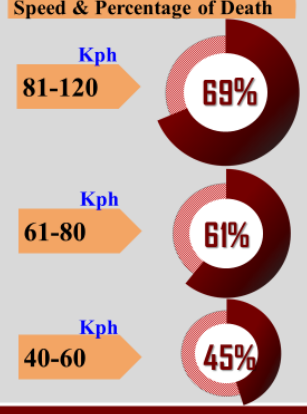

- **Model Results**

Variable		M1	M2	M3	M4
Rider attributes					
Gender:	Male	*2.041***	*2.240**	0.439	NA
Age:	Teen	-0.988	-1.760	*-2.640**	-2.068
	Young	1.407	*2.439**	1.678	*3.437**
	Adult[a]				
Experience:	A little	*-1.676***	*-5.525****	*-5.102***	*-5.241***
	Moderate	*-4.189****	*-2.963***	*-6.137****	-1.889
	Extensive[b]				
License:	No_license	*1.736***	*3.303****	*5.413****	*4.254***
Helmet Use:	Not use	*1.489***	*1.554***	*2.112**	0.614
Environmental conditions					
Light Condition:	Daytime	*-1.631***	*-1.901**	*-2.88***	NA
Urbanization:	Suburban	*1.489***	*2.026***	*2.569***	NA
	Rural	*1.850**	*2.733***	*4.702**	NA
	Urban[c]				
MC attributes					
Transmission:	Auto	*1.734***	*2.579***	*2.585***	NA
Brake system:	ABS/CBS	*-1.804**	*-3.246***	*-6.033***	NA
Crash scenes					
Impact Speed:	Speed	*0.063****	*0.092****	0.101**	*0.08***
Vehicle type:	OVPC	*-1.687**	*-2.609***	-0.411	*-3.105***
	OVPickup	-0.300	0.109	1.495	0.801
	OVMC	-1.436	0.543	2.574	NA
	OVTruck[d]				
Distance:	POI to POR	*0.117***	0.094	NA	NA
Attention:	Attention failure	*1.231**	*3.287***	*2.394***	NA
Human Failure:	Decision	-0.832	-0.672	NA	NA
	Reaction	*-2.824***	-1.991	NA	NA
	Perception[e]				
Faulty MC:	Faulty	-1.116	-1.262	NA	*-2.516**

Note: *, $p<0.1$; **, $p<0.05$; ***, $p<0.005$

Conclusion

For considering rear-end collision model, motorcyclists are more likely to be severe injuries from the following risk factors: no license, light condition (night-day), un-waring helmet, brake systems (no ABS or CBS) and attention failure.

Type of vehicles, MC hit OVPC has a low probability of occurring injury when compared with OVTruck.

- **Recommendations**

For driving license, youngers and teenagers are expected for improving knowledge related to safe driving and speed.

Enforcing extensive policies, the wearing helmet, controlling speed, should be implemented in particular suburban and rural areas.

TARC Knowledge Saves Life
AIT Asian Institute of Technology 8-10 December 2020
9th Joint Student Seminar on Civil Infrastructures

School of Engineering and Technology
FoS: Transportation Engineering
Phanuphong Prajongkha email: st120592@ait.asia

Rapid Identification of Seismic Damage in Tall Buildings by using Acceleration Response Time Histories

Navindra Liyanarachchi[1], Chananwath Sinthumongkhonchai[2], Pennung Warnitchai[3]

[1]Post-graduate Student in Structural Engineering, Asian Institute of Technology (AIT) – Sri Lankan
[2]Graduate in Structural Engineering, Asian Institute of Technology (AIT) - Thai
[3]Professor in Structural Engineering, Asian Institute of Technology (AIT) – Thai

Abstract: This poster presents a novel technique to identify the seismic damage to a Tall building by using accelerometers in a limited number of floors. The procedure is based on modal decomposition considering the concept of mode of vibration where any complex response of the structure could be defined as a sum of modal responses. The importance of modal decomposition is that a modal pushover analysis could be done before hand and the damage to the structure from each mode could be calculated. These could be combined to find the total damage to the structure. The modal decomposition is to be carried out by a novel technique called "Orthogonal Filter" approach where the orthogonality of the modes is taken into consideration to obtain the real acceleration of all the floors of the building from accelerometers placed in a limited number of floors of the building. These acceleration records could then be used to identify the internal forces of the structure and compared with the capacity of the structure to identify the damage to the structure.

Traditional Approach

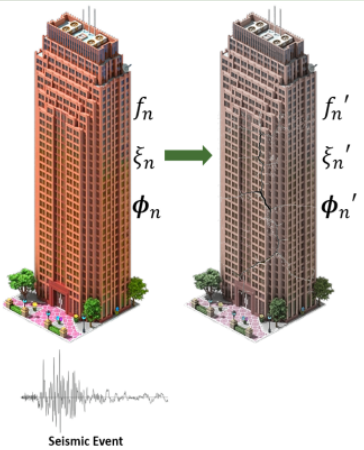

- Influence of Environmental Factors
- Significant change in stiffness required to make a modest change in Frequency
- Insensitivity to Damage
- Damage localization is challenging

Importance of Modal Decomposition

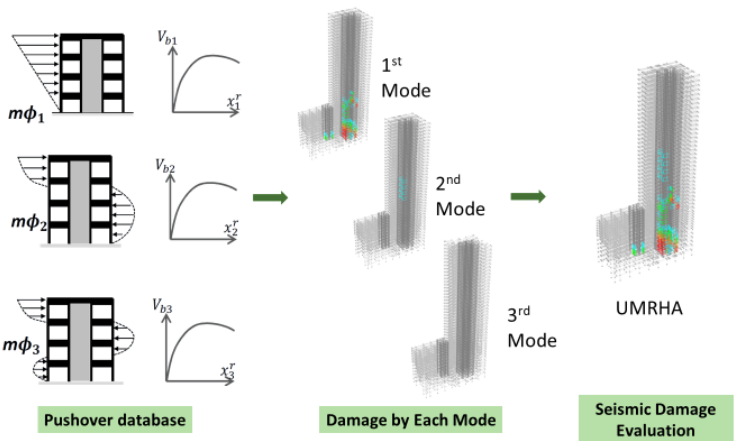

Concept of Mode of Vibration

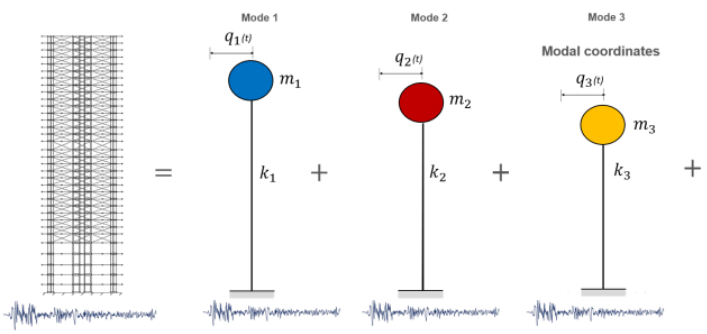

Results

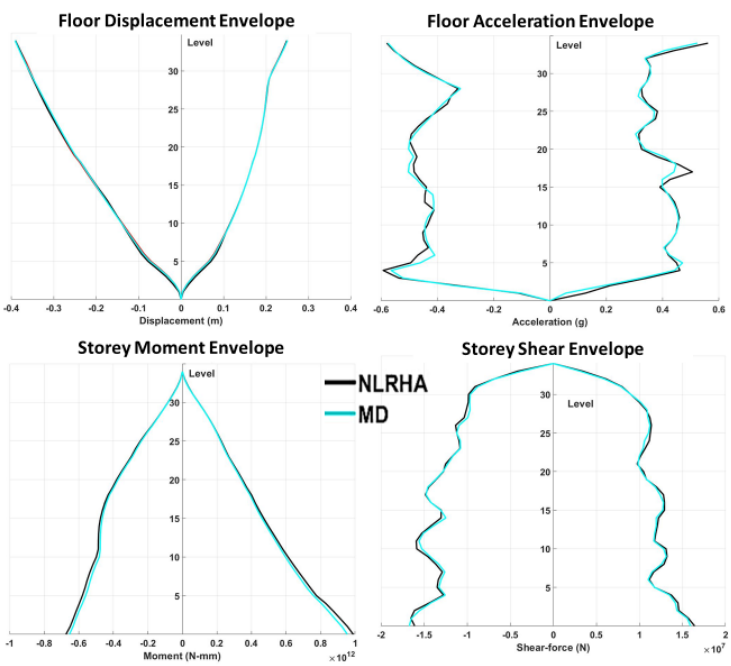

Orthogonal Filter Approach

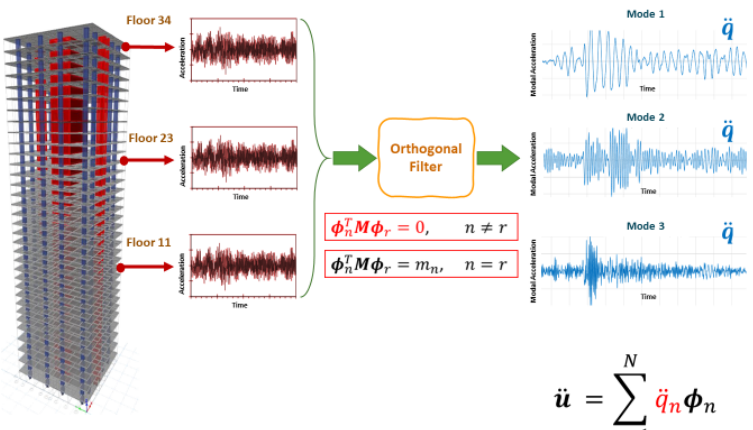

$$\ddot{u} = \sum_{n=1}^{N} \ddot{q}_n \phi_n$$

Conclusion

- This technique shows impressive potential to be used to estimate Floor accelerations, floor displacements and Internal Forces due to a seismic event
- Compared to rigorous Non-Linear Response History Analysis (NLRHA), this procedure requires very less computational time and effort

For further information, contact below.
Name: Navindra Liyanarachchi, TEL: +66-631506001 E-mail: st120863@ait.ac.th

・Award

・Awardees

・**Mr. Martin Garcia-Fry, Tohoku University, Japan**

・**Ms. Achini Uppeka Ranasinghe, Asian Institute of University**

・**Mr. Phattarasuda Witchayaphong, Asian Institute of University**

・**Mr. Nyi Linn Maung, The University of Tokyo**

・**Ms. Srikulnath Nilnoree, Asian Institute of University**

・**Mr. Zamzam Multazam, The University of Tokyo**

Excellent Presentation Award

Presented to

Mr. Zamzam Multazam,
The University of Tokyo

In appreciation for its cooperation towards

the 9th Joint Student Seminar on Civil Infrastructures
on
8 - 10 December, 2020

With Compliments from

International Center for Urban Safety Engineering (ICUS)
Institute of Industrial Science, The University of Tokyo, Japan
&
Regional Network Office for Urban Safety (RNUS)
Asian Institute of Technology, Thailand

Prof. Dr. Wataru TAKEUCHI
Institute of Industrial Science,
The University of Tokyo, Japan

Prof. Dr. Pennung WARNITCHAI
Dept. of Civil and Infrastructure Eng,
Asian Institute of Technology, Thailand

・Questionnaire

Q1. What was the most important (significant, crucial) thing you have learned in this seminar?

1 Simulation studies
2 It was great to learn about the research happening in different field. It helps to boost my understanding
3 Usually we get the opportunity to participate or update our knowledge in our own filed of specialization. This seminar covered a big scope in civil engineering, it was a great opportunity to learn about the newest researches in other specializations. Although it was in brief, I learned a lot about the current research topics in civil engineering field.
4 Criticle thinking about each research topic. Also, we've learnt how to ask and answer the questions to presenters
5 How to make an academic poster
6 Developing time based pre-presentation and discussing with other researchers regarding their and own research.
7 special lectures on various research topics
8 Understanding international research perspective on disaster resilient infrastructure
9 I learned that as an architect I have a good background knowledge on applied engineering and I gained deeper knowledge on seismic dissipator technology
10 Get to know about different fields (Transportation, Geotech, Earthquake) and studies carried out in the field.
11 I learned about how to ask a question related to their research, so this is the great experience that we learned from other English accents.
12 Communication in English
13 Respond to questions. We make a easy poster.
14 Make others understand the content by giving a presentation in English.
15 It is difficult to discuss in English about academic topic.
16 The lecture by Professor Wataru Takeuchi about the ecological footprint.
17 I learned the importance of communicating my research to people overseas in English in an easy-to-understand way. I should have been more visual in my poster, such as using larger figures and tables.
18 We have learnt a lot on how to construct the research work and many updated knowledge part from over the sea country.
19 The process and methodology of their research especially earthquake.
20 How to ask questions
21 Different new ideas in Civil Engineering Field
22 Summarize the research work so that it can be presented in 5 mins.
23 Presentation and communication skills
24 The process and methodology of their research especially earthquake.
25 Presentation skill with a time limitation and other reseach from different field of study and countries
26 The discussion after each presentation was very rich
27 An opportunity to present the research in front of international student, get feedback for our research, and also get a lot of idea from other speakers.
28 To use and discuss in English. To be stimulated by different viewpoints from those in Japan.
29 How to communicate my research. Not only I was not able to answer questions in zoom, in English, but my explanation in the video seems to have given the wrong messeage.
30 I learned about many latest researches in various fields.
31 Question and answer session

Q2. What question(s) do you have about what you have learned in this seminar?

1	If the researches can be explained in detail it will be more useful.
2	What are the main components to make a good research and publish in high rank of international journal??
3	How can I learn from other schoolmates even if I don't know about his/her research topic or methodology?
4	no question but handouts are needed.
5	I asked questions during the seminar itself and the presenters replied them during the seminar.
6	About structural retrofit mechanisms used in developing countries, how often are these applied to buildings and which uses are often more critical (besides hospitals and schools of course)?
7	I have learned how to deliver poster presentation and prepare poster
8	There are many things. For example, I analyzed the MC rear-end collision by the order regression model. So, can I apply results to be recommendations to other kinds of accidents without MC rear-end collisions?
9	Is it okay to make an announcement without questions?
10	(About the research by Nyu Linn Maung) How are historical facts related to today's situation of Yangon?
11	It's a little different from my research field.
12	In your own recorded presentation, I felt it was very good that someone was presenting the poster while using the zoom-in/out function.How did you do it?(I apologize if this is the wrong way to answer your question.)
13	Shall we have the PowerPoint presentation instead of poster presentation cuz it's too small fonts and hard to understand?
14	How can I variate or calibrate my work.
15	Everything is clear, Thank you!
16	How can I variate or calibrate my work.
17	No, the participants can provide clearly answers
18	i would prefer to make much more sections for research fields to be contact with more specialist
19	Is it possible to extend the presentation time? I think 5 minutes is not enough to explain a whole research
20	It was very helpful to clearly present the results of various faults, not just the sagaing fault.

Q3. Any suggestions for this seminar?

1 More time for presentation

2 It's better to have online presentation rather than video presentation

3 Instead of poster if the presentations can be presented in ppt format it will be more clear to see the content.

4 Time for video presentation is too short.

5 From my point of view, this seminar is of great value in that it provides a platform for students in different countries to share their research achievements and communicate with each other. I think the software used for the seminar (zoom） could be improved in its video and audio connection

6 The poster size can be made more bigger for video based presentation.

7 each poster should be presented more than 10 mins included q&a.

8 It was well organised and smooth. Great work and efforts by ICUS & IIS team.

9 I think it went pretty well for 5-min presentations. Moreover, presentation skills were developed, thank you!

10 Poster font were very small and Five minute presentation is not enough

11 In the past seminar, everything was perfect. In the further seminar, could we invite universities in EU and US to join us? If we can do this, it will be more beneficial to students.

12 I think PPT is better than posters online.

13 We make a power point , not only poster.

14 Since it was a remote seminar, I thought it would be better to present it with PowerPoint slides rather than posters.

15 The session I joined was occupied by a lot of Thais, and the discussion between Thais and Japanese was very rare. Sessions should be more diverse.

16 I think it would be great to include the researches which will be the combination of social sciences and engineering. Thank you very much.

17 It would have been nice if we could have used the breakout room function to break up into several groups and have students interact with each other.

18 According to Q2, we can limited the presentation time and number of slides for all presenters to follow the rule
Moreover, it's really good place for student to practice and present through the online method. Great activity!

19 The seminar is effective to share and discuss about the new innovation but in the time limit of presentation affected the audiences to understand the research because presenter had to present in time limit

20 If next year we need to do it online again, please consider the different way to present the project. Using the poster is hard to explain the detail and no one could understand the project clearly.

21 It would be easy for some presenters if 5mins presentation can be submitted as a video file without recording it in PowerPoint. It allows the presenter to make presentation more clearer in there own way.

22 Should not use powerpoint for poster online presentation

23 The seminar is effective to share and discuss about the new innovation but in the time limit of presentation affected the audiences to understand the research because presenter had to present in time limit

24 Unfortunately, the seminar was performed via online platform so they are our obstructions about the internet connection also the participants need to submit the presentation video and some have problems with this step

25 providing much more time for presentation

26 Hopefully, this seminar can be held offline. And for me, recording the presentation is a new things. I prefer to directly present intead of record the presentation. Overall, this seminar give me a good opportunity, during this pandemic.

27 I think it is better to use PowerPoint instead of posters for online presentations.

28 For many people, online seminars are good because they are easy to attend.
Some might say that face-to-face is better...

・Appendix

1. Registration number 73

2. Prefix

prefix	
Dr.	4
Mr.	44
Ms.	19
Prof.	6
	73

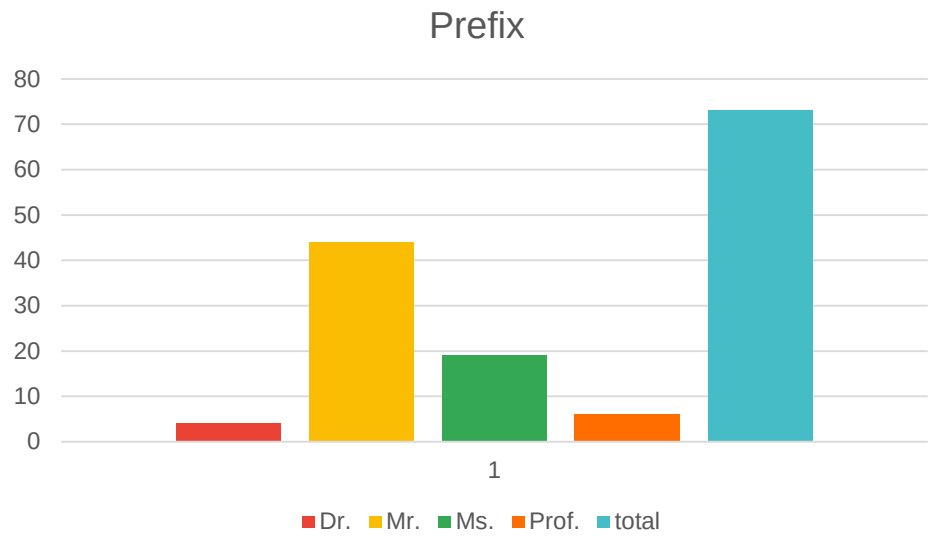

3. Nationality

	Nationality	
1	Cambodia	1
2	China	5
3	Egypt	1
4	India	7
5	Indonesia	2
6	Iran	1
7	Japan	18
8	Korea	1
9	Myanmar	3
10	Nepal	9
11	Nigeria	1
12	Peru	1
13	Philippines	4
14	Sri Lanka	5
15	Thailand	13
16	Vietnum	1
	total	73

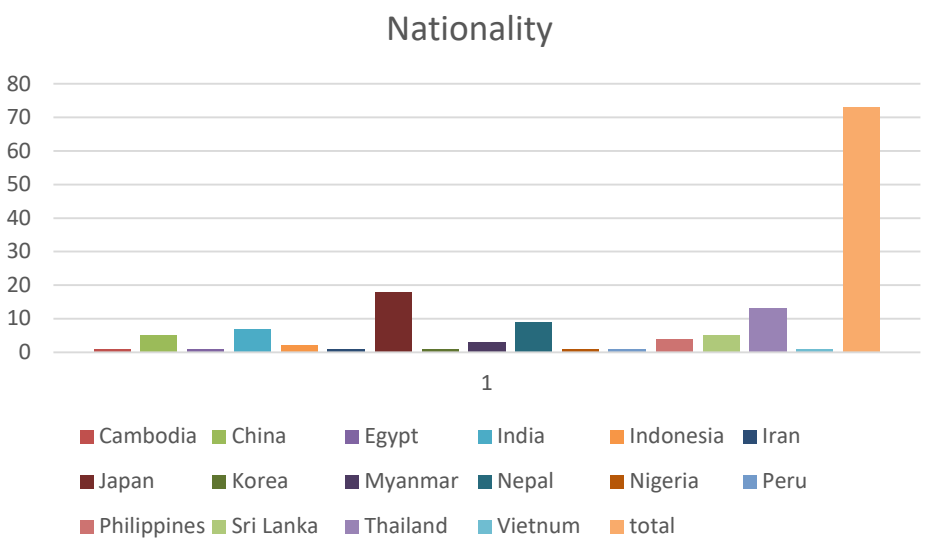

3. Field of study

Field of study	
Disaster prevention field	14
Environmental field	14
Infrastructure field, Others	25
Others	16
Secretary	4
total	73

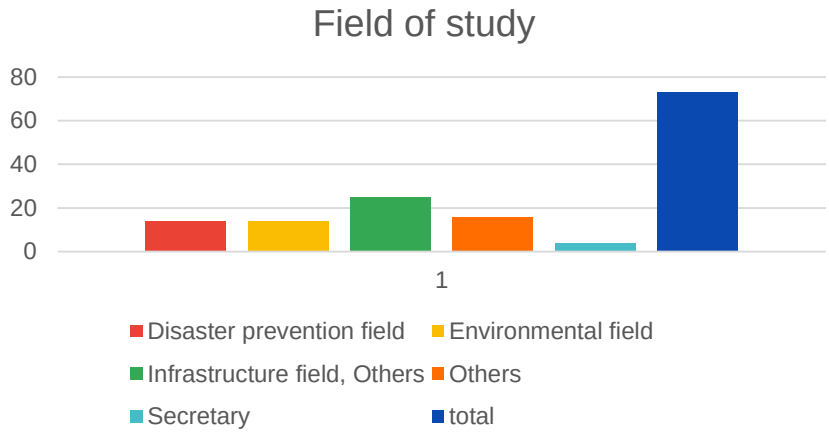

4. Access number

	8th	9th	10th
19:30	70	58	58
19:40	70	60	56
19:50	73	57	54
20:00	72	57	53
20:10	74	56	52
20:20	75	55	55
20:30	75	54	54
20:40	71	51	52
20:50	70	51	52
21:00	65	52	50
21:10	58	50	55
21:20		47	44
21:20		45	

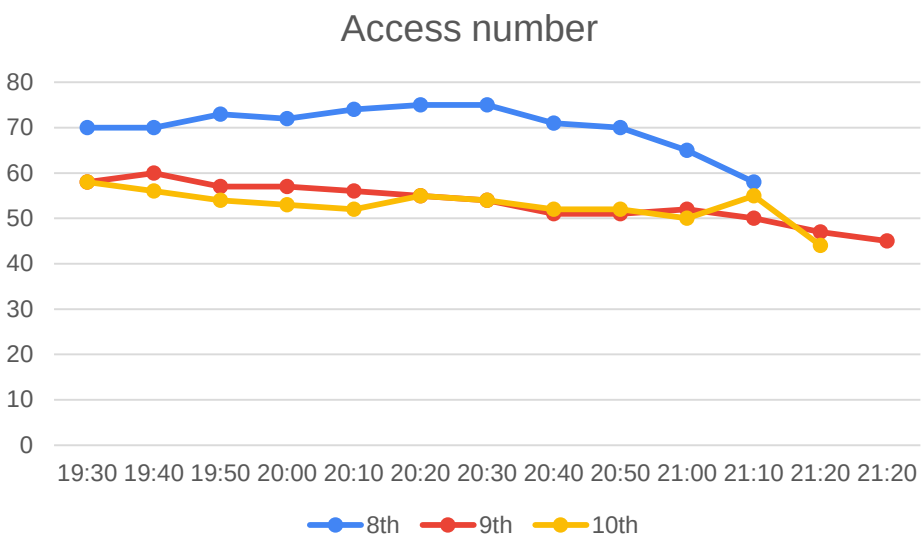

・Photos

From 3 countries,

Chairman, Prof. Takeuchi, UTokyo, Japan, Co- chairman, Prof. Pennung, AIT, Thailand, Prof. Huang, Thingha, China

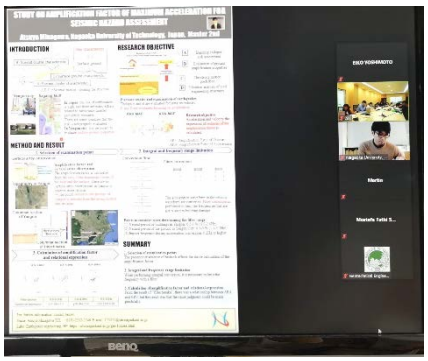

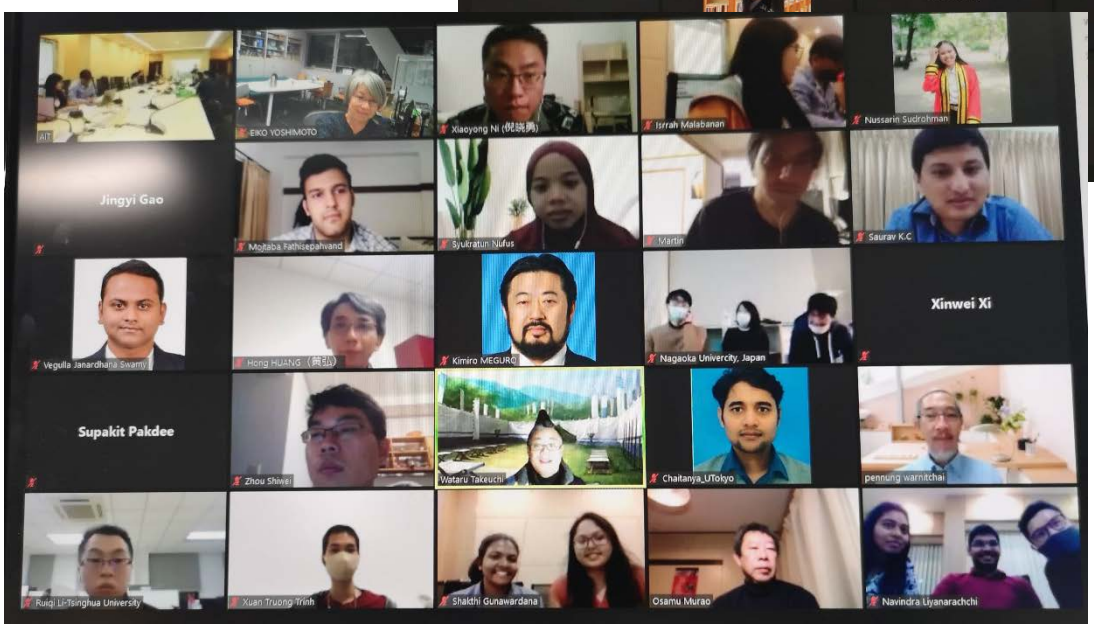

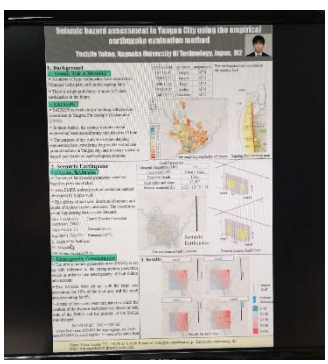

8th Dec., participants and poster

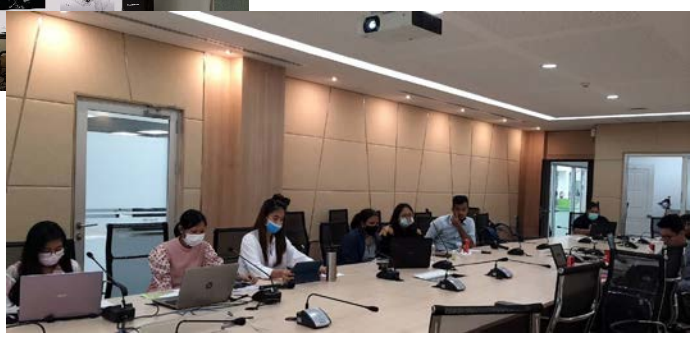

MC: Ms. Isrrah Malabanan AIT IIS, UTOKYO

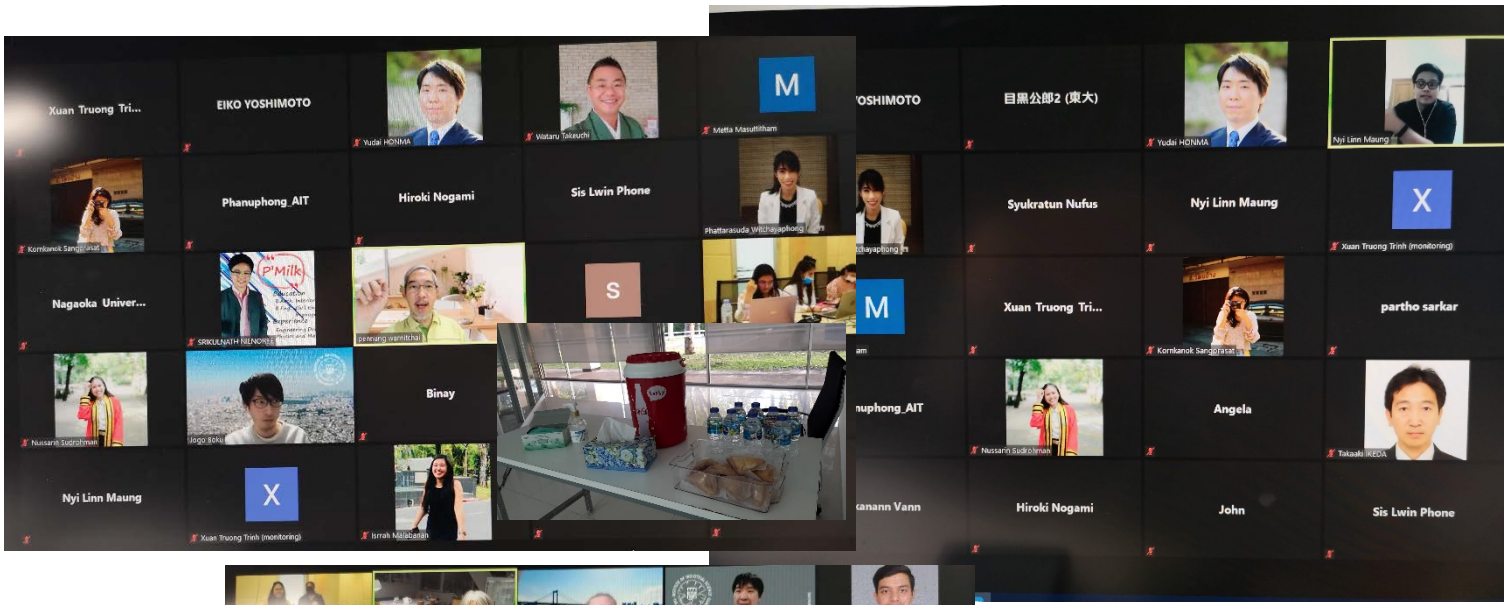

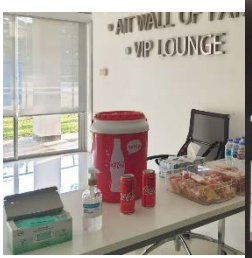

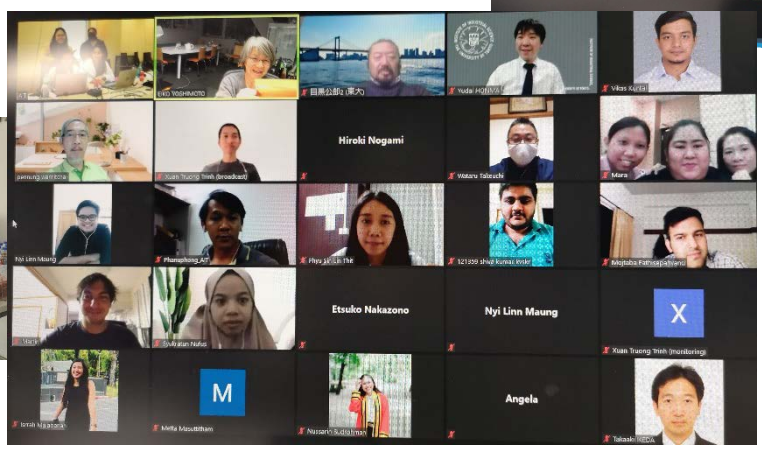

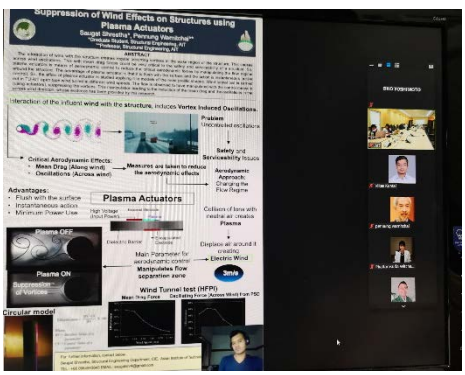

9th Dec., 2020, participants and poster

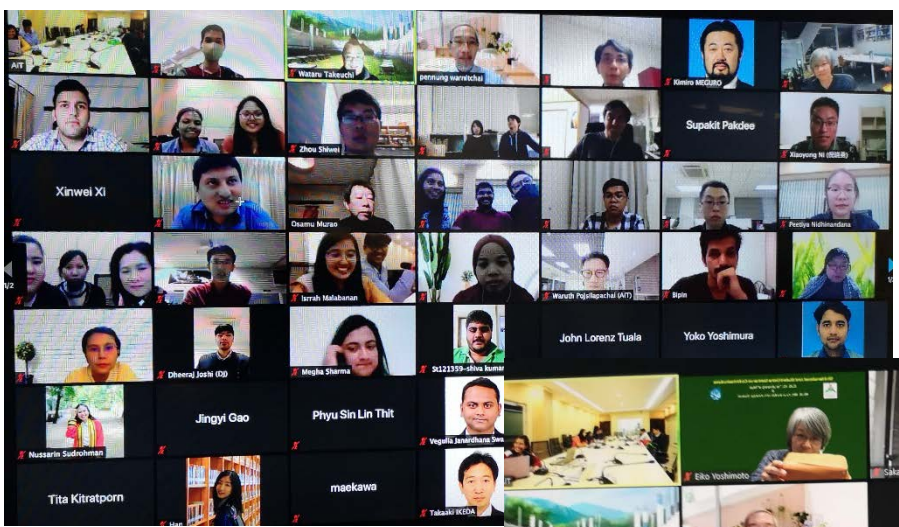

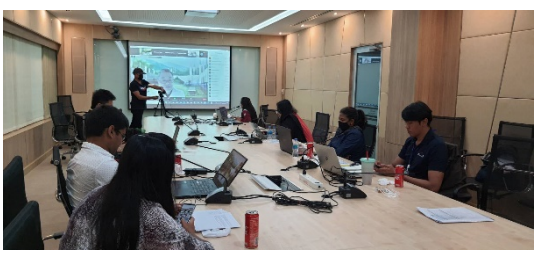

AIT

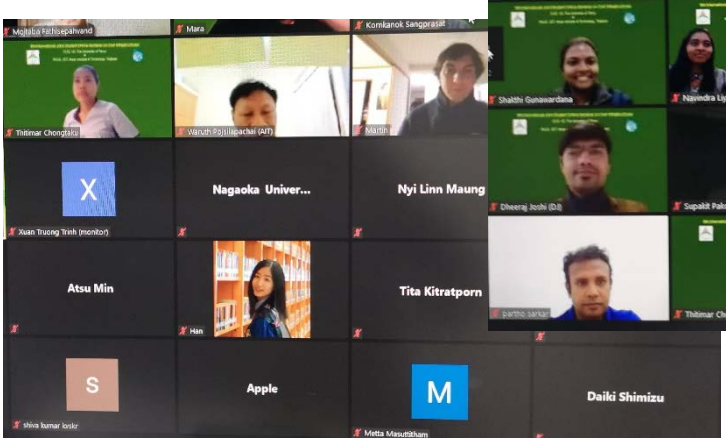

10th Dec., 2020, participants

REPORTS

9th Joint Student Seminar for Civil Infrastructure オンライン開催

2020年12月8日（火）～10日（木）に9th Joint Student Seminar for Civil Infrastructureがオンラインで開催された。本セミナーは、本所がアジア工科大学院（AIT）に設置しているRegional Office for Urban Safety (RNUS)と共同で、2007年以来タイで開催しているが、今回は初めてオンラインでの開催となった。初日はPennung Warnitchai AIT土木工学科長が「Vibration control of building and structures-an Overview」、2日目は本所 本間 雄大 准教授が「Mathematical Model for Social Distancing-Close relationship with architectural planning」、3日目は本所 竹内 渉 教授が「Geospatical technologies towards one world, one health and earth」と題して講義を実施した。学生セッションは、事前に録画した5分間のポスター発表ののちに、5分間の質疑を行う形で行われた。ネット環境が不安定な国からの接続が心配であったが、chatでの質問がモデレーターによってうまく共有され予想以上に学生間での議論が進んだこと、事前に録画することで自分の発表を短時間に伝える工夫と努力が見られたことは、オンライン開催のメリットであると思われた。参加者の国籍は実に多様で、タイ、日本、ミャンマー、インド、スリランカ、カンボジア、ペルー、エジプト、インドネシア、ネパール、中国、韓国、フィリピンの13カ国から36名の学生の発表があり、聴講を含めた3日間の参加者は132名であった。タイ周辺のアジア諸国では、社会インフラ整備が着実に進む中、大気汚染や林野火災をはじめとした環境問題に対する社会の関心が高まりつつある。ICUS（都市基盤安全工学国際研究センター）が中心になって進めてきた生研タイオフィスの活動は、今後は国際産学連携室などと連携しつつ、全所的な活動へと貢献できるように進めていく所存である。

（人間・社会系部門　教授　竹内 渉）

学生セミナー集合写真

Prof. Pennung 発表

AIT 会場の様子

Thank you for joining 9th Student Seminar

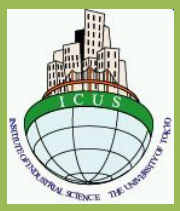

RNUS
School of Civil Engineering (N201), AIT
Tel: +66-2-524-6418
http://rnus.ait.ac.th
&
Takeuchi laboratory, IIS, UTokyo
&
International Center for Urban Safety Engineering
IIS, UTokyo
4-6-1 Komaba, Meguro-ku,
Tokyo 153-8505, Japan

Tel: +81-3-5452-6472
Fax: +81-3-5452-6476
http://icus.iis.u-tokyo.ac.jp

Edited & photos by Eiko YOSHIMOTO,
Issued in February 2021